



UNIVERSIDAD
DE LA REPÚBLICA
URUGUAY

Mecanismos de tolerancia al déficit hídrico en clones puros e híbridos de *Eucalyptus* de uso comercial: una contribución para la selección de genotipos con mayor tolerancia

José Manuel Gándara García

Doctor en Ciencias Agrarias

Noviembre, 2025

**Mecanismos de tolerancia al déficit
hídrico en clones puros e híbridos de
Eucalyptus de uso comercial: una
contribución para la selección de
genotipos con mayor tolerancia**

José Manuel Gándara García

Doctorado en Ciencias Agrarias

Noviembre, 2025

Esta tesis de doctorado se distribuye bajo licencia

Creative Commons **reconocimiento – no comercial – sin obra
derivada.**



Tesis aprobada por el tribunal integrado por (Ing. For. Dr. José Macedo Pezzopane), (Ing. Agr. Dra., Cecilia Rachid) y (Lic. Biol. Dra. Sandra Bucci) el (día) de (mes) de (año). Autor/a: (Ing. Agr. Mag. José Gándara). Director/a: (Lic. Biol. Dra. María Elena Fernández). Codirector/a: (Ing. Agr. Dr. Jaime González-Tálice).

Dedico este trabajo a Luis Viega.

Agradecimientos

A mi directora de tesis, María Elena Fernández, por su apoyo constante, capacidad de trabajo, comprensión y su estímulo permanente, especialmente cuando más lo necesitaba.

A mi codirector, Jaime González-Tálice, por su apoyo en todo momento, por su paciencia y entusiasmo durante el proceso.

A mis compañeros del Laboratorio de Fisiología Vegetal, por su ayuda permanente, desde lo profesional y lo personal.

Al Centro Universitario de Tacuarembó (Cenur Noreste) e INIA por su colaboración durante todo el trabajo y por permitirme el uso de sus instalaciones y servicios.

A la empresa Lumin, por su apoyo constante de todo tipo; el intercambio con sus profesionales fue fundamental para resolver las dificultades y los desafíos que surgieron durante el trabajo.

A la Comisión Sectorial de Investigación Científica (CSIC) de Udelar, por el financiamiento otorgado para llevar a cabo el proyecto de tesis.

A mis seres queridos, muchas gracias.

Tabla de contenido

	Página
<u>Página de aprobación</u>	III
<u>Agradecimientos</u>	VI
<u>Resumen</u>	IX
<u>Summary</u>	X
<u>1. Introducción</u>	11
1.1. Respuesta al estrés hídrico en leñosas: evitación vs. tolerancia	12
1.2. Adaptabilidad al déficit hídrico y plasticidad fenotípica	15
1.3. Respuestas al estrés hídrico en <i>Eucalyptus</i> sp.	16
1.4. Hipótesis	17
1.5. Objetivo general.....	17
1.6. Objetivos específicos	18
1.7. Revisión bibliográfica.....	18
<u>1.7.1. Intercambio gaseoso y actividad transpiratoria</u>	18
<u>1.7.2. Relaciones hídricas foliares y respuesta al estrés</u>	21
<u>1.7.3. Suministro de agua al follaje y variables hidráulicas</u>	23
<u>1.7.4. Antecedentes nacionales</u>	29
<u>2. Similares pero contrastantes: respuesta fisiológica a la sequía y crecimiento en especies puras y clones híbridos interespecíficos de <i>Eucalyptus</i></u>	30
2.1. Resumen.....	30
<u>3. Anatomía funcional del xilema en especies puras y clones híbridos interespecíficos de <i>Eucalyptus</i> con diferente resistencia a la sequía</u>	47
3.1. Resumen.....	47

<u>4. Diferencias en el estado hídrico, eficiencia del uso del agua y crecimiento en híbridos clonales de <i>Eucalyptus grandis</i>, durante temporadas de crecimiento con distinto régimen de precipitaciones</u>	<u>73</u>
4.1. Resumen.....	73
<u>5. Resultados y discusión.....</u>	<u>87</u>
5.1. Contribuciones a los objetivos específicos	87
5.2. Integración de resultados a la luz del objetivo general	88
<u>6. Conclusiones.....</u>	<u>103</u>
<u>7. Bibliografía.....</u>	<u>106</u>

Resumen

Eucalyptus grandis es una especie ampliamente utilizada por la industria forestal en Uruguay debido a su potencial de crecimiento y calidad de madera. Sin embargo, el aumento en la frecuencia de sequías exige genotipos más adaptados, obtenidos principalmente por hibridación con eucaliptos de mayor rusticidad. El objetivo de esta tesis fue estudiar los efectos del déficit hídrico (sequía) sobre atributos anatómico-funcionales y desempeño en clones comerciales de *Eucalyptus grandis* (GG), *E. grandis* × *camaldulensis* (GC), *E. grandis* × *tereticornis* (GT) y *E. grandis* × *urophylla* (GU1 y GU2) para contribuir al desarrollo de criterios de selección de genotipos más tolerantes. Se evaluaron plantines en invernáculo y árboles juveniles a campo. Los clones difirieron en sus estrategias de uso del agua y resistencia a la sequía. GC y GT presentaron un comportamiento anisohídrico, con menor control estomático durante la sequía, lo que promovió la transpiración y la fijación de C, y permitió sostener su potencial de crecimiento, especialmente en GC. Los ajustes osmóticos o elásticos les permitieron mantener turgencia durante el estrés. Además, presentaron alta pérdida de conductividad hidráulica por bajos potenciales hídricos, una estrategia hidráulicamente riesgosa. Estos clones mantuvieron la fracción de lúmenes de vasos e incrementaron la densidad de la madera lo cual favoreció tanto la eficiencia como la seguridad hidráulica. *E. grandis*, y en menor medida GU1 y GU2, adoptaron una estrategia más conservadora del agua y evitadora de la deshidratación, con estricto control estomático y baja transpiración. Esto provocó una fuerte caída del crecimiento en el clon GG bajo sequía, seguido de GU2, aunque ambos mostraron respuestas plásticas de aclimatación. Los resultados sugieren que en tallos se prioriza la eficiencia, y en ramas, la seguridad hidráulica, pero cada clon presenta un conjunto de caracteres distintivo que confiere diferente sensibilidad al estrés hídrico. El clon GC presentó mejor desempeño ante la sequía y un alto crecimiento con buena disponibilidad hídrica, con lo que demostró combinaciones de caracteres que maximizan productividad y adaptabilidad. Se discuten caracteres potencialmente útiles en la selección temprana de genotipos tolerantes a la sequía.

Palabras clave: *Eucalyptus grandis*, híbridos interespecíficos, resistencia a sequía, conductividad hidráulica, anatomía xilemática

Mechanisms of drought tolerance in pure and hybrid clones of commercial *Eucalyptus*: a contribution to the selection of more tolerant genotypes

Summary

Eucalyptus grandis is widely used in Uruguayan forestry for its growth potential and wood quality, but increasing drought severity requires genotypes better adapted through hybridization with drought-resistant eucalypts. This thesis aimed to investigate the effects of drought on anatomical-functional and performance traits in commercial clones of *Eucalyptus grandis* (GG), *E. grandis* × *camaldulensis* (GC), *E. grandis* × *tereticornis* (GT) and *E. grandis* × *urophylla* (GU1 and GU2) to contribute to the development of selection criteria for more tolerant genotypes. Seedlings were evaluated in the greenhouse and juvenile trees were evaluated in the field. The clones exhibited distinct water-use strategies and varying levels of drought resistance. GC and GT clones exhibited an anisohydric behavior, characterized by a weak stomatal response under drought conditions, which promoted transpiration and carbon fixation, thereby sustaining their growth capacity, particularly in the GC clone. Osmotic and/or elastic adjustments allowed these clones to maintain cell turgor. Additionally, they exhibited a high loss of hydraulic conductivity due to lower water potential, a hydraulically risky strategy. *E. grandis* and, to a lesser extent, GU1 and GU2 adopted a more conservative water use and dehydration-avoidance strategy, characterized by strict stomatal control and reduced transpiration. This resulted in a steep decline in growth in the GG clone under drought, followed by GU2, although both genotypes exhibited plasticity in their acclimation response. The results suggest that stems prioritize hydraulic efficiency, while branches prioritize safety; however, each clone exhibits a distinctive set of traits that confer different sensitivities to water stress. Clone GC showed better performance under drought and high growth under favorable water availability, demonstrating trait combinations that maximize productivity and adaptability. Traits with potential use in the early selection of more drought-tolerant clones are discussed.

Keywords: *Eucalyptus grandis*, interspecific hybrids, drought resistance, hydraulic conductivity, xylem anatomy

1. Introducción

La superficie forestada en Uruguay supera un millón de hectáreas y la mayor parte (>70 %) corresponde a plantaciones de especies del género *Eucalyptus* (DIEA, 2023), caracterizado por su notable capacidad adaptativa (Stape y Binkley, 2010). Los productos de mayor valor económico se obtienen a partir de *Eucalyptus grandis*, especie de alta productividad en la región y probada calidad industrial. Más allá de sus características intrínsecas, la productividad de las especies comerciales depende, en gran medida, de los avances en el mejoramiento genético y el manejo silvícola (Gonçalves et al., 2017), que han hecho grandes progresos en las últimas décadas. Sin embargo, el aumento de la variabilidad climática en todo el mundo, y en el Cono Sur en particular (IPCC, 2022; Linderman et al., 2013;), favorece la ocurrencia de sequías severas y olas de calor, hecho que condiciona el crecimiento de las plantas (Harper et al., 2009; Tyree y Jarvis, 1982) y el rendimiento de los rodales (Pyrke y Kirkpatrick, 1994). Por lo tanto, es importante que los programas de mejoramiento incorporen criterios de selección no solo basados en el aumento de la productividad y calidad industrial, como ha sido históricamente, sino también en caracteres de respuesta al estrés ambiental (Lachenbruch y McCulloh, 2014).

En este sentido, los programas de mejoramiento de eucaliptos se orientan hacia el uso de híbridos de *E. grandis* con especies de mayor rusticidad como los eucaliptos colorados (*E. camaldulensis*, *E. tereticornis*) y *E. urophylla*, buscando combinar atributos deseables —productividad y resistencia a estrés— de ambos parentales. Debido a que, en general, existen compromisos entre ambas características (*e. g.*, especies/genotipos altamente productivos suelen presentar menor resistencia al estrés y viceversa), la optimización de atributos mediante hibridación requiere de un conocimiento sólido acerca de caracteres morfofisiológicos que se expresan en la descendencia de distintas combinaciones, especialmente, aquellos de mayor relevancia en etapas tempranas del desarrollo. Estos caracteres son clave para el establecimiento de las plantaciones. Los antecedentes específicos vinculados a estos conceptos, en general y en el contexto del sistema de estudio, se presentan en los siguientes apartados .

1.1. Respuesta al estrés hídrico en leñosas: evitación vs. tolerancia

Las plantas desarrollan diferentes estrategias de resistencia frente al déficit hídrico (*i. e.*, sequía). Tienen como objetivo retrasar el mayor tiempo posible la deshidratación (especies evitadoras) o bien mantener la funcionalidad y la fijación de carbono aún con cierto grado de deshidratación de los tejidos (especies tolerantes) (Lambers et al., 2008; Levit, 1980). Sin embargo, entre estos extremos hipotéticos existe un gradiente de respuestas intermedias. Según Lambers et al. (2008), los caracteres más importantes asociados a una especie evitadora son *a*) un estricto control estomático promovido por la reducción del potencial hídrico y *b*) el desarrollo de un sistema radical amplio o una elevada conductancia hidráulica (K_h) de la planta. El aumento en K_h puede lograrse mediante una alta relación entre el área de xilema conductivo y el área foliar asociada (relación de Huber) o a través de una mayor eficiencia en el transporte de agua debido a una menor resistencia al flujo. La reducción de la resistencia implica la formación de elementos de conducción (vasos, traqueidas) con mayor diámetro. Asimismo, los diferentes tipos de regulación estomática modifican la eficiencia en el uso del agua —a escala de hoja o de planta— y afectan el balance entre la fijación de carbono y la actividad transpiratoria (Anderegg et al., 2018; Lin et al., 2015).

Las respuestas al déficit hídrico ocurren básicamente en dos fases (Choat et al., 2018). En la primera fase, el control estomático es el principal mecanismo de regulación del estado hídrico, ya que supera por varios órdenes de magnitud a la pérdida de agua por otras vías (Kerstiens, 1996). Durante la segunda fase, una vez que los estomas se cerraron, la pérdida de agua persiste a través de la cutícula, el ritidoma (*bark*) y, en menor medida, por una apertura estomática residual. Posteriormente, si el déficit hídrico persiste, la deshidratación favorece la propagación del embolismo, lo que provoca distintos grados de pérdida de conductividad hidráulica y, en casos extremos, puede producir la muerte de tejidos, órganos o incluso del individuo completo (Blackman et al., 2016; Hammond y Adams, 2019).

En las hojas la tolerancia al déficit hídrico depende de distintos mecanismos que permiten mantener la turgencia a medida que el potencial hídrico disminuye. Los más importantes son los ajustes de tipo osmótico (acumulación de osmolitos compatibles)

y elástico (modificación de la rigidez de la pared celular) (Choat et al., 2018; Larcher, 2003, Pallardy, 2008). Asimismo, existen mecanismos que modifican la permeabilidad de las membranas mediante cambios en la expresión o actividad de acuaporinas (Kapilan et al., 2019). Si bien se trata de un tipo respuesta al estrés ampliamente estudiada en especies herbáceas, existen solo reportes recientes en diferentes leñosas de interés productivo (Carraro y Di Lorio, 2022).

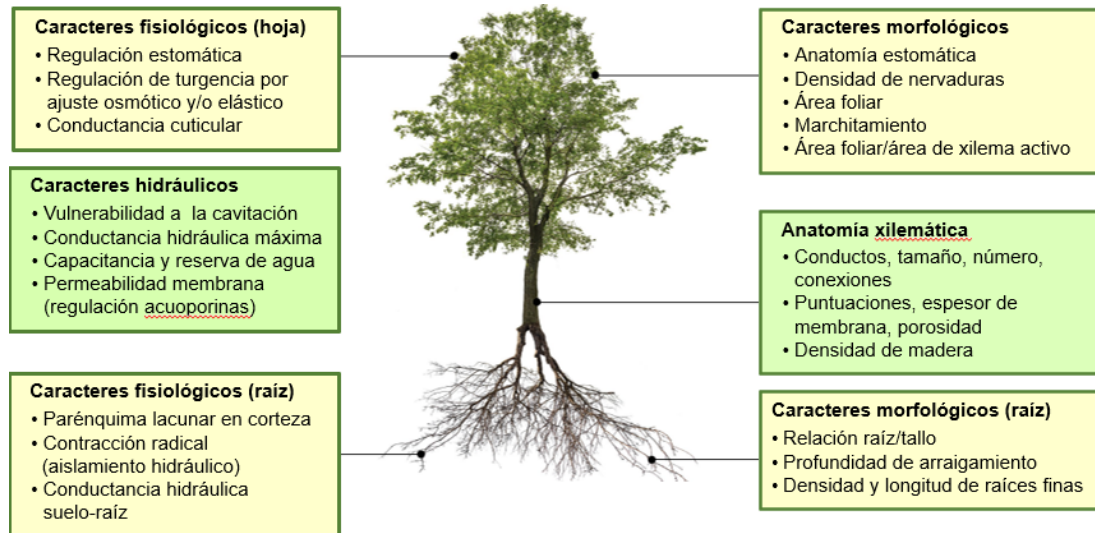
En términos hidráulicos, la tolerancia a la sequía se asocia con una menor vulnerabilidad a la cavitación de la columna de agua dentro del xilema (Choat et al., 2012). La resistencia a la cavitación depende de rasgos anatómicos que limitan la entrada o la propagación del aire en los elementos de conducción (Jacobsen et al., 2007; Willson et al., 2008), como así también del engrosamiento de las paredes celulares en conductos y células acompañantes (fibras y fibrotraqueidas). Este refuerzo estructural es fundamental para preservar la funcionalidad del sistema conductivo, ya que aumenta la estabilidad mecánica frente a la cavitación y al colapso (Hacke et al., 2001; Matos et al., 2024; Zanne et al., 2010). Así, la relación entre el espesor de pared y el diámetro de lumen de los elementos individuales de conducción constituye un indicador clave de la resistencia a la cavitación (Hacke et al., 2006; Lens et al., 2011).

Estos cambios morfológicos promueven un aumento en la densidad de la madera (Hacke et al., 2001; Meinzer y McCulloh, 2013) y evidencian la transición hacia un tejido con mayor seguridad hidráulica (menor vulnerabilidad a la cavitación) a costa de una menor eficiencia (baja conductividad hidráulica) (Li et al., 2024; Martínez-Vilalta et al., 2002; Zimmermann et al., 2021; Soro et al., 2023). El balance entre seguridad y eficiencia define la arquitectura hidráulica de las especies leñosas (Sperry et al., 2008) y determina el potencial de adaptabilidad de las especies al estrés abiótico (Johnson et al., 2022; Li et al., 2023). No obstante, existen distintos patrones de respuesta asociados a los rasgos anatómicos y al grado de vulnerabilidad a la cavitación. Por ejemplo, en angiospermas de ambientes áridos, el balance entre seguridad y eficiencia conlleva un descenso marcado en el diámetro de los vasos (Jacobsen et al., 2007; y Schenk, 2012; Pfautsch, 2016). Sin embargo, en géneros como *Populus* se ha observado una gran variabilidad de respuestas en cuanto a los atributos anatómicos y la seguridad hidráulica (Fichot et al., 2015).

Existen otras características estructurales del xilema, surgidas del conjunto de los elementos de conducción, que también afectan la relación entre la eficiencia del transporte y la seguridad hidráulica. Entre ellas, algunas de simple cuantificación son la fracción de lúmenes (F) y la composición de los conductos (S), que mide la distribución de tamaños de estos en el tejido. El análisis en conjunto de ambos atributos ofrece una visión integrada de la coordinación funcional del xilema frente a la variación de las condiciones ambientales (Zanne et al., 2010). Asimismo, la capacitancia de los tejidos (*e. g.*, McCulloh et al., 2014; Scholz et al., 2007) y la morfología de las puntuaciones intervasculares (*e. g.*, Sperry y Hacke, 2004) son caracteres que también afectan la conductividad hidráulica, la vulnerabilidad a la cavitación y, eventualmente, la reparación del embolismo (Brodersem et al., 2013). Por otro lado, se ha reportado que las fibras xilemáticas desempeñan un rol importante en la recuperación del embolismo en *Populus nigra* (Tricerri et al., 2025), al proveer agua estructural almacenada. En la figura 1 se presentan algunas de las respuestas al déficit hídrico en especies leñosas.

Figura 1

Principales caracteres fisiológicos y morfológicos asociados con la respuesta al estrés en especies leñosas



Nota. Modificado de Choat et al. (2018).

1.2. Adaptabilidad al déficit hídrico y plasticidad fenotípica

Para evaluar el potencial de adaptación de una especie, es esencial identificar el valor adaptativo de diferentes caracteres morfofuncionales, analizando su relación con el crecimiento y con la supervivencia de las plantas en condiciones de estrés. Así, existen determinados rasgos anatómicos que desempeñan un rol clave en algunas especies, mientras que en otras su impacto es limitado. Por ejemplo, la vulnerabilidad a la cavitación del xilema es un carácter determinante de la respuesta a la sequía en *Pseudotsuga menziesii* (Dalla-Salda et al., 2011); sin embargo, en *Pinus pinaster* su papel es poco relevante (Lamy et al., 2014), como se deduce de su baja variabilidad entre procedencias creciendo en distintos ambientes. Para comprender el valor adaptativo de un rasgo dentro de una especie o genotipo, es necesario conocer cómo se integra en el conjunto de mecanismos de ajuste en órganos aéreos y subterráneos. Este enfoque permitiría conocer tanto las respuestas de la planta entera (Rowland et al., 2023) como los efectos compensatorios que operan en función de la exposición al estrés (Martínez-Vilalta et al., 2023).

Además de la variación genética, es fundamental considerar la plasticidad fenotípica de los caracteres de interés, entendida como la norma de reacción ante diferentes condiciones ambientales. La magnitud de la plasticidad varía en función del genotipo y del carácter evaluado y está asociada a la heterogeneidad ambiental a la que el taxón ha estado expuesto durante su historia evolutiva (Balaguer et al., 2002). Esta respuesta condiciona la capacidad de aclimatación del individuo al factor de estrés y afecta su desempeño funcional, así como su aptitud en ambientes variables. Por lo tanto, la comprensión de respuestas plásticas constituye un elemento primordial para predecir y gestionar los efectos del cambio climático en los vegetales (Nicotra et al., 2010; Valladares et al., 2014). Estudiar la plasticidad fenotípica implica identificar posibles interacciones genotipo-ambiente.

1.3. Respuestas al estrés hídrico en *Eucalyptus* sp.

En *Eucalyptus*, los mecanismos más importantes para mantener la turgencia celular y evitar la deshidratación son el control estomático y los ajustes de tipo osmótico y elástico (White et al., 2000; Whitehead y Beadle, 2004; Zhang et al., 2015). Sin embargo, más allá de las respuestas plásticas —como la acumulación de osmolitos— existe una amplia diversidad de caracteres de la madera que determinan distintos grados de adaptación a la sequía. Por ejemplo, *E. grandis* es más vulnerable a la cavitación que *E. camaldulensis* (Barotto et al., 2016; Fernández et al., 2019). La anatomía y la densidad de la madera sugieren una estrategia de evitación en la primera especie y de tolerancia en la segunda (Monteoliva et al., 2015). Por este motivo, es importante identificar cambios en caracteres morfofisiológicos relacionados con la resistencia al estrés hídrico que puedan surgir a partir de la hibridación entre *E. grandis* y especies consideradas más rústicas o tolerantes, como *E. camaldulensis*. Al mismo tiempo, es importante evaluar el impacto del estrés sobre la tasa de crecimiento potencial de los individuos.

Al igual que en otros géneros, se espera una coordinación entre las respuestas de las hojas y de los órganos leñosos, como así también variaciones en sus relaciones alométricas. Identificar dichas respuestas contribuiría al ajuste y ampliación de los caracteres que pueden emplearse en la selección precoz de genotipos con mayor

tolerancia al déficit hídrico. En este contexto, resulta relevante determinar si la combinación de características de *E. grandis* con las de especies más tolerantes se traduce en un desempeño diferencial bajo condiciones contrastantes de disponibilidad de agua. En particular, interesa conocer si los híbridos exhiben un compromiso entre el crecimiento y la capacidad de regular su estado hídrico en condiciones de alta disponibilidad de agua, pero una ventaja funcional en situaciones de déficit, asociada a mayores tasas de transpiración, mantenimiento de la turgencia y eficiencia en el transporte de agua. De esta manera, será posible seleccionar o desarrollar clones — mediante cruzamientos interespecíficos— que mejoren la adaptabilidad del género al cambio climático, sin comprometer la producción ni la calidad de la madera.

1.4. Hipótesis

a) Los clones híbridos de *E. grandis* con eucaliptos colorados (*E. camaldulensis* y *E. tereticornis*) y con *E. urophylla* presentan menor crecimiento que *E. grandis* en condiciones de alta disponibilidad hídrica; sin embargo, bajo condiciones de déficit hídrico, presentan una mayor actividad transpiratoria y capacidad de crecimiento, debido a la activación de mecanismos que mantienen la turgencia, la apertura estomática y la eficiencia del transporte de agua, además de relaciones alométricas que maximizan el abastecimiento de agua al follaje.

b) El mejor desempeño de los clones híbridos bajo déficit hídrico está asociado a valores intrínsecos más altos en caracteres funcionales relacionados con la tolerancia al estrés, así como con una mayor plasticidad fenotípica en dichos caracteres.

c) Existen correlaciones significativas entre variables anatómicas y funcionales, así como también entre atributos funcionales de distintos órganos, que permiten utilizar determinados caracteres como *proxy* de otros caracteres en la selección precoz de clones de alto valor.

1.5. Objetivo general

Determinar mecanismos morfofisiológicos involucrados en la respuesta al déficit hídrico en clones comerciales de *Eucalyptus grandis* e híbridos con eucaliptos

colorados (*E. camaldulensis* y *E. tereticornis*) y con *E. urophylla*, para contribuir al desarrollo de criterios de selección de genotipos más tolerantes.

1.6. Objetivos específicos

- a) Caracterizar y comparar variables asociadas a las relaciones hídricas y al intercambio gaseoso en los diferentes clones durante la estación de crecimiento, en el estado de plantín.
- b) Cuantificar variables anatómico-funcionales del xilema y de la planta entera, relacionados con la arquitectura hidráulica de los diferentes genotipos.
- c) Cuantificar el grado de plasticidad fenotípica en caracteres funcionales (anatómicos, fisiológicos, morfológicos, de asignación de biomasa) en función de la disponibilidad hídrica del sustrato.
- d) Identificar cómo los mecanismos fisiológicos, las características anatómico-funcionales (objetivos *a* y *b*) y la plasticidad fenotípica (objetivo *c*) se relacionan con el desempeño de clones puros e híbridos bajo condiciones contrastantes de disponibilidad hídrica.
- e) Estudiar las relaciones hídricas y la fijación de carbono en individuos juveniles de los diferentes taxones, creciendo a campo con distinta disponibilidad hídrica del suelo (condiciones medias del sitio o la disponibilidad hídrica estacional), e interpretar los patrones de crecimiento, comparándolos con los observados en el estado de plantín (objetivos anteriores).

1.7. Revisión bibliográfica

1.7.1. Intercambio gaseoso y actividad transpiratoria

La apertura estomática es el proceso más importante mediante el cual las plantas regulan su estado hídrico. Se expresa frecuentemente a través de la conductancia estomática (g_s) y es una limitante importante de la productividad en rodales de *Eucalyptus* (Whitehead y Beadle, 2004). En *E. grandis*, la g_s depende principalmente de la irradiancia (PAR), del déficit de presión de vapor del aire (D_{pv}) y de la disponibilidad hídrica en el suelo (Mielke et al., 2000). Así, bajo condiciones óptimas de luz (PAR $\sim 800 \mu\text{mol m}^{-2} \text{s}^{-1}$) y agua, presenta una mayor tasa transpiratoria que

varias otras especies del género (Brodribb y Holbrook, 2004; Valverde et al., 2025). Los eucaliptos colorados —llamados así por la tonalidad de su madera, en contraste con los blancos— presentan un comportamiento estomático diferente a *E. grandis*. Por ejemplo, *E. tereticornis* es menos sensible al Dpv que *E. grandis* (Bourné et al., 2015) y transpira más activamente bajo condiciones de déficit hídrico en la atmósfera. A su vez, *E. camaldulensis* es más sensible que *E. tereticornis*, pero activa mecanismos compensatorios que le permiten mantener el intercambio gaseoso; entre ellos, un mayor desarrollo radical y un aumento de la conductividad hidráulica en raíz y tallo (Whitehead y Beadle, 2004). En general, los eucaliptos colorados presentan una estrategia menos conservativa en el uso del agua (*i. e.*, menor control estomático), similar a lo reportado en *E. urophylla* (Singh, 2005).

El estado hídrico de los tejidos se mide habitualmente a través del potencial hídrico (Ψ). Este parámetro indica la capacidad energética del agua y permite predecir la dirección del flujo en el sistema suelo-planta-atmósfera. El agua pura posee un Ψ igual a cero, tomando valores negativos el agua en el suelo, en la planta o la atmósfera de acuerdo a su concentración en estos compartimientos. El agua se mueve por difusión desde zonas con potenciales más cercanos a cero hacia zonas con mayor déficit de agua, es decir, con valores de Ψ más negativos. Debido a que es una medida de la concentración relativa de agua en un tejido, el Ψ influye sobre procesos fisiológicos clave, como la turgencia y la expansión celular, por lo que se trata de un indicador fundamental para comprender las estrategias de respuesta de las plantas al déficit hídrico. En este contexto, la transpiración desempeña un rol central, ya que genera tensión ($\Delta\Psi$) en los conductos xilemáticos, lo que promueve la absorción de agua desde el suelo. Bajo condiciones de elevada tensión en el xilema (*i. e.*, estrés severo) se pueden desencadenar eventos de cavitación y embolia en el xilema (Sperry et al., 2002; Tyree, 2003; Martínez-Vilalta y Garcia-Forner, 2016) que comprometen la funcionalidad hidráulica y la supervivencia de los árboles (McDowell et al., 2008). Las leñosas regulan su apertura estomática (gs) para evitar que el Ψ descienda por debajo de un valor crítico (umbral) a partir del cual se induce el embolismo de manera progresiva (Martin-St. Paul et al., 2017; Ryan et al., 2006).

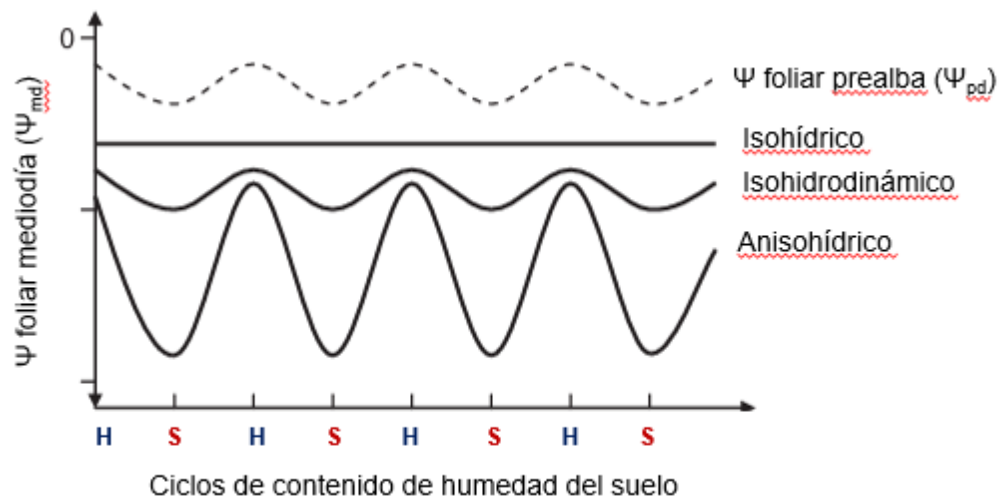
En condiciones de estrés severo, la embolia masiva puede interrumpir el transporte xilemático y comprometer la integridad del tejido, con la consiguiente muerte de órganos o, en situaciones extremas, del propio individuo. En *E. grandis* el umbral está próximo a $\Psi = -2$ MPa (Mielke et al., 2000), aunque en otras especies del género es menor a -4 MPa (White et al., 2000). Así, *E. grandis* reduce significativamente la apertura estomática a medida que disminuye el potencial hídrico, lo que evidencia su elevada sensibilidad al déficit hídrico (Bourné et al., 2015). El Ψ máximo se registra al final del período nocturno (prealba, Ψ_{pd}) y su valor refleja el potencial hídrico del suelo en contacto con las raíces, siempre que no exista transpiración nocturna, que el suelo que rodea las raíces mantenga una humedad relativamente homogénea y que no haya aporte externo de agua. En *Eucalyptus* existe una relación lineal entre el Ψ_{pd} y la g_s , inclusive en condiciones de bajo contenido hídrico del suelo (Körner y Cochrane, 1985; Mielke et al., 2000; White et al., 2000; Zhang et al., 2015).

El potencial hídrico foliar de mediodía (Ψ_{md}) representa el Ψ mínimo diario en los tejidos y su variación en relación con la actividad transpiratoria y humedad del suelo define patrones característicos (figura 2). Cabe mencionar que la tasa de transpiración de una planta ϵ es directamente proporcional a su conductancia hidráulica total (K_h) y a la diferencia de potencial entre el suelo y las hojas. En numerosas especies, el Ψ_{md} permanece relativamente constante, al margen de la disponibilidad hídrica en el suelo. Este comportamiento se denomina *isohídrico* y, en general, supone un importante control estomático en condiciones de elevada demanda atmosférica o bajo contenido hídrico del suelo (Hubbard et al., 2001; Ripullone et al., 2007). En especies o genotipos isohídricos se minimiza la pérdida de agua —y consecuente deshidratación de los tejidos— a pesar de una disminución en la transpiración y fijación de carbono. Contrariamente a esta estrategia, los eucaliptos —aunque en diferente grado según la especie— se consideran especies anisohídricas, ya que su Ψ_{md} disminuye proporcionalmente en función del contenido de agua en el suelo (figura 2). Por otra parte, Franks et al. (2007) definieron en *Eucalyptus gomphocephala* un comportamiento denominado *isohidrodinámico*. Consiste en mantener relativamente constante la actividad transpiratoria durante ciclos estacionales de distinto contenido

de agua del suelo a través de un ajuste coordinado de la conductancia estomática y la conductividad hidráulica. Así, en especies isohídricas, el potencial mínimo se mantiene relativamente constante (figura 2), de modo que el $\Delta\Psi$ —y, por ende, la transpiración— disminuye a medida que se reduce la disponibilidad de agua del suelo. En las especies anisohídricas, el potencial mínimo desciende junto con el potencial de prealpa a medida que el suelo se seca (figura 2), de manera que el gradiente de potencial ($\Delta\Psi = \Psi_{pd} - \Psi_{md}$) se incrementa. La transpiración en este caso se mantiene en mayor o menor medida en función de la reducción de la conductancia hidráulica (K_h) que produce la cavitación. En las especies isohidrodinámicas, el $\Delta\Psi$ es menos variable que en las especies anisohídricas y más estable que en las isohídricas, lo que permite mantener la capacidad de transporte de agua (K_h) y, por lo tanto, la transpiración.

Figura 2

Patrones generales que representan la variación del potencial hídrico foliar mediodía (Ψ_{md}) en función de los ciclos estacionales de humedad del suelo.



Nota. H: suelo húmedo, S: suelo seco. Modificado de Franks et al. (2007).

1.7.2. Relaciones hídricas foliares y respuesta al estrés

Para evaluar el estado hídrico de un tejido es importante la determinación del Ψ y de sus principales componentes: el potencial osmótico ($\Psi\pi$) y el potencial de

turgencia o presión (Ψ_p), no solo en un momento puntual, sino antes y después de los eventos de sequía. Es posible determinar valores *normales* con los que opera la planta —los cuales pueden ser intrínsecamente más o menos favorables para el mantenimiento de la turgencia en condiciones de bajo contenido de agua en el suelo— así como su capacidad para modificar activamente (ajustar) dichos valores (Fernández y Gyenge, 2010).

Una respuesta frecuente al estrés hídrico es el ajuste elástico, el cual implica un cambio en el módulo de elasticidad de la pared celular (ϵ). La reducción de ϵ conlleva una disminución de la rigidez de la pared, lo que permite mantener la presión de turgencia frente a un descenso del potencial hídrico. Si bien ϵ depende en gran medida del genotipo (Leuschner et al., 2019) y de la edad de los tejidos (Saito y Terashima, 2004), en *Eucalyptus* su modificación es muy marcada, tanto en la magnitud como en la dirección del cambio. Por ejemplo, en *E. platypus* disminuye frente a sequía (de 20 a 15 MPa) pero en *E. camaldulensis* aumenta (de 18 a 23 MPa). En la primera especie, la estrategia consiste en incrementar la elasticidad de la pared, mientras que en la segunda se trata de aumentar su rigidez (White et al., 2000). Las paredes rígidas (alto ϵ) permiten generar un gradiente de potencial hídrico que promueve la absorción de agua en suelos secos, a partir de pequeñas variaciones del contenido relativo de agua en los tejidos. En general, el incremento de ϵ está asociado a un mayor control estomático (Lenz et al., 2006).

El ajuste osmótico es otro mecanismo de respuesta que consiste en la acumulación de solutos —osmolitos compatibles— para reducir el potencial osmótico (Ψ_π) y, de esta manera, promover un gradiente de potencial hídrico que facilita el ingreso de agua en las células. La disminución del Ψ_π es un indicador de tolerancia a la sequía en los vegetales (Choat et al., 2018; Larcher, 2003; Wang et al., 2018) y, aunque presenta gran variabilidad genotípica, es un mecanismo de respuesta frecuente en *Eucalyptus* (Pita y Pardos, 2001; Lemcoff et al., 2002). Por ejemplo, en *E. globulus* se observó un aumento de carbohidratos solubles y prolina en respuesta a la sequía (Guarnaschelli et al., 2003). Sin embargo, en varios híbridos interespecíficos los resultados no han sido consistentes, como por ejemplo, en *E. nitens* \times *E. grandis* (Mokotedi, 2013). El ajuste osmótico presenta menor dependencia de la especie que

el ajuste elástico (Merchant et al., 2007) y también menor dependencia de la edad de los tejidos. Existen especies que combinan ambas estrategias (alto ε y bajo $\Psi\pi$) para mantener un $\Delta\Psi$ suelo-planta favorable para la absorción de agua en suelos secos, lo que les permite sostener el crecimiento (Corcuera, 2003).

1.7.3. Suministro de agua al follaje y variables hidráulicas

En especies leñosas el agua circula por una vasta red de conducción, donde las resistencias al flujo y la capacitancia desempeñan un rol clave para comprender el comportamiento en diferentes condiciones ambientales. La resistencia al déficit hídrico depende de factores relacionados con la eficiencia del transporte (Tyree y Zimmermann, 2002), cuya principal medida es la conductividad hidráulica (k_h). Esta refleja la capacidad de suministro de agua al follaje y se relaciona directamente con la apertura estomática y con la fijación de carbono (Hubbard et al., 2001). En este sentido, la reducción de k_h induce el cierre estomático, y si bien se desconoce cómo opera el mecanismo, se sabe que influye de manera directa sobre la eficiencia en el uso del agua de la planta (Gleason et al., 2016).

La conductividad hidráulica (k_h) se calcula como la masa de agua (Q , kg) que atraviesa un segmento de longitud conocida (l) por unidad de tiempo (s) y por unidad de diferencia de presión (ΔP , MPa) entre sus extremos, $k_h = Ql \times \Delta P^{-1}$ ($\text{kg m s}^{-1} \text{MPa}^{-1}$). Para estandarizar las mediciones, se corrige por el área de xilema activo (A_S) y se obtiene la conductividad hidráulica específica, $k_S = Ql (A_S \Delta P)^{-1}$ ($\text{kg m}^{-1} \text{s}^{-1} \text{MPa}^{-1}$). Así, por ejemplo, luego de sequías prolongadas, el diámetro medio de los elementos de conducción disminuye (*i. e.*, los nuevos elementos son más pequeños) y su número por unidad de superficie aumenta. Estos cambios reducen significativamente la k_S , dado que esta variable depende directa y exponencialmente (a la cuarta potencia) del diámetro de los conductos. Por otro lado, para conocer la capacidad de suministro de agua al follaje, se normaliza la k_h (medida o teórica, ver más abajo) por el área foliar alimentada por el segmento de xilema considerado (A_F) y se obtiene la conductividad hidráulica foliar específica, $k_L = Ql (A_F \Delta P)^{-1}$ ($\text{kg m s}^{-1} \text{MPa}^{-1}$). Tanto la k_S como la k_L son variables que definen propiedades intensivas, dado que, al haber sido

estandarizadas (por longitud y áreas de xilema o foliar), no dependen de las dimensiones del material.

Es importante considerar que, al medir la k_s de un órgano extraído directamente de una planta (ejemplo, una rama terminal), este generalmente contiene cierto nivel de embolismos. Estos pueden ser removidos mediante perfusión de agua a presión (de aproximadamente 0,1-0,2 MPa), para así obtener la k_h máxima (o la k_{Smax} , al estandarizarla por el tamaño), propiedad que hace referencia a la capacidad conductiva del segmento. A su vez, una aproximación a esta medida puede hacerse a partir de las dimensiones de los elementos de conducción del xilema. Así, es posible calcular la k_s máxima teórica (k_{Stheo}) asumiendo que todos los conductos son funcionales y despreciando las resistencias de las puntuaciones intervasculares. En este sentido, la k_s máxima teórica siempre es mayor que la k_s máxima real medida, ya que esta integra las resistencias de las puntuaciones. La $k_{Stheo} = \sum_i (d_i^4 \pi \rho / 128 \eta_w)$, donde d_i es el diámetro del conducto, ρ es la densidad del agua a 20 °C (998,2 kg m⁻³) y η_w es la viscosidad del agua ($8,9 \times 10^{-10}$ MPa).

Otra propiedad hidráulica clave para comprender la resistencia a la sequía es la vulnerabilidad a la cavitación del xilema (e. g., Maherali et al., 2004), que se describe a partir de los parámetros de la curva sigmoidea que relaciona el porcentaje de pérdida de k_h (PLC) y el potencial hídrico del segmento considerado. Esta curva se conoce como *curva de vulnerabilidad a la cavitación* y su parámetro más comúnmente reportado es el P_{50} (i. e., potencial hídrico en el cual el segmento pierde 50% de k_h). La elaboración de estas curvas en laboratorio requiere llevar los tejidos a la máxima pérdida de k_h posible, lo que en varias especies de eucaliptos suele implicar valores muy bajos de potencial hídrico (entre -8 y -10 MPa). A su vez, el grado de embolismo que la planta tiene *in situ* en un determinado momento se calcula relacionando la k_s medida inmediatamente después de la extracción del segmento con los valores posteriores a la remoción del embolismo, es decir, la k_{Smax} . Así, se calcula la reducción porcentual de la conductividad hidráulica como $PLC = 1 - (k_s/k_{Smax})$, la cual refleja la cavitación real en la condición ambiental en la que se cosechó el material. La vulnerabilidad a la cavitación es una propiedad intensiva de los tejidos, pero la

cavitación real depende de esta y de los niveles de tensión alcanzados en cada momento como consecuencia de la disponibilidad de agua y la apertura estomática.

Todas las medidas hidráulicas mencionadas permiten comparaciones entre órganos o tratamientos (ejemplo, distinta disponibilidad hídrica) y son útiles para estimar respuestas adaptativas. Asimismo, en estudios ecofisiológicos es habitual calcular una variable que define una propiedad extensiva, la conductancia hidráulica (K_h). Se trata de una variable funcional que integra todos los valores de conductividad hidráulica de un órgano o de la planta entera y es el cociente entre la transpiración (E) y el $\Delta\Psi$ entre los extremos del segmento, órgano o planta (Bond y Kavanagh, 1999). La K_h de una planta varía durante el transcurso del día debido a la interdependencia entre la g_s , el Ψ y la k_h de los distintos órganos. Cuando la transpiración es intensa, pueden ocurrir eventos de cavitación que reducen la k_h en segmentos u órganos de la planta. Por ello, la mayoría de las especies leñosas mantiene la g_s en un rango que evita una disminución significativa de k_h , dado el incremento de $\Delta\Psi$.

En especies angiospermas, la k_s y la vulnerabilidad a la cavitación del xilema están determinadas principalmente por características anatómicas de los vasos. La mayoría de los estudios que describen las relaciones entre estructura y función provienen de especies con vasos agrupados. Sin embargo, en *Eucalyptus* se han observado vasos solitarios y poco numerosos, generalmente rodeados por traqueidas vasicéntricas y parénquima axial. Estudios recientes también muestran diferencias en la vulnerabilidad a la cavitación de algunos eucaliptos y su relación con la anatomía xilemática (Fernández et al., 2019). En dicho estudio se reportan relaciones particulares para especies del género en materiales utilizados comercialmente, es decir, que han sufrido algún tipo de selección y mejoramiento genético. A diferencia de lo postulado para la mayoría de las angiospermas y coníferas, la vulnerabilidad a la cavitación disminuye en las especies comerciales de *Eucalyptus* con vasos más anchos (Barotto et al., 2016). La mayor vulnerabilidad de los vasos con menor diámetro podría explicarse por la presencia de puntuaciones intervasculares de mayor tamaño (Fernández et al., 2019) o por la presencia de membranas delgadas en ellas (Pfautsch et al., 2018). Las células que rodean a los vasos los interconectan radialmente y desempeñan un rol fundamental, actuando como puentes hidráulicos que aumentan el

pasaje de agua radialmente entre vasos solitarios a la vez que reducen la propagación del aire (embolismo) entre conductos (Fernández et al., 2019). Asimismo, estas conexiones contribuirían a la reparación del embolismo a través de la liberación de solutos en los vasos, como potasio (Hmidi et al., 2025) o carbohidratos no estructurales (Li et al., 2025).

La relación entre los lúmenes de los elementos de conducción, el grosor de las paredes celulares y la presencia de otros tipos celulares —como las fibras y fibrotraqueidas en angiospermas— resulta en distintas relaciones peso seco:volumen de madera. Así, la densidad de madera es una propiedad emergente de la anatomía que tiene un rol central en el funcionamiento de las leñosas. La densidad de la madera es una propiedad muy variable en *Eucalyptus* (400-1000 kg m⁻³) (Zanne et al., 2010) y su valor aumenta debido a los ajustes morfológicos y anatómicos en respuesta al estrés hídrico, tales como la reducción de lúmenes y engrosamiento de paredes celulares. Existen trabajos que relacionan la densidad de la madera en este género con propiedades hidráulicas, tanto entre especies (Barotto et al., 2017; Fernández et al., 2019; Searson et al., 2004) como dentro de una misma especie (Barotto et al., 2018). El compromiso entre seguridad y eficiencia hidráulica es mayor en *E. grandis*, especie que presenta una elevada k_h teórica en tallos, principalmente debido a su mayor densidad de vasos con diámetros más amplios, en comparación, por ejemplo, con *E. viminalis* (Barotto et al., 2017). Así, la densidad de madera en los genotipos de *E. grandis* de alto crecimiento en Sudamérica es de alrededor de 350-400 kg m⁻³. Es posible que estos valores bajos de densidad de madera sean una consecuencia del mejoramiento genético enfocado en la productividad, ya que los reportes de densidad básica de madera de esta especie en bosques de Australia son mucho mayores, del orden de 600 kg m⁻³ (Ilic et al., 2000). Por el contrario, *E. camaldulensis* (Nouri, 2012; Tampori et al., 2024), *E. tereticornis* (Pillai et al., 2013) y *E. urophylla* (Vieira et al., 2021) son especies con valores de densidad básica mayores a 500 kg m⁻³ que sugieren un tejido xilemático menos eficiente, más resistente y seguro en términos hidráulicos. En *E. tereticornis* se han reportado promedios por encima de 800 kg m⁻³ (USDA Forest Service, 2023), lo que sugiere que es una especie con alta seguridad hidráulica.

El déficit hídrico produce cambios anatómicos y morfológicos que reflejan la capacidad de aclimatación a ambientes con déficit hídrico. Los cambios plásticos de conductividad hidráulica que surgen como respuesta de aclimatación a condiciones de mayor estrés hídrico afectan el proceso fotosintético (Eamus et al., 2000; Santiago et al., 2004; Xu et al., 2021). En varias especies de *Eucalyptus* las respuestas más comunes de tipo no estomático (fase fotoquímica) implican una reducción en la tasa máxima de transferencia de electrones (J_{\max}) y en la tasa máxima de carboxilación ($V_{C\max}$), aunque con recuperación de los valores a largo plazo (Zhou et al., 2016). En *E. globulus*, la sequía prolongada reduce el diámetro y número de los nuevos vasos, lo que disminuye la k_h y, eventualmente, la g_s y la fijación de carbono por unidad de área foliar. En los híbridos *E. grandis* × *camaldulensis* y *E. grandis* × *urophylla* se observó que la k_h máxima y la vulnerabilidad a la cavitación no presentan variaciones entre sitios con distinta condición hídrica, aunque sí dependen del genotipo, lo que determina su respuesta diferencial al déficit hídrico (Vander Willigen y Pammenter, 1998).

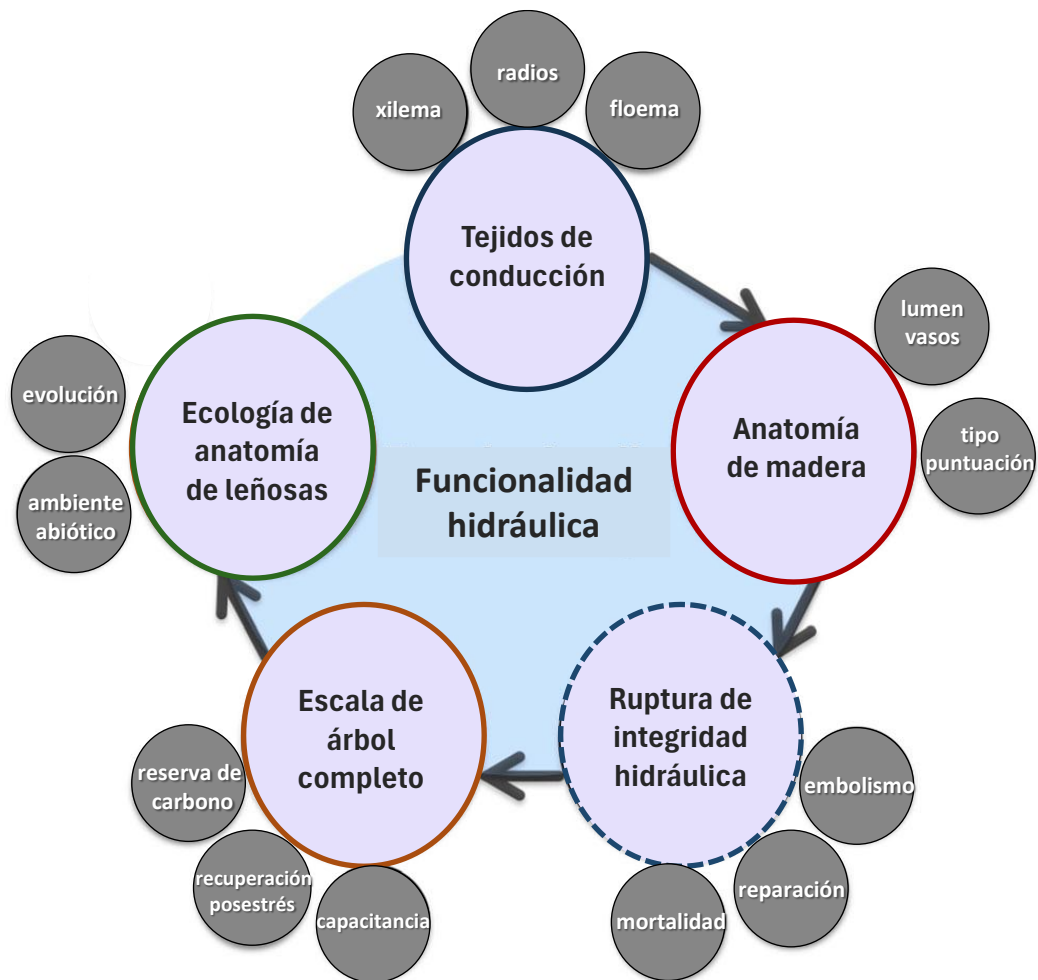
Otras respuestas plásticas frente a la sequía incluyen modificaciones en la relación de Huber (área foliar / área de xilema activo) y en el área foliar específica (AFE, área de lámina / peso seco de lámina). Si bien ambas relaciones disminuyen en condiciones de estrés, existe una gran variación genotípica en la respuesta, particularmente en especies como *E. globulus* (Pita y Pardos, 2001). Asimismo, el estrés hídrico reduce la densidad y frecuencia estomáticas, aunque la evidencia para varios híbridos —como *E. grandis* × *camaldulensis*— no es concluyente (Eksteen et al., 2013).

En este contexto, resulta relevante analizar las relaciones entre el intercambio gaseoso y variables hídrico-funcionales, analizando los efectos de distintos factores —intrínsecos y extrínsecos— sobre la funcionalidad e integridad hidráulica en condiciones de déficit hídrico. Así, será posible identificar mecanismos de respuesta a la sequía en clones de interés silvícola y, al mismo tiempo, podrá conocerse el impacto potencial sobre la economía del agua y del carbono a diferentes escalas (órgano, individuo, bosque) (figura 3). Este análisis es fundamental para contribuir a la

selección de genotipos con mayor capacidad de resiliencia, tratando de minimizar los compromisos con la productividad de los rodales.

Figura 3

Principales aspectos que afectan la funcionalidad hidráulica en árboles



Nota. Esquema conceptual que integra los principales aspectos (círculos de colores) que definen la funcionalidad hidráulica del árbol, abarcando múltiples escalas, desde las células (xilema y floema) y tejidos hasta el individuo. Los círculos más pequeños (grises) indican variables o procesos específicos que afectan la funcionalidad hidráulica en cada una de las escalas representadas. Modificado de Pfautsch (2016).

1.7.4. Antecedentes nacionales

En Uruguay, aunque ya se habían realizado estudios de fisiología vegetal en rodales comerciales, los primeros trabajos integrados de ecofisiología —incluyendo relaciones hídricas, fotosíntesis y área foliar— se iniciaron en 2008 en plantaciones de *Pinus taeda* (Gándara, 2013). En ellos se evaluó el impacto del manejo silvícola sobre parámetros hídricos y fotosintéticos, área foliar y crecimiento de árboles sometidos a poda y raleo en sitios contrastantes (Gándara et al., 2014). Se obtuvieron modelos que relacionan potencial hídrico, crecimiento e índice de área foliar del rodal. Los trabajos se enmarcaron en un estudio de cuencas pareadas establecidos en Tacuarembó por la North Carolina State University y la empresa forestal Lumin (ex Weyerhaeuser Uruguay), cuyo objetivo principal fue analizar el efecto de la forestación sobre los pastizales nativos, estimando la evapotranspiración en ambos sistemas y evaluando diferencias en las propiedades físicas y químicas de suelo (Amatya et al., 2014; Cano et al., 2023; Skaggs et al., 2008). Luego, se desarrollaron una serie de trabajos en el Departamento de Biología Vegetal de la Facultad de Agronomía de la Universidad de la República (Udelar), en los cuales se estudió el impacto del manejo silvícola sobre el estado hídrico y la eficiencia en el uso del agua en plantaciones de pinos (Pechi y Ramírez, 2012) y eucaliptos (Dellacassa y Figarola, 2016; Dellepiane, 2023).

Por otro lado, se evaluó el efecto del déficit hídrico en *Eucalyptus* en condiciones de crecimiento controladas (invernáculo). Se utilizaron clones comerciales de *E. grandis* y *E. grandis* × *camaldulensis* y *E. grandis* × *tereticornis*. Se caracterizó la actividad fotosintética —fases bioquímica y fotoquímica— y el consumo de agua de las plantas, donde se destacó el desempeño fotosintético y la notable capacidad de disipación de energía bajo estrés del clon de *E. grandis* × *tereticornis* (Nión et al., 2024). Más adelante, en distintos trabajos del Departamento Forestal de la Facultad de Agronomía (Udelar), se midieron variables ambientales asociadas a sistemas silvopastoriles con *E. grandis*, como la radiación fotosintéticamente activa, el índice de área foliar y el contenido de humedad del suelo, a través de observaciones a campo complementadas con análisis de la estructura arbórea mediante teledetección (Dogliotti et al., 2023; González-Tálice y Dogliotti, 2024).

2. Similares pero contrastantes: respuesta fisiológica a la sequía y crecimiento en especies puras y clones híbridos interespecíficos de *Eucalyptus*

2.1. Resumen

Mensaje clave: *Eucalyptus grandis* e híbridos con eucaliptos colorados y con *E. urophylla* presentan diferentes estrategias frente a la sequía en el largo plazo, con implicancias en la regulación estomática, la hidráulica de la planta y el crecimiento.

Resumen: Las especies de eucalipto son importantes en la silvicultura comercial debido a su rápido crecimiento y gran adaptabilidad. Sin embargo, en el contexto actual de cambio climático, es fundamental evaluar la respuesta a la sequía de diferentes genotipos para mejorar la resiliencia y la productividad. El mejoramiento genético a menudo implica el cruzamiento de especies de rápido crecimiento y alta calidad con especies tolerantes a la sequía. Para optimizar la gestión forestal, resulta esencial comprender las ventajas y desventajas de las especies puras y de los híbridos. Este estudio examinó las respuestas fisiológicas y de crecimiento a la restricción hídrica (RH) de los clones de *E. grandis* (GG), *E. grandis* × *E. camaldulensis* (GC), *E. grandis* × *E. tereticornis* (GT) y *E. grandis* × *E. urophylla* (GU1 y GU2) en la etapa de plántulas durante dos ciclos de sequía. Las mediciones incluyeron el potencial hídrico foliar (Ψ), el contenido relativo de agua (RWC), la conductancia estomática (g_s), curvas de presión-volumen, conductividad hidráulica (k_s , k_L), el porcentaje de pérdida de conductividad hidráulica (PLC), el área foliar específica (AFE) y el contenido de clorofila en hojas. Los resultados revelaron diferentes estrategias de respuesta a la sequía entre los clones. Los híbridos GC y GT fueron más consumidores de agua, presentando un alto PLC (>80 %) debido al cierre estomático limitado. Además, mostraron mayor contenido de clorofila lo cual maximizó la ganancia de carbono y el crecimiento en condiciones de sequía. GC presentó ajuste elástico y osmótico, mientras que GT solo mostró ajuste elástico. GG fue el clon más sensible a la sequía, debido a un fuerte control estomático, ajuste osmótico y baja cavitación, lo que limitó la asimilación de carbono y provocó la mayor reducción del crecimiento. Los híbridos GU compartieron similitudes fisiológicas con GG, pero mostraron respuestas de crecimiento variables a WR. Estos hallazgos sugieren que algunos clones

híbridos podrían superar a *E. grandis* puro bajo WR, con una variación genotípica significativa incluso entre híbridos que comparten especies parentales similares.

Palabras clave: intercambio gaseoso · conductividad hidráulica · resistencia al estrés · embolismo



Similar but unique: physiological response to drought and growth of pure species and interspecific hybrid clones of *Eucalyptus*

José Gándara¹ · Matías Nión¹ · Jaime González-Tálice¹ · Silvia Ross¹ · Juan Villar¹ · María Elena Fernández^{2,3}

Received: 2 August 2024 / Revised: 24 January 2025 / Accepted: 27 January 2025
© The Author(s), under exclusive licence to Springer-Verlag GmbH Germany, part of Springer Nature 2025

Abstract

Key message *Eucalyptus grandis* and hybrids with red gums and *E. urophylla* exhibit different strategies to deal with long-term drought, involving differences in stomatal regulation, plant hydraulics, and growth.

Abstract *Eucalyptus* species are important in commercial forestry for their rapid growth and adaptability. In the context of climate change, evaluating the drought responses of different genotypes is critical for enhancing resilience and productivity. Genetic improvement often involves crossing fast-growing, high-quality species with drought-tolerant ones. Understanding trade-offs in pure species and hybrids is essential for optimizing forest management. This study examined physiologic and growth responses to water restriction (WR) of *E. grandis* (GG), *E. grandis* × *E. camaldulensis* (GC), *E. grandis* × *E. tereticornis* (GT), and *E. grandis* × *E. urophylla* (GU1 and GU2) clones at the sapling stage across two drought cycles. Measurements included leaf-water potential (Ψ), relative water content (RWC), stomatal conductance (g_s), pressure–volume traits, hydraulic conductivities (k_s , k_L), percentage loss of hydraulic conductivity (PLC), specific leaf area (SLA), and chlorophyll content. Results revealed different drought response strategies among clones. GC and GT hybrids were more “water spenders”, exhibiting high PLC (> 80%) due to limited stomatal closure, along with higher chlorophyll levels that maximized carbon gain and growth under drought. GC exhibited both elastic and osmotic adjustment, while GT showed only elastic adjustment. GG was the most drought-sensitive clone, relying on strong stomatal control, osmotic adjustment, and low cavitation, which limited carbon assimilation and resulted in the greatest growth reduction. GU hybrids shared physiologic similarities with GG but showed varying growth responses to WR. These findings suggest some hybrid clones may outperform pure *E. grandis* under WR, with significant genotype variation even among hybrids sharing similar parental species.

Keywords Leaf gas exchange · Hydraulic conductivity · Stress resistance · Xylem embolism

Introduction

Eucalyptus is a globally important genus for planted forests, with over 22-million ha cultivated across more than 95 countries (Zhang and Wang 2021). Of its more than 700 species, only a few are widely used in intensively managed plantations. These have undergone genetic selection and improvement to enhance traits that boost profitability and industrial value. Among them, *E. grandis* is known for its high productivity and valuable wood properties. However, its sensitivity to low temperatures and increased drought conditions (Fernández et al. 2019) across many cultivation regions (IPCC 2023) has driven efforts to enhance abiotic stress tolerance through breeding programs. A main strategy involves hybridizing *E. grandis* with species that are more resistant to abiotic stress, such as red gums (*E. camaldulensis*, *E. tereticornis*) and white gum (*E. urophylla*).

Communicated by V. Resco de Dios.

✉ José Gándara
jgandara@fagro.edu.uy

¹ Departamento de Biología Vegetal, Facultad de Agronomía, Universidad de La República, Av. Eugenio Garzón 780, 12900 Montevideo, Uruguay

² CONICET, Consejo Nacional de Investigaciones Científicas y Técnicas, Buenos Aires, Argentina

³ INTA, Instituto Nacional de Tecnología Agropecuaria, Ecología Forestal, UEDD INTA-CONICET IPADS, Tandil, Argentina

Published online: 03 March 2025

Springer

These hybrids may retain desirable traits like rapid growth and wood quality, while improving adaptability to climate-induced stresses (Janes and Hamilton 2017).

Plants adopt various strategies for drought resistance, including delaying dehydration (avoidant species) or sustaining function during water scarcity (tolerant species) (Levitt 1980; Lambers et al. 2008). Drought avoidance traits include strong stomatal control influenced by water potential (Ψ), extensive root systems, and high hydraulic conductance (K). Increased K can be achieved by a low leaf area to xylem area ratio or by high tissue hydraulic conductivity (k_H), both increasing carbon gain per unit leaf area (Eamus et al. 2000). Drought tolerance, in turn, depends largely on osmotic and elastic adjustments that maintain cell turgor under water deficit, influencing the turgor loss point (TLP)—the leaf-water potential at which turgor pressure reaches zero. This parameter serves as a key indicator of drought tolerance (Zhu et al. 2018). In this context, some species exhibit both a lower osmotic potential at full turgor ($\Psi\pi$) and an increased modulus of elasticity (ϵ), allowing them to maintain turgor as Ψ declines. In contrast, other species reduce ϵ to delay turgor loss at lower leaf-water content (RWC) without osmotic adjustment (Kozlowsky and Palardy 2002). Both strategies help maintain protoplast volume, thereby extending stomatal opening and photosynthesis during drought (Meinzer et al. 2014). Moreover, variations in ϵ are influenced by factors such as leaf age (Saito and Terashima 2004) and genotype (Leuschner et al. 2019), adding complexity to drought responses. These drought tolerance traits at leaf level are often linked to lower vulnerability to xylem cavitation (Pfautsch 2018), reinforced xylem cell walls and increased wood density of woody organs (Meinzer and McCulloh 2013).

Eucalyptus species exhibit adaptations to prevent turgor loss and dehydration, primarily through stomatal regulation and adjustments in osmotic and elastic tissue properties (White et al. 2000; Whitehead and Beadle 2004; Zhang et al. 2015). Elastic adjustment, involving shifts in the cell wall's elasticity, can either increase or decrease as an adaptive response (Schulte 1992; Leuschner et al. 2019). Stiffer walls (high ϵ) create a water potential gradient that facilitates water uptake in dry soils with minimal changes in relative water content (RWC). While high ϵ aligns generally with stronger stomatal control (White et al. 2000; Lenz et al. 2006), it has been also observed in *E. camaldulensis*, a species with relatively weak stomatal regulation (White 2000). The capacity for osmotic adjustment is also particularly relevant in the adaptation of eucalypts to drought, being strongly genotype-dependent (Pita and Pardos 2001; Lemcoff et al. 2002). Osmotic adjustment in *E. camaldulensis* and *E. globulus* occurs through the accumulation of solutes such as sugars, cyclitols, and proline to retain water (Souden et al. 2020; Guarnaschelli et al. 2003). On the other hand, drought impacts leaf-level photosynthesis

in several ways, including reducing chlorophyll content due to increased degradation or slowed biosynthesis (Xue 2011). Yet, some species like *E. grandis* (Silva et al. 2017), hybrids with *E. tereticornis* (Nión et al. 2024), and with *E. robusta* (Michelozzi et al. 1995), show increased chlorophyll content in response to drought.

Regarding hydraulic traits, eucalypts exhibit distinctive wood characteristics with different functional consequences in terms of drought adaptability. For example, *E. grandis* is more susceptible to cavitation than *E. camaldulensis* (Fernández et al. 2019; Barotto et al. 2016), yet it shows stronger stomatal control, as evidenced by a rapid decrease in stomatal conductance (g_s) as water potential drops (Bournè et al. 2015). Wood anatomy and density suggest that *E. grandis* follows an avoidance strategy, whereas *E. camaldulensis* employs a more drought-tolerant strategy (Monteoliva et al. 2015; Fernández et al. 2019; Barigah et al. 2021). A seminal study about vulnerability to cavitation in *Eucalyptus* demonstrated that interspecific hybrids (*E. grandis* × *camaldulensis* and *E. grandis* × *urophylla*) exhibited significantly lower vulnerability to cavitation than the pure species *E. grandis*. However, overall, all taxa studied showed high vulnerability to cavitation (substantially higher than *E. camaldulensis* reported in other studies), with values characteristic of drought avoidant species (Vander Willigen and Pammenter 1998).

As exposed above, *Eucalyptus* taxa demonstrate diverse drought-resistance mechanisms, from avoidance to tolerance, making it difficult to predict traits in hybrids coming from the combination of parental species with contrasting strategies. Moreover, as genetic improvement prioritizes fast-growing species, it is essential to evaluate potential trade-offs between drought resistance and growth potential in hybrids. This study aimed to analyze the effects of medium-term water restriction (over an entire growing season) on leaf-water status, plant hydraulics, and growth in six-month old plantlets of *E. grandis* and its hybrids with *E. camaldulensis* and *E. tereticornis* (red gums) and *E. urophylla* (white gum). We hypothesized that hybrids with red gum species would outperform *E. grandis* under drought due to the higher drought resistance of the parental pure species, while hybrids with white gum (*E. urophylla*) would show intermediate responses. We also hypothesized a correlation between the type of drought resistance strategy (avoidance vs. tolerance) and growth under stress, resulting in a more marked decrease in growth in avoidant taxa than in drought-tolerant ones.

Materials and methods

Plant material and culture conditions

The study was conducted using commercial clonal materials typically used in forest plantations in Uruguay,

South-America. *Eucalyptus* is the most widely planted genus in this country, covering 1 million hectare (MGAP 2022), and supporting a well-developed paper industry. The experiment took place in a greenhouse at the Plant Biology Department of Centro Universitario de Tacuarembó, Uruguay (31.73° S; 55.97° W). Ahead of the experiment, rooted cuttings of *Eucalyptus grandis* (GG), *E. grandis* × *camaldulensis* (GC), *E. grandis* × *E. tereticornis* (GT), and *E. grandis* × *E. urophylla* (GU1 and GU2) were grown for 5 months in a clonal nursery (Lumin forestry company) in 120 cm³ tubes filled with inert substrate, maintained at 20–22 °C and 90–95% of relative humidity. The plantlets were periodically watered with a Biorend® solution (10 cm³ L⁻¹) until transplantation into 3 L pots containing Carolina Soils® substrate (58% peat, 40% vermiculite, 1.5% dolomitic limestone, and 0.5% trace minerals). At 6 months of age, the plantlets were put in 18-L plastic pots filled with Carolina Soils® substrate and moved to a greenhouse in Tacuarembó, to acclimate them to the environmental conditions where the experiment was conducted.

Experimental design

Two drought-stress cycles were imposed from 29 October 2019 (austral spring) to 22 March 2020 (early fall), each lasting 60 days, with a 15-day recovery phase in-between. A split-plot design was applied using six plants per clone of each treatment (totaling 60 plants), with the water regime (well-watered (WW) or water-restricted (WR) plants) being the main plot and the clone (GG, GC, GT, GU1, and GU2) representing the subplot. Plants were organized in four rows of 15 individuals. An automatic drip irrigation system operated twice daily for 15-min intervals, at 6:30 am and 7:30 pm. Each pot was fitted with two drip emitters placed opposite to each other at a depth of 5 cm, each delivering a flow rate of 8 mL per 15 min. Half of the plants received a water volume (mL) sufficient to offset losses due to evapotranspiration and were classified as well-watered (WW) plants. The remaining half, designated as WR plants, received 30% of the volume supplied to the WW plants. This reduced water dose had been previously shown to induce drought stress in these clones. In all cases, water loss was measured by the gravimetric method. During the recovery phase -the interval between drought-stress cycles- all plants received the same amount of water as the WW plants. Substrate water content (θ ; %, w/w) was monitored biweekly using a TDR equipment (Decagon®, Pullman, WA), averaging 36.1% in WW and 9.7% in WR plants over both cycles (see below for further methodological details on these measurements).

Plant measurements

Six-month-old plants, grown as described above, were used in this experiment. The study examined the impact of water availability on plant water status, functional parameters, plant hydraulics, and growth. RWC, stomatal conductance, and water potential were assessed over two consecutive days at the beginning and end of each drought cycle. Pressure–volume (P–V) curves were constructed at the end of each cycle to calculate functional parameters. Shoot hydraulic conductivity, specific leaf area, plant leaf area, leaf chlorophyll content, and plant size (to estimate growth through the comparison with initial size) were measured at the end of the study period (i.e., at the end of the second drought cycle).

Leaf relative water content

Leaf RWC was evaluated biweekly in all experimental plants. Two freshly collected disks (2.49 cm²) were taken from two opposite leaves per plant, weighed to obtain the fresh weight (FW, mg), and placed in 1.5 mL Eppendorf tubes containing distilled water for 72 h. Daily weight measurements were taken until a stable value was obtained (TW). Then, disks were dried at 60 °C for 48 h, and dry weight was measured (DW). RWC (%) was calculated as $RWC = [(FW - DW)/(TW - DW)]100$

Stomatal conductance

Stomatal conductance to water vapor (g_s , mmol m⁻² s⁻¹) was assessed with a steady-state diffusion leaf porometer (Model SC-1 Decagon Devices®, Pullman, WA) on three randomly selected plants per clone and treatment. Measurements were taken between 8:00 and 10:00 a.m. on the abaxial surface of three subapical, healthy, fully expanded, and illuminated leaves.

Leaf-water potential

Bulk leaf-water potential was recorded on four randomly selected plants per clone and treatment in two daily time intervals -pre-dawn and midday- to capture daily maximum and minimum values, respectively. Measurements were taken between 4:30 and 5:30 a.m. (Ψ_{pd} , MPa) and between 12:00 and 2:00 p.m. (Ψ_{md} , MPa) using a pressure chamber (M3005 Soil and Moisture®, Santa Barbara, CA) on subapical shoots. Each shoot had an equal number of fully expanded and illuminated leaves. Diurnal fluctuation of Ψ ($\Delta\Psi$, MPa) was calculated as $\Delta\Psi = \Psi_{pd} - \Psi_{md}$.

Pressure–volume curves and leaf hydric parameters

Measurements were performed at the end of each drought cycle on four randomly selected plants per clone and treatment (totaling 40 plants). A branch, approximately 15 cm in length (comprising six leaves with very short petioles), was excised from the main stem and rehydrated in the dark for 3 h in glasses containing distilled water and covered with plastic bags. To construct pressure–volume curves, the pressurization method (Hinckley et al. 1980) was applied by releasing water from the cut end of the branch in intervals of 0.2 MPa. Each branch underwent ten measurements, with pressure increasing until it reached 2 MPa, using a Schölander-type chamber (M3005; Soil and Moisture[®], Santa Barbara, CA). Water expelled was collected onto filter paper and weighed (± 0.1 mg) using an analytical balance (MT42022, Shimadzu[®]). P–V curves were then constructed for each branch, and the following functional parameters were calculated: elasticity modulus of the cell wall (E , MPa), the osmotic potential at saturation ($\Psi\pi_{\text{sat}}$, MPa), and the water potential at incipient plasmolysis (Ψ_{ILP} , MPa).

Shoot hydraulic conductivity

Hydraulic conductivity (k_{H}) was measured in all 60 plants at the end of the second drought-stress cycle. To minimize cavitation during the sampling prior to the conductivity measurements, the plants were watered the evening before sampling. Previous studies on *E. camaldulensis* indicate that the cavitated vessels are not repaired in the short term, even when the plant exhibits a high (near-zero) water potential (Barigah et al. 2021). By irrigating plants prior to sampling, we reduce xylem tension, enabling the measurement of the percent loss of conductivity resulting from prior cavitation (i.e., cavitation that occurred during the experimental period). The following morning, between 7:00 and 9:30 a.m., a subapical shoot segment 5–8 cm long was excised from each plant and defoliated under distilled water. The segments were cut 30 cm from the shoot apex, and perpendicular diameters (mm) were measured at both the proximal and distal ends. The time taken (s) to pass 0.4 mL of distilled water through each segment was measured using a conductivity meter designed according to “the pipette method” (Sperry et al. 2002). The first measurement was recorded without embolism removal (k_{H}), while the second (k_{Hmax}) was performed after perfusing distilled water under pressure (0.1 MPa) using a 60 mL syringe. Values were recorded after obtaining three consecutive stable measurements. Percentage loss of hydraulic conductivity (PLC) was calculated as $\text{PLC} = [1 - k_{\text{H}}/k_{\text{Hmax}}]$. Specific hydraulic conductivity (k_{S} , k_{Smax}) was determined by standardizing k_{H} by the cross-sectional area of each segment. Leaf-specific hydraulic conductivity (k_{L} , k_{Lmax}) was calculated by normalizing k_{H} by

the leaf area of each segment (LA_{S} , m^2), where LA_{S} was calculated as $LA_{\text{S}} = \text{SLA} \times \text{DW}_{\text{b}}$. Here, SLA represents the specific leaf area (methodological details provided in the next section), and DW_{b} is the segment’s foliage DW. Hydraulic conductivity ($\text{kg s}^{-1} \text{m MPa}^{-1}$) was calculated as $k_{\text{H}} = Q \times L / \Delta P$, where Q represents the water flow per unit time (0.0004 kg s^{-1}), L represents length of the segment (m), and $\Delta P = 0.01$ MPa (determined by a water column of 1 m above the sample).

Plant leaf area and specific leaf area

After measuring hydraulic conductivity, 20 leaf discs (1.71 cm^2 each) were randomly collected from various parts of each plant. These discs were dried at 60 °C for 72 h to obtain the dry weight of each disc (DW_{d}). Subsequently, all leaves were completely removed from each plant, dried at 60 °C for 72 h, and weighed to quantify the total dry leaf mass (DW_{t}). The specific leaf area (SLA , $\text{cm}^2 \text{g}^{-1}$) was calculated as $\text{SLA} = 1.71 / \text{DW}_{\text{d}}$. Total plant leaf area (LA , cm^2) was calculated as $LA = \text{SLA} \times \text{DW}_{\text{t}}$.

Leaf chlorophyll content

Relative chlorophyll content (SPAD index) was assessed using a SPAD-502[®] chlorophyll meter, which measures leaf absorbance within the near-red (650 nm) and infrared (940 nm) wavelength ranges. Measurements were taken on the adaxial surfaces of four subapical, healthy, and fully mature leaves from three plants per clone and treatment at the end of the second drought cycle.

Plant growth

Plant height (H_{t} , cm) and ground-level stem diameter (Φ , mm) of all 60 plants were measured at the beginning and end of each drought cycle using a millimeter tape and a digital caliper. Relative growth (RG, %) was estimated as the relative increment in H_{t} and Φ between the beginning of the experiment and the end of the second cycle, as follows: $\text{RG} = [(G_{\text{n}} - G_{\text{n-1}}) / (G_{\text{n-1}})] 100$, where G represents the plant height (H_{t}) or diameter (Φ).

Meteorological variables and soil water content

Air temperature (T , °C) and relative humidity (HR, %) were automatically logged every 15 min at a height of 1 m using an RHT10 sensor (EXTECH[®] Instruments). The air vapor pressure deficit (Vpd) was calculated according to Allen et al. (1998), with an average of 1.51 kPa in the morning (8:00 to 10:00 a.m.) and 4.21 kPa at midday (12:00 to 2:00 p.m.) during the study period. Substrate volumetric water content (θ ; % Vol) was recorded biweekly in 30 randomly

selected pots using a time-domain reflectometer (GS1 ruggedized sensor, Decagon®, Pullman, WA). Two measurements were taken at opposing positions within each pot at a depth of 10 cm.

Statistical analysis

A split-plot design was employed, with the irrigation treatment as the main plot factor and clone as the subplot factor. The analysis focused on specific clones and treatment levels rather than on broader populations of inference, making fixed effects appropriate for examining clone \times treatment \times block interactions within a controlled setting (Steel and Torrie 1980). A two-way ANOVA was performed for each measured variable to analyze treatment effects and the clone \times treatment interaction within each drought-stress cycle. Data were verified for normality using the Shapiro–Wilk test. Analyses were conducted using InfoStat® software (UNC, Córdoba, Argentina), and mean comparisons were performed by Tukey's test ($p < 0.05$). The model analyzed was as follows:

$$Y_{ijk} = \mu + \alpha_i + \beta_j + \gamma_k + (\alpha\beta)_{ij} + (\alpha\gamma)_{ik} + (\alpha\beta\gamma)_{ijk} + \varepsilon_{ijk}$$

where, Y_{ijk} : response variable, μ : overall mean of the model, α_i : effect of the i^{th} genotype (GG, GC, GT, GU1, GU2), β_j : effect of the j^{th} treatment (WW and WR), γ_k : the effect of the k^{th} block (irrigation row, 1 to 4), $(\alpha\beta)_{ij}$: interaction between the i^{th} level of α and the j^{th} level of β , $(\alpha\gamma)_{ik}$: interaction between the i^{th} level of α and the k^{th} level of γ , $(\beta\gamma)_{jk}$: interaction between the j^{th} level of β and the k^{th} level of γ , $(\alpha\beta\gamma)_{ijk}$: interaction between the i^{th} level of α , the j^{th} level of β , and the k^{th} level of γ , ε_{ijk} : experimental error with $\varepsilon_{ij} \sim N(0, \sigma^2\varepsilon)$.

Multivariate analysis was carried out by means of Principal Component Analysis (PCA) with the FactoMineR package (Husson et al. 2007) to assess grouping of clones based on their functional response to the water regime treatments. Correlation between traits (Pearson's R) and associated p -values are also reported.

Results

Plant water status

Water restriction (WR) reduced RWC by 12% ($p = 0.0295$), with WW plants maintaining $81 \pm 1\%$ compared to $69 \pm 1\%$ in WR plants. The RWC decreased slightly but significantly between cycles (75% in the first cycle vs. $71 \pm 1\%$ in the second one), a trend consistent across biweekly measurements. No significant clonal differences in RWC were observed ($p = 0.080$).

Predawn leaf-water potential (Ψ_{pd}) was significantly influenced by the water availability treatment and the drought cycle ($p < 0.0001$). Mean Ψ_{pd} was 37% lower in the first cycle ($\Psi_{pd} = -0.58 \pm 0.03$ MPa) than in the second one ($\Psi_{pd} = -0.37 \pm 0.03$ MPa). On average, WR plants exhibited a 38% reduction in Ψ_{pd} throughout the experiment. During the second cycle, Ψ_{pd} declined further in red gum hybrids (GC and GT), with a twofold decrease in GT (Fig. 1a).

Midday leaf-water potential (Ψ_{md}) also varied significantly among clones, water regimes, and cycles ($p < 0.0001$), with the lowest mean Ψ_{md} observed in the second cycle, 13% lower than in the first drought period (mean value across all the clones: -1.83 ± 0.06 MPa). The WR treatment reduced Ψ_{md} by 23% on average, with red gum hybrids declining 27%, especially GT ($\Psi_{md} < -2.0$ MPa) in comparison with their well-irrigated counterparts. The GG clone exhibited the highest mean Ψ_{md} ($\Psi_{md} > -1.55$ MPa), followed by the GU hybrids, with no clonal differences under WW conditions (Fig. 1b).

Diurnal fluctuation in Ψ ($\Delta\Psi$) differed significantly by clone, cycle, and water regimes ($p < 0.01$). The GT clone exhibited the highest $\Delta\Psi$ (1.26 ± 0.07 MPa), while the GG clone had the lowest (0.89 ± 0.07 MPa). Under WR, the GC and GT clones showed a 35% increase in $\Delta\Psi$ in the first cycle, with the GT clone maintaining this trend in the second cycle, too. GU clones exhibited reduced $\Delta\Psi$ under drought, while the GG clone was unaffected compared to WW conditions ($p = 0.0064$) (Fig. 1c).

Stomatal conductance (g_s)

Stomatal conductance (g_s) varied significantly with water regime ($p < 0.0001$), clone ($p < 0.0001$), and their interaction ($p = 0.0296$). The GC clone exhibited the highest mean g_s (607 ± 30 mmol m $^{-2}$ s $^{-1}$), followed by GT (477 ± 27 mmol m $^{-2}$ s $^{-1}$), with both clones maintaining elevated g_s across water regimes. Under WR conditions, the GC clone achieved the highest g_s (432 ± 32 mmol m $^{-2}$ s $^{-1}$), whereas the GU1 clone showed the lowest values (286 ± 28 mmol m $^{-2}$ s $^{-1}$). The GG and GU2 clones displayed intermediate g_s levels. On average, water restriction reduced g_s by 60%, with reductions of up to 70% observed in the GG and GU1 clones (Table 1).

Leaf stomatal conductance exhibited a moderate-to-strong positive correlation with Ψ_{pd} in GT ($R = 0.74$, $p = 0.03$) and GC ($R = 0.56$, $p = 0.02$) hybrids. Regression models revealed that Ψ_{pd} explained a greater proportion of g_s variance in red gum hybrids, as denoted by the highest R^2 values. In contrast, this relationship was weaker in the other clones, with an average $R^2 = 0.25$ ($p < 0.05$) across treatments, and even lower R^2 under WR than WW conditions. Notably, the slope of the Ψ_{pd} - g_s relationship became negative under WR in *E. grandis* (GG) and *E. grandis* \times *E. urophylla* hybrids (Fig. 2).

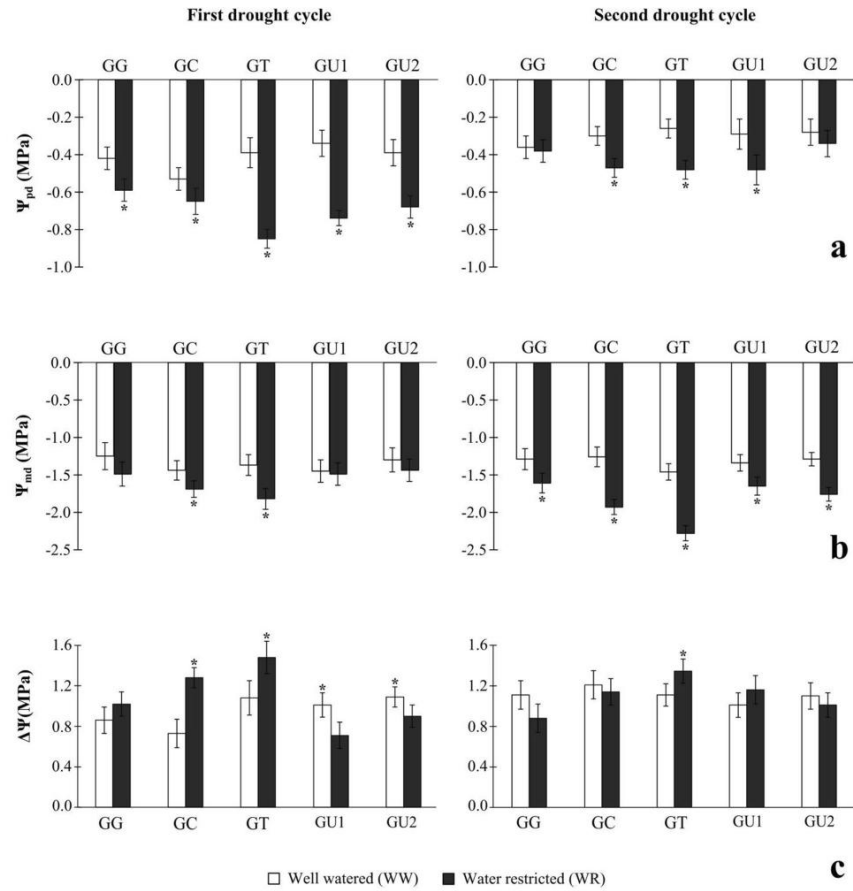


Fig. 1 **a** Mean predawn leaf water potential (Ψ_{pd} , MPa), **b** Midday leaf-water potential (Ψ_{md} , MPa), **c** Diurnal fluctuation in leaf-water potential ($\Delta\Psi$, MPa) for *E. grandis* (GG), *E. grandis* × *E. camaldulensis* (GC), *E. grandis* × *E. tereticornis* (GT), and *E. grandis* × *E. wro-*

phylla (GU1 and GU2) clones under well-watered (WW) and water-restricted (WR) conditions during the first and the second drought cycles. Asterisks indicate significant differences ($p < 0.05$) between WW and WR within each clone and cycle

Pressure–volume curve parameters

Across all the studied clones, the modulus of elasticity (ϵ) of leaf tissue was significantly higher in the first drought cycle than in the second cycle ($\epsilon = 8.59 \pm 0.76$ MPa and 4.81 ± 0.76 MPa, respectively, $p = 0.0005$). Under WW conditions, the GT clone exhibited the highest ϵ (16.74 ± 1.97 MPa, $p = 0.015$), which was twice as high

as that of the other clones. This clone was also the one that exhibited the greatest reduction in ϵ under WR conditions, decreasing by 45% during the first drought cycle, ($p = 0.0187$). In the second cycle, however, WR decreased ϵ only in the GC clone, with even a steeper reduction (75%) than that observed in the GT clone in the first cycle (Table 2). Both red gums hybrids were those that displayed

Table 1 Mean stomatal conductance (g_s , $\text{mmol H}_2\text{O m}^{-2} \text{s}^{-1}$) for *E. grandis* (GG), *E. grandis*×*E. camaldulensis* (GC), *E. grandis*×*E. tereticornis* (GT) and *E. grandis*×*E. urophylla* (GU1 and GU2) clones under well-watered (WW) and water-restricted (WR) regimes

	Stomatal conductance (g_s) ($\text{mmol H}_2\text{O m}^{-2} \text{s}^{-1}$)	
	WW	WR
GG	564.52 ± 29.26b	197.10 ± 25.99bc
GC	709.45 ± 28.01a	432.52 ± 32.58a
GT	698.54 ± 29.26a	289.69 ± 23.91b
GU1	489.66 ± 32.35b	145.08 ± 23.91c
GU2	503.11 ± 24.52b	227.25 ± 23.91bc

Data are presented as mean ± SE of multiple dates throughout the experiment. Different lowercase letters indicate significant differences between clones or treatments ($p < 0.05$)

a higher change in their cell wall elasticity, but in different periods of the experiment.

Across the evaluated clones, the osmotic potential at saturation ($\Psi\pi_{\text{sat}}$) averaged -1.04 ± 0.07 MPa, with no significant difference between drought cycles ($p = 0.0621$). The GC clone showed the highest mean $\Psi\pi_{\text{sat}}$ (-0.93 ± 0.10 MPa), while GU hybrids had the lowest (-1.25 ± 0.09 MPa, $p = 0.0217$). In the second cycle, GC exhibited the largest osmotic adjustment, as indicated by the high and significant difference in $\Psi\pi_{\text{sat}}$ between WW and WR plants (Table 2), showing also a high difference between Ψ_{TLP} and $\Psi\pi_{\text{sat}}$ (0.90 ± 0.07 MPa) in WR plants, corresponding to a 2.4-fold reduction in Ψ_{TLP} . Similarly, a significant decrease in Ψ_{TLP} was also observed in *E. grandis*, with reductions of 34% in

the first cycle ($p = 0.032$) and 19% during the second cycle ($p = 0.040$) (Table 2).

Plant hydraulics

Specific hydraulic conductivity (k_s) exhibited a significant clone × treatment interaction ($p = 0.0003$). On average, plants subjected to the WR treatment showed 44% lower k_s ($2.87 \pm 0.34 \text{ kg m}^{-1} \text{ MPa}^{-1}$) compared to WW plants ($k_s = 4.12 \pm 0.32 \text{ kg m}^{-1} \text{ MPa}^{-1}$). However, the red gum hybrids (GC, $p = 0.0110$; GT $p = 0.0013$) experienced a 73% reduction in k_s and PLC exceeding 80%, both of which were significantly higher in magnitude than those observed in the other clones. Moreover, *E. grandis* exhibited an increase in k_s under WR conditions ($p = 0.0162$) relative to control plants, attributed to a reduction in PLC (43%, $p = 0.0162$). In contrast, *E. urophylla* hybrids (GU1, $p = 0.6373$; GU2, $p = 0.4515$) showed no difference in k_s or PLC between water availability treatments. After embolism removal, $k_{s\text{max}}$ was unaffected by either water regime ($p = 0.0013$) or genotype ($p = 0.2332$), indicating that the observed k_s differences were due to the variation in native embolism among clones and drought treatments. As a result of cavitation, leaf-specific hydraulic conductivity (k_L) decreased by 75% in GC ($p = 0.088$) and GT ($p = 0.0096$) clones under WR, whereas no significant changes occurred in the other clones (Table 3). Furthermore, $k_{L\text{max}}$ did not differ significantly between clones or drought treatments (Table 3).

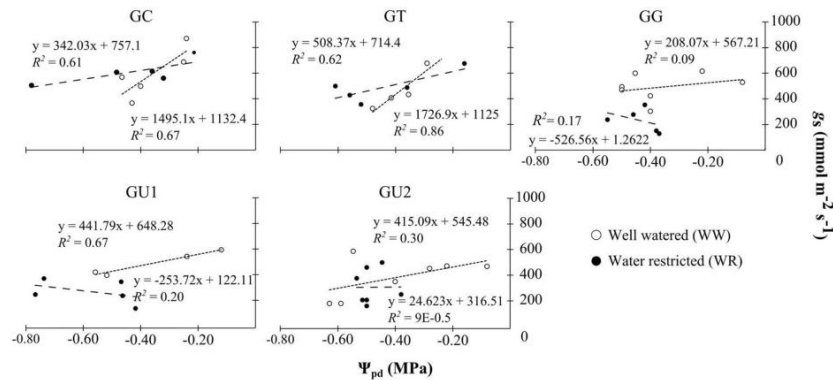


Fig. 2 Relationship between mean predawn water potential (Ψ_{pd} , MPa) and mean mid-morning leaf stomatal conductance (g_s , $\text{mmol H}_2\text{O m}^{-2} \text{s}^{-1}$) for *E. grandis* (GG), *E. grandis*×*E. camaldulensis* (GC), *E. grandis*×*E. tereticornis* (GT), and *E. grandis*×*E. urophylla* (GU1 and GU2) clones under well-watered (WW) and water-restricted

(WR) regimes. Each point represents the mean of three replicates (i.e., three plants); the different points correspond to measurements carried out on different dates across the study period. Each panel shows the response of each clone under both water regimes

Table 2 Mean modulus of elasticity (ϵ , MPa), osmotic potential at saturation ($\Psi_{\pi_{\text{sat}}}$, MPa), and water potential at turgor loss point (Ψ_{TLP} , MPa) for *E. grandis* (GG), *E. grandis* × *E. camaldulensis* (GC), *E. grandis* × *E. tereticornis* (GT) and *E. grandis* × *E. urophylla* (GU1 and GU2) clones under well-watered (WW) and water-restricted (WR) regimes during the first and the second drought cycles

	First drought cycle			Second drought cycle		
	ϵ (MPa)	Ψ_{TLP} (MPa)	$\Psi_{\pi_{\text{sat}}}$ (MPa)	ϵ (MPa)	Ψ_{TLP} (MPa)	$\Psi_{\pi_{\text{sat}}}$ (MPa)
GG						
WW	7.42 ± 2.42a	-1.22 ± 0.16a	-1.03 ± 0.09a	3.22 ± 0.56a	-1.24 ± 0.10a	-1.06 ± 0.05a
WR	10.73 ± 2.10a	-1.64 ± 0.18b	-1.09 ± 0.15a	3.30 ± 1.31a	-1.47 ± 0.07b	-1.22 ± 0.05b
GC						
WW	5.85 ± 1.19a	-0.96 ± 0.15a	-0.84 ± 0.09a	9.94 ± 1.31a	-1.51 ± 0.10a	-0.64 ± 0.07a
WR	6.74 ± 1.19a	-1.19 ± 0.21a	-0.94 ± 0.17a	2.54 ± 1.31b	-1.54 ± 0.07a	-1.29 ± 0.07b
GT						
WW	16.74 ± 1.97a	-0.98 ± 0.15a	-0.86 ± 0.09a	7.35 ± 2.76a	-1.27 ± 0.10a	-1.20 ± 0.08a
WR	8.39 ± 1.97b	-1.13 ± 0.21a	-1.05 ± 0.17a	5.05 ± 1.95a	-1.40 ± 0.07a	-1.14 ± 0.08a
GU1						
WW	6.63 ± 1.80a	-1.31 ± 0.19a	-0.96 ± 0.11a	4.24 ± 1.04a	-1.23 ± 0.10a	-1.13 ± 0.09a
WR	6.92 ± 1.47a	-1.23 ± 0.21a	-0.99 ± 0.17a	3.84 ± 1.04a	-1.36 ± 0.07a	-1.02 ± 0.09a
GU2						
WW	5.79 ± 2.65a	-1.32 ± 0.14a	-1.11 ± 0.09a	4.23 ± 1.13a	-1.18 ± 0.10a	-1.08 ± 0.09a
WR	6.28 ± 2.65a	-1.19 ± 0.14a	-1.08 ± 0.17a	3.84 ± 0.93a	-1.26 ± 0.10a	-1.06 ± 0.09a

Data are presented as mean ± SE. Different lowercase letters indicate significant differences between treatments within each clone and drought cycle ($p < 0.05$)

Table 3 Shoot specific hydraulic conductivity (k_s , $\text{kg s}^{-1} \text{m}^{-1} \text{MPa}^{-1}$), shoot leaf-specific hydraulic conductivity (k_l , $\text{kg s}^{-1} \text{m}^{-1} \text{MPa}^{-1}$), and percentage loss of hydraulic conductivity (PLC, %) after embolism removal for *E. grandis* (GG), *E. grandis* × *E. camaldulensis* (GC), *E. grandis* × *E. tereticornis* (GT) and *E. grandis* × *E. urophylla* (GU1 and GU2) clones under well-watered (WW) and water-restricted (WR) regimes at the end of the second drought cycle

	k_s ($\text{kg s}^{-1} \text{m}^{-1} \text{MPa}^{-1}$)	PLC (%)	k_l ($\text{kg s}^{-1} \text{m}^{-1} \text{MPa}^{-1}$)
GG			
WW	3.23 ± 0.74b	52.21 ± 6.91a	1.83 ± 0.39a
WR	5.27 ± 0.55a	29.88 ± 7.18b	1.70 ± 0.19a
GC			
WW	5.61 ± 0.80a	48.72 ± 7.46b	2.09 ± 0.42a
WR	1.02 ± 0.55b	84.18 ± 7.18a	0.59 ± 0.19b
GT			
WW	4.68 ± 0.80a	50.95 ± 7.46b	1.47 ± 0.42a
WR	0.98 ± 0.50b	87.54 ± 6.56a	0.40 ± 0.17b
GU1			
WW	3.45 ± 0.80a	49.29 ± 7.46a	0.91 ± 0.42a
WR	4.00 ± 0.55a	62.59 ± 7.18a	1.14 ± 0.19a
GU2			
WW	3.80 ± 0.80a	47.10 ± 7.46a	1.38 ± 0.42a
WR	3.24 ± 0.50a	55.94 ± 6.56a	1.22 ± 0.17a

Data are presented as mean ± SE. Different lowercase letters indicate significant differences between treatments within each clone ($p < 0.05$)

The percentage of hydraulic conductivity (PLC) and midday leaf-water potential (Ψ_{md}) exhibited a negative

Table 4 Correlation between the percentage loss of hydraulic conductivity (PLC, %) and midday leaf water potential (Ψ_{md} , MPa) for *E. grandis* (GG), *E. grandis* × *E. camaldulensis* (GC), *E. grandis* × *E. tereticornis* (GT), and *E. grandis* × *E. urophylla* (GU1 and GU2) clones at the end of the second drought cycle

	Correlation (Pearson's R)	* p -value
GG	0.20	0.65
GC	-0.60	0.11
GT	-0.42	0.30
GU1	-0.64	0.09
GU2	-0.60	0.17

relationship in all hybrids (GC, GT, GU1, and GU2), but a positive relationship in the *E. grandis* clone (GG). However, Pearson's correlation coefficient (R) indicated no statistical significance for any clone ($*p > 0.05$ in all cases), likely due to the limited sample size (Table 4).

Plant leaf area and specific leaf area

Plant leaf area decreased by 75% ($p < 0.0001$) under WR with no clonal effect ($p = 0.2248$, data not shown). Specific leaf area (SLA) varied among genotypes ($p = 0.0025$) and water regimes ($p < 0.0001$), with GU1 exhibiting the highest average SLA ($16.88 \pm 2.37 \text{ cm}^2 \text{ gr}^{-1}$) and red gum hybrids, the lowest SLA (11.29 ± 0.73 and $11.92 \pm 0.68 \text{ cm}^2 \text{ gr}^{-1}$, for GC and GT, respectively). SLA increased by 20% under the WR treatment in most of the genotypes, GC being the exception with no significant change in response to drought (Table 5).

Table 5 Specific leaf area (SLA, cm² g⁻¹) for *E. grandis* (GG), *E. grandis* × *E. camaldulensis* (GC), *E. grandis* × *E. tereticornis* (GT), and *E. grandis* × *E. urophylla* (GU1 and GU2) clones at the end of the second drought-stress cycle under well-watered (WW) and water-restricted (WR) regimes

		SLA (cm ² g ⁻¹)	
GG	WW	12.69 ± 1.17b	
	WR	15.17 ± 1.26a	
GC	WW	11.06 ± 0.93a	
	WR	12.58 ± 1.10a	
GT	WW	10.31 ± 0.96b	
	WR	13.54 ± 0.96a	
GU1	WW	12.82 ± 1.25b	
	WR	16.37 ± 1.25a	
GU2	WW	12.57 ± 1.04b	
	WR	16.87 ± 1.13a	

Data are presented as mean ± SE. Different lowercase letters indicate significant differences between treatments within each clone ($p < 0.05$)

Leaf chlorophyll content

Leaf chlorophyll content, assessed through the SPAD index, was higher ($p < 0.0001$) in GC (40.84 ± 1.12) and GT (38.76 ± 1.22) clones compared to *E. grandis* × *E. urophylla* hybrids, exceeding their index by 22%. The index significantly decreased ($p = 0.0010$) in WR plants of GU1 (28%), GU2 (31%), and GG (13%) clones, while GC and GT remained unaffected (Table 6).

Height and diameter relative increment

Relative height increment decreased by 40% in WR compared to WW plants ($p < 0.0001$), while the relative increment in basal diameter decreased by 21% under drought across all studied clones. However, there was a significant effect of the genotype on the magnitude of growth reduction in response to drought. Clones GG and GT exhibited the most significant growth reductions under WR ($p < 0.0001$),

Table 6 SPAD index at the end of the second drought-stress cycle for *E. grandis* (GG), *E. grandis* × *E. camaldulensis* (GC), *E. grandis* × *E. tereticornis* (GT), and *E. grandis* × *E. urophylla* (GU1 and GU2) clones under well-watered (WW) and water-restricted (WR) regimes

SPAD index	SPAD index	
	WW	WR
GG	37.07 ± 1.73a	32.43 ± 1.41b
GC	42.12 ± 2.42a	39.57 ± 1.71a
GT	40.19 ± 0.73a	37.34 ± 1.27a
GU1	38.26 ± 1.08a	27.73 ± 0.61b
GU2	34.67 ± 1.73a	23.95 ± 0.82b

Data are presented as mean ± SE. Different lowercase letters indicate significant differences between treatments within each clone ($p < 0.05$)

with GG exhibiting the lowest average height of all studied clones ($p = 0.04$). In contrast, the GC clone had the greatest final height ($p = 0.0238$). Notably, the GC clone maintained both height and diametric growth under WR (Table 7). Differences were observed between the *E. grandis* × *urophylla* clones in the response of relative height and diameter increment to drought: GU2 showed reductions in both height and diameter increments, while GU1 exhibited a decrease only in diameter increment (Table 7).

Multivariate analysis

The PCA indicated that the first two dimensions (Dim1 and Dim2) accounted for 50.68% of the total variance, with Dim 1 and Dim 2 explaining 27.9% and 22.8%, respectively. Including Dim 3 increased the explained variance to 64.83%. Leaf-water potential (Ψ_{pd} and Ψ_{md}) contributed most to Dim1 (0.60 and 0.56, respectively), followed by stomatal conductance (g_s , 0.46). Dim2 was primarily driven by the PLC (0.56), with smaller contributions from specific hydraulic conductance (k_s , 0.34), leaf-specific hydraulic conductance (k_l , 0.33), and the specific leaf area (SLA, 0.31) (Fig. 3a).

Although all the studied clones had a rather similar general physiologic behavior and growth under control (high water) conditions, PCA ordination revealed distinct physiologic responses among the clones under WR (Fig. 3b). Red

Table 7 Height and diameter relative increment (%) for *E. grandis* (GG), *E. grandis* × *E. camaldulensis* (GC), *E. grandis* × *E. tereticornis* (GT) and *E. grandis* × *E. urophylla* clones under well-watered (WW) and water restricted (WR) regimes

Clone	Relative increment (%)		
	Height (H _t)	Diameter (Φ)	
GG	WW	195.48 ± 38.51a	200.93 ± 18.16a
	WR	95.78 ± 38.51b	96.60 ± 18.16b
GC	WW	316.23 ± 47.31a	150.09 ± 40.38a
	WR	245.72 ± 47.31a	175.36 ± 40.38a
GT	WW	293.01 ± 20.73a	210.76 ± 20.55a
	WR	121.38 ± 20.73b	74.59 ± 20.55b
GU1	WW	208.91 ± 30.41a	195.35 ± 28.53a
	WR	182.30 ± 30.41a	132.20 ± 28.53b
GU2	WW	261.57 ± 32.31a	283.84 ± 32.91a
	WR	157.58 ± 32.35b	90.77 ± 32.91b

Data are expressed as mean ± SE measured at the end of the experiment. Different lowercase letters indicate significant differences between treatments ($p < 0.05$)

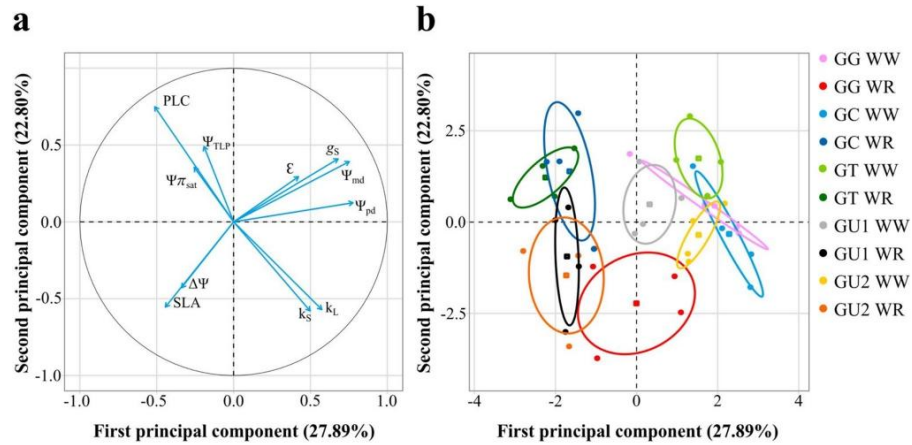


Fig. 3 **a** Principal component analysis of eleven physiological parameters: leaf predawn (Ψ_{pd}) and midday (Ψ_{md}) water potential, daily fluctuation of leaf water potential ($\Delta\Psi$), stomatal conductance (g_s), elasticity modulus (ϵ), osmotic potential at saturation ($\Psi_{\pi_{sat}}$), water potential at turgor loss point (Ψ_{TLP}), specific hydraulic conductivity (k_s), leaf-specific hydraulic conductivity (k_l), percentage loss of

hydraulic conductivity (PLC), and specific leaf area (SLA). **b** Confidence ellipses representing clone × treatment groups for *E. grandis* (GG), *E. grandis* × *E. camaldulensis* (GC), *E. grandis* × *E. tereticornis* (GT), and *E. grandis* × *urophylla* (GU1 and GU2) clones in well-watered (WW) and water-restricted conditions (WR)

gum hybrids (GC and GT) clustered in the upper-left part of the diagram, reflecting higher covariance among variables and greater values specially in PLC. White gum hybrids (GU1 and GU2) clustered in the lower left of the diagram, indicating lower covariance and reduced values compared to red gum hybrids, but higher SLA. *E. grandis* (GG) clone exhibited a unique behavior, showing the highest homogeneity in variance and the lowest variable values, as illustrated by its ellipse spanning two quadrants (Fig. 3b). Correlations among variables are detailed in the supplementary material.

Discussion

This study assessed the effects of water restriction on water status, leaf morphological and physiologic variables, plant hydraulics, and growth in *Eucalyptus grandis* and interspecific hybrids to characterize the functional strategies in response to drought of each species group. Hybrids with red gum species (*E. camaldulensis*, *E. tereticornis*) were expected to outperform *E. grandis* under drought due to the higher drought resistance of red gums as parental species, while hybrids with white gum (*E. urophylla*) were anticipated to show intermediate responses. We also hypothesized a correlation between drought resistance strategies (avoidance vs. tolerance) and growth under stress, resulting in a

more marked decrease in growth in avoidant taxa than in drought tolerant ones. To this end, plants were exposed to moderate-to-severe drought, with midday measurements taken under V_{pd} exceeding 4 kPa (Amirano et al. 2019). Soil water content decreased by one-third, with greater effects during the first cycle, while plants acclimated better during the second cycle by activating additional drought-response mechanisms. Overall, hybrid clones demonstrated lower drought sensitivity than *E. grandis*, with physiologic responses clustering as expected in PCA. However, no consistent relationship was observed between physiologic strategies and growth performance under drought. Specific responses and behaviors observed in the different taxa are discussed in the following subsections.

Different water-use strategies among clones

Two distinct water-use strategies were identified among the studied clones under varying soil moisture levels. Hybrids of *E. grandis* with red gums (GC and GT) demonstrated a “water-spending” strategy, characterized by higher transpiration rates under drought. This was reflected in elevated stomatal conductance (g_s), a steep water potential gradient ($\Delta\Psi$), and the lowest midday leaf-water potential (Ψ_{md}), particularly in the GT clone (Fig. 1b, Table 1). A lower slope in the linear relationship between g_s and predawn leaf

water potential (Ψ_{pd}) was observed in these hybrids under drought conditions compared to those under high-water availability (Fig. 2), indicating reduced stomatal sensitivity as water availability declines. This response supports the maintenance of high gas exchange during drought and reflects anisohydric behavior. In contrast, the *E. grandis* clone (GG) and the white gum hybrids (GU1 and GU2) followed a “water-conservative” strategy, showing increased stomatal responsiveness to Ψ_{pd} under WR (Fig. 2), indicative of isohydric-like behavior.

These results align with previous studies on field-grown trees (Gándara et al. 2020) and rooted cuttings (Niñón et al. 2024), which reported similar patterns than those observed in this study regarding leaf-level water-use efficiency under drought in *E. grandis* clones and hybrids with red gum and with white gum species. Regarding hybrids with red gum species, similarly low stomatal sensitivity was reported in parental species such as *E. camaldulensis* (Merchant et al. 2007; Bournè et al. 2017; Souden et al. 2020) and *E. tereticornis* (Bournè et al. 2015; Aspinwall et al. 2016). These species, along with certain GC hybrids, demonstrate morpho-physiologic adaptations that maintain hydraulic conductivity under high xylem tension (Whitehead and Beadle 2004; Eksteen et al. 2013; Barotto et al. 2016; Saunders and Drew 2022; De Kauwe et al. 2022), thereby supporting continued stomatal opening under drought stress. However, our single-time-point g_s highlights the need for further research to determine whether these hybrids exhibit sensitivity to Ψ_{pd} comparable to that of their parental species.

Adaptive mechanisms to drought in red gum hybrids: the role of elastic and osmotic adjustments

Cell-wall elasticity appears to play a more critical role than osmotic adjustment in maintaining turgor pressure in red gum hybrids, a finding that aligns with observations in related eucalypts (White et al. 2000; Lemcoff et al. 2002; Callister et al. 2008). These hybrids were able to sustain stomatal opening, transpiration, and water uptake during drought conditions by enhancing the elasticity of their cell walls, as indicated by a reduced modulus of elasticity (E). The increased cell wall elasticity can be attributed to the production of new leaves with cell properties adapted to drought conditions. These adaptations involve modifications to the cellulose microfibrils and the cell matrix polysaccharides in the new foliage (Joly and Zaerr 1987). The newly formed leaves are expected to have thinner cell walls and larger intercellular spaces (Niinemets 2001). In our study, the GC clone likely developed such foliage in the spring, while the GT clone exhibited these changes later, in late summer.

Furthermore, the GC clone also exhibited osmotic adjustment later in the growing season, likely through the accumulation of soluble sugars in response to water stress, a pattern

also observed in *E. camaldulensis* (Lemcoff et al. 2002; Souden et al. 2020). Notably, the $\Psi_{TLP} - \Psi_{sat}$ difference in GC was three times greater (0.90 ± 0.07 MPa) than the value reported for *E. camaldulensis* by Lemcoff et al. (2002), highlighting the extent of its osmotic adjustment capacity. The *E. grandis* clone (GG) exhibited reduced Ψ_{TLP} in both cycles and a decrease in Ψ_{sat} in the second cycle. This suggests active osmolyte accumulation in WR plants of this *E. grandis* clone, particularly in spring (first drought cycle), while recognizing that other clones may display different behaviors. Interestingly, the lowest Ψ_{TLP} observed in the GG clone contrasts with the typical drought-avoidance strategy, which generally involves a reduction in stomatal conductance (g_s) to maintain turgor, rather than altering the TLP (Levitt 1980; Barlett et al. 2016). However, although this clone exhibited a significant osmotic adjustment in response to drought, it was not enough to maintain its g_s compared to the well-watered plants.

Photosynthetic and leaf morphologic responses to drought

Drought reduced chlorophyll content in GG, GU1, and GU2 clones, while the red gum hybrids were not significantly affected and maintained higher chlorophyll levels compared to the other taxa, suggesting better preservation of the photosynthetic capacity under drought conditions. In agreement with previous research, it was observed that red gum hybrids acclimated their photosynthetic structure, including both the photochemical and biochemical phases, to cope with prolonged drought, potentially exhibiting “hermetic” behavior (Niñón et al. 2024). Conversely, specific leaf area increased during drought for all clones except GC, which showed a relatively stable leaf surface-to-leaf weight ratio. The smallest SLA increase was observed in GT, suggesting low plasticity in this leaf trait, similar to that of GC.

Hydraulic traits and drought-response mechanisms

Regarding hydraulic traits, there were varying degrees of percent loss in conductivity (PLC) among the clones, depending on their stomatal behavior. In this context, red gum hybrids exhibited the most significant decrease in stem hydraulic conductivity (k_s) due to cavitation, reaching values of PLC around 85%. This value is close to the non-return point threshold described for *E. camaldulensis*, which did not resprout when the main stem reached PLC values above 85% (Barigah et al. 2021). The higher stomatal conductance of red gum hybrids suggests a reduced vulnerability to drought-induced xylem embolism, a characteristic similar to that of their red gum parental species. These species are known to develop compensatory mechanisms that maintain hydraulic conductivity under

water stress (Lemcoff 2002; Whitehead and Beadle 2004; Maseda and Fernández 2016). Indeed, *E. camaldulensis* is a dehydration postponement species, losing hydraulic conductivity at lower Ψ compared to *E. grandis* and other eucalypts (Barotto et al. 2016; Fernández et al. 2019). The GU clones also showed relatively high PLC values, but these were lower than in red gums hybrids (55–62% of the maximum PLC), with all hybrid clones demonstrating a more risk-prone hydraulic strategy than the pure-species GG clone (PLC around 30% under the drought treatment).

Our findings in the hybrid clones align with those of Saunders and Drew (2022), who also reported a high-risk hydraulic strategy linked to other GC and GU hybrid clones. This strategy allows plants to maintain relatively high hydraulic conductance despite the associated safety trade-offs, mainly due to vessel diameter modifications and functional traits of cells surrounding vessels. However, the underlying mechanisms remain a subject of debate (Nardini et al. 2011; Fernández et al. 2019). In our study, considering the clones exhibiting this “risky” strategy, only the two white gum hybrids (GU1 and GU2) were able to maintain high water transport capacity per unit leaf area (i.e., similar k_H in control and water-restricted plants) by the end of the experiment. In contrast, although some hydraulic conductance was maintained, both red-gum hybrids showed highly reduced hydraulic efficiency under relatively long-lasting drought conditions. Saunders and Drew (2022) reported that GC hybrids are more resistant to embolism formation but have lower levels of hydraulic recovery after water refilling. In our study, we did not measure the effect of long-term water recovery to evaluate the impact of PLC on plant’s resilience. However, in the short term, no mortality was observed in any of the plants, suggesting that non-recovery thresholds were not exceeded in any case.

There is an interdependent relationship between stomatal conductance (g_S) and hydraulic conductivity (k_H), which is crucial for maintaining plant-water status, especially under drought conditions (Sperry et al. 2002; Brodribb et al. 2003; Crous et al. 2018; De Kauwe et al. 2022; Johnson and Brodribb 2023). In response to drought conditions, plants usually undergo morpho-physiologic changes in roots (Sperry and Saliendra 1994; Carminati and Javaux 2020; Bourbia et al. 2021), stem (Li et al. 2019), and leaves (Cochard 2002) that reduce hydraulic conductivity, inducing stomatal closure to prevent further xylem dysfunction. Unexpectedly, we observed increased cavitation and reduced k_H with high transpiration rates in GC and GT clones. This behavior may indicate a decoupling of the influence of k_H on g_S as the soil dries, as reported in some fast-growing species (Ocheltree et al. 2016; Müllers et al. 2022), including some *Eucalyptus* species (Creek et al. 2018).

Drought response strategies and growth dynamics

As described previously, hybrid clones exhibited different drought-response strategies compared to the GG clone, with hybrids being more drought-tolerant and GG more drought-avoidant. Among the hybrids, the GU clones differed in their response from GC and GT. Red-gums clones showed a riskier strategy for hydraulic maintenance, with higher elastic/osmotic adjustment and no changes in SLA or chlorophyll content. GU clones displayed intermediate PLC levels and stomatal control of minimum water potential, but no significant elastic/osmotic adjustments, an increased SLA, and a marked decrease in chlorophyll content under WR. Although these patterns suggest a common growth response within each group, drought reduced height growth twice as much as diameter growth in four of the five clones, with GC being the only genotype maintaining both traits at control levels. This behavior indicates GC’s ability to activate diverse drought-response mechanisms. While GC exhibited high height growth under well-watered conditions, it did not show a trade-off between growth potential and drought resistance. In contrast, the studied GT clone, similar to GC in its tolerance strategy, showed a substantial growth reduction under drought, resembling the avoidant GG clone. Among GU hybrids, GU2 was particularly drought-sensitive based on its growth reduction, but the physiologic measurements could not explain this particular response.

Conclusions

This study identified varying drought responses among the studied GG, GC, GT, and GU hybrid clones, leading to different growth capacities under both control and water restricted conditions. While all clones exhibited strategies ranging from water spenders to water savers, only the GC clone maintained high growth under drought. One GU clone (GU1) showed relatively low growth reduction, particularly in height, highlighting the need to explore the physiological differences between GU1 and the more sensitive GU2. Overall, hybrid clones outperformed GG in growth under both conditions; however, significant variation exists among clones, and no single strategy can reliably predict growth under drought. Ongoing research aims to examine the impact of drought on wood anatomy to better understand the underlying drought-response mechanisms.

Acknowledgements Plant material was provided by Lumin Forest Products Company (Tacuarembó, Uruguay). We want to thank Roberto Scoz and INIA (Instituto Nacional de Investigación Agropecuaria) for providing technical support throughout the study, Gabriel Gatica (CONICET) for assisting with the statistical analyses, and Unidad de

Posgrados y Educación Permanente de Facultad de Agronomía for its permanent academic support.

Authors contributions José Gándara, María Elena Fernández, Jaime González-Tálice and Silvia Ross conceived and designed the experiment. Material preparation, data collection, and analysis were performed by José Gándara, Matías Nión and Juan Villar. Statistical analyses were performed by José Gándara and Matías Nión. The first draft of the manuscript was written by José Gándara and Ma Elena Fernández. All authors commented on previous versions of the manuscript and approved the final manuscript.

Funding This research was supported by Comisión Sectorial De Investigación Científica, Universidad De La República, Uruguay. Programa Iniciación a la Investigación 2017 ID233, José Gándara.

Data availability “The datasets generated during and/or analyzed during the current study are available from the corresponding author on reasonable request.” The authors utilized ChatGPT (OpenAI 2024) and Grammarly Premium (Grammarly Inc. 2023) for language correction and text improvement, with all suggestions being supervised and carefully evaluated.

Declarations

Conflict of interest The authors have no relevant financial or non-financial interests to disclose.

References

- Allen RG, Pereira LS, Raes D, Smith M (1998) Crop evapotranspiration. Guidelines for computing crop water requirements. FAO Irrigation and drainage paper 56. FAO, 300(9):D05109.
- Amitrano C, Arena C, Roupael Y et al (2019) Vapour pressure deficit: the hidden driver behind plant morphofunctional traits in controlled environments. *Ann Appl Biol* 175(3):313–325. <https://doi.org/10.1111/aab.12544>
- Aspinwall MJ, Drake JE, Campamy C et al (2016) Convergent acclimation of leaf photosynthesis and respiration to prevailing ambient temperatures under current and warmer climates in *Eucalyptus tereticornis*. *New Phytol* 212:354–367. <https://doi.org/10.1111/nph.14035>
- Barigah TS, Gyenge JE, Barreto F, Rozenberg P, Fernández ME (2021) Narrow vessels cavitate first during a simulated drought in *Eucalyptus camaldulensis*. *Physiol Plant* 173(4):2081–2090. <https://doi.org/10.1111/ppl.13556>
- Barlett M, Klein T, Jansen S et al (2016) The correlations and sequence of plant stomatal, hydraulic, and wilting responses to drought. *Proc Natl Acad Sci* 113(46):13098–13103. <https://doi.org/10.1073/pnas.160408811>
- Barotto AJ, Fernandez ME, Gyenge J et al (2016) First insights into the functional role of vasicentric tracheids and parenchyma in *Eucalyptus* species with solitary vessels: do they contribute to xylem efficiency or safety? *Tree Physiol* 36:1485–1497. <https://doi.org/10.1093/treephys/tpw072>
- Bourbia I, Pritzkow C, Brodribb TJ (2021) Herb and conifer roots show similar high sensitivity to water deficit. *Plant Physiol* 186(4):1908–1918. <https://doi.org/10.1093/plphys/kiab207>
- Bournè AE, Haigh AM, Ellsworth DS (2015) Stomatal sensitivity to vapour pressure deficit relates to climate of origin in *Eucalyptus* species. *Tree Physiol* 35(3):266–278. <https://doi.org/10.1093/treephys/tpv014>
- Bournè AE, Creek D, Peters JMR et al (2017) Species climate range influences hydraulic and stomatal traits in *Eucalyptus* species. *Ann Bot* 120:123–133. <https://doi.org/10.1093/aob/mcx020>
- Brodribb TJ, Holbrook LM, Edwards EJ et al (2003) Relations between stomatal closure, leaf turgor and xylem vulnerability in eight tropical dry forest trees. *Plant, Cell Environ* 26(3):443–450. <https://doi.org/10.1046/j.1365-3040.2003.00975.x>
- Callister A, Arndt SK, Ades PK et al (2008) Leaf osmotic potential of *Eucalyptus* hybrids responds differently to freezing and drought, with little clonal variation. *Tree Physiol* 28(8):1297–1304. <https://doi.org/10.1093/treephys/28.8.1297>
- Carminati A, Javaux M (2020) Soil rather than xylem vulnerability controls stomatal response to drought. *Trends Plant Sci* 25(9):868–880. <https://doi.org/10.1016/j.tplants.2020.04.003>
- Cochar H (2002) Xylem embolism and drought-induced stomatal closure in maize. *Planta* 215(3):466–471. <https://doi.org/10.1007/s00425-002-0766-9>
- Corcuera L (2003) Comparación de dos métodos para generar curvas presión-volumen en especies del género *Quercus*. *Investigación Agraria: Sistemas y Recursos Forestales* 12(1):111–121
- Creek D, Blackman C, Brodribb T et al (2018) Coordination between leaf, stem, and root hydraulics and gas exchange in three arid-zone angiosperms during severe drought and recovery. *Plant, Cell Environ* 41(12):2869–2881. <https://doi.org/10.1111/pce.13418>
- Crous CJ, Greyling I, Wingfield M (2018) Dissimilar stem and leaf hydraulic traits suggest varying drought tolerance among co-occurring *Eucalyptus grandis* × *E. urophylla* clones. *Southern Forests J Forest Sci* 80(2):175–184. <https://doi.org/10.2989/20702620.2017.1315546>
- De Kauwe MG, Sabot MEB, Medlyn BE et al (2022) Towards species-level forecasts of drought-induced tree mortality risk. *New Phytol* 235(1):94–110. <https://doi.org/10.1111/nph.18129>
- DIEA. 2023. Anuario Estadístico Agropecuario (2022) MGAP, Uruguay. Available at www.gub.uy/ministerio-ganaderia-agricultura-pesca/comunicacion. Accessed 12 May 2024
- Eamus D, O’Grady AP, Hutley L (2000) Dry season conditions determine wet season water use in the wet-tropical savannas of Northern Australia. *Tree Physiol* 20(18):1219–1226. <https://doi.org/10.1093/treephys/20.18.1219>
- Eksteen AB, Grzeskowiak V, Jones NB, Pammenter NW (2013) Stomatal characteristics of *Eucalyptus grandis* clonal hybrids in response to water stress. *Southern Forests J Forest Sci* 75(3):105–111. <https://doi.org/10.2989/20702620.2013.804310>
- Eucalyptus* species. *Annals of Botany*: 123–133. <https://doi.org/10.1093/aob/mcx020>
- Fernández ME, Barotto AJ, Martínez-Meier A, Monteoliva S (2019) New insights into wood anatomy and function relationships: how *Eucalyptus* challenges what we already know. *Forest Ecol Manag* 454:117638. <https://doi.org/10.1016/j.foreco.2019.117638>
- Gándara J, Ross S, Quero G et al (2020) Differential water-use efficiency and growth among *Eucalyptus grandis* hybrids under two different rainfall conditions. *Forest Systems* 29(2):e006. <https://doi.org/10.5424/fs/2020292-16011>
- Guarnaschelli AB, Lemcoff JH, Prystupa P et al (2003) Responses to drought preconditioning in *Eucalyptus globulus* Labill. provenances. *Trees* 17(6):501–509. <https://doi.org/10.1007/s00468-003-0264-0>
- Hinckley TM, Duhme F, Hinckley AR, Richter H (1980) Water relations of drought hardy shrubs: osmotic potential and stomatal reactivity. *Plant, Cell Environ* 3(2):131–140. <https://doi.org/10.1111/1365-3040.ep11580919>
- Husson F, Josse J, Lê S, Mazet J (2007) FactoMineR: Factor Analysis and Data Mining with R. R package version 1.04. <http://CRAN.R-project.org/package=FactoMineR>. Accessed 12 May 2024
- in seedlings from six *Eucalyptus* provenances. *Tree Physiology* 36: 2433–251. <https://doi.org/10.1093/treephys/tpv137>

- Intergovernmental Panel on Climate Change (IPCC) (2023) Climate change 2023: Synthesis report. Contribution of Working Groups I, II and III to the Sixth Assessment Report of the Intergovernmental Panel on Climate Change (Core Writing Team, H. Lee & J. Romero, Eds.). IPCC. <https://doi.org/10.59327/IPCC/AR6-9789291691647>
- Janes J, Hamilton JA (2017) Mixing it up: the role of hybridization in forest management and conservation under climate change. *Forest* 8(7):237. <https://doi.org/10.3390/f8070237>
- Johnson K, Brodribb TJ (2023) Evidence for a trade-off between growth rate and xylem cavitation resistance in *Callitris rhochoide*. *Tree Physiol* 43(7):1055–1065. <https://doi.org/10.1093/treephys/tpad037>
- Joly R, Zaerr JB (1987) Alteration of cell-wall water content and elasticity in douglas-fir during periods of water deficit. *Plant Physiol* 83(2):418–422. <https://doi.org/10.1104/pp.83.2.418>
- Kozlowski TT, Pallardy SG (2002) Acclimation and adaptive responses of woody plants to environmental stresses. *Bot Rev* 68:270–334. [https://doi.org/10.1663/0006-8101\(2002\)068\[0270:AAAROW\]2.0.CO;2](https://doi.org/10.1663/0006-8101(2002)068[0270:AAAROW]2.0.CO;2)
- Lambers H, Chapin FS, Pons TL (2008) *Plant physiological ecology*. Springer, New York
- Lemcoff JH, Guarnaschelli AB, Garau AM, Prystupa P (2002) Elastic and osmotic adjustments in rooted cuttings of several clones of *Eucalyptus camaldulensis* Dehnh. From southeastern Australia after a drought. *Flora* 197(2):134–142. <https://doi.org/10.1078/0367-2530-00023>
- Lenz TI, Wright JJ, Westoby M (2006) Interrelations among pressure-volume curve traits across species and water availability gradients. *Physiol Plant* 127:423–433. <https://doi.org/10.1111/j.1399-3054.2006.00680.x>
- Leuschner C, Wedde P, Lübke T (2019) The relation between pressure-volume curve traits and stomatal regulation of water potential in five temperate broadleaf tree species. *Ann for Sci* 76:60. <https://doi.org/10.1007/s13595-019-0838-7>
- Levitt J (1980) Responses of plants to environmental stresses. Academic Press Inc., New York
- Li X, Blackman CJ, Peters JMR, Choat B et al (2019) More than iso/anisohydry: Hydroscales integrate plant water use and drought tolerance traits in 10 eucalypt species from contrasting climates. *Funct Ecol* 33(9):1811–1812. <https://doi.org/10.1111/1365-2435.13320>
- Maseda P, Fernandez R (2016) Growth potential limits drought morphological plasticity in seedlings from six *Eucalyptus* provenances. *Tree Physiology* 36:2433–251. <https://doi.org/10.1093/treephys/tpv137>
- Meinzer FC, Woodruff DR, Marias DE et al (2014) Dynamics of leaf water relations components in co-occurring iso- and anisohydric conifer species. *Plant Cell Environ* 37(11):2577–2586. <https://doi.org/10.1111/pce.12327>
- Meinzer FC, McCulloh KA (2013) Xylem recovery from drought-induced embolism: where is the hydraulic point of no return? *Tree Physiol* 33:331–334. <https://doi.org/10.1093/treephys/tp022>
- Merchant A, Callister A, Arndt S et al (2007) Contrasting physiological responses of six *Eucalyptus* species to water deficit. *Ann Bot* 100(7):1507–1515. <https://doi.org/10.1093/aob/mcm234>
- Michelozzi M, Johnson J, Warrag E (1995) Response of ethylene and chlorophyll in two *Eucalyptus* clones during drought. *New for* 9:197–204. <https://doi.org/10.1007/BF00035487>
- Monteoliva S, Barotto J, Fernández ME (2015) Anatomía y densidad de la madera en *Eucalyptus*: variación interespecífica e implicancia en la resistencia al estrés abiótico. *Rev Fac Agron* 114(2):209–217
- Müllers Y, Postma J, Poorter H, van Dusschoten D (2022) Stomatal conductance tracks soil-to-leaf hydraulic conductance in faba bean and maize during soil drying. *Plant Physiol* 190(4):2279–2294. <https://doi.org/10.1093/plphys/kiac422>
- Nardini A, Lo Gullo MA, Salleo S (2011) Refilling embolized xylem conduits: Is it a matter of phloem unloading? *Plant Sci* 180(4):604–611. <https://doi.org/10.1016/j.plantsci.2010.12.011>
- Niinemets Ü (2001) Global-scale climate controls of leaf dry mass per area, density and thickness in trees and shrubs. *Ecology* 82(2):453–469. <https://doi.org/10.2307/2679872>
- NiÓN M, Gándara J, Ross S et al (2024) Photosynthesis adaptation to long- and short-term water restriction in commercial plantlets of *Eucalyptus grandis* and hybrids with Red Gums. *Trees* 38:537–547. <https://doi.org/10.1007/s00468-024-02503-y>
- Ocheltree T, Nippert JB, Vara Prasad PV (2016) A safety vs efficiency trade-off identified in the hydraulic pathway of Grass leaves is decoupled from photosynthesis, stomatal conductance and precipitation. *New Phytol* 210(1):97–107. <https://doi.org/10.1111/nph.13781>
- Pfautsch S, Aspinwall M, Drake J et al (2018) Traits and trade-offs in whole-tree hydraulic architecture along the vertical axis of *Eucalyptus grandis*. *Ann Bot* 121:129–141. <https://doi.org/10.1093/aob/mcx137>
- Pita P, Pardos JA (2001) Growth, leaf morphology, water use and tissue water relations of *Eucalyptus globulus* clones in response to water deficit. *Tree Physiol* 21(9):599–607. <https://doi.org/10.1093/treephys/21.9.599>
- Saito T, Terashima I (2004) Reversible decreases in the bulk elastic modulus of mature leaves of deciduous *Quercus* species subjected to tow drought treatments. *Plant, Cell Environ* 27:863–875. <https://doi.org/10.1111/j.1365-3040.2004.01192.x>
- Saunders A, Drew DM (2022) Measurements done on excised stems indicate that hydraulic recovery can be an important strategy used by *Eucalyptus* hybrids in response to drought. *Trees* 36:139–151. <https://doi.org/10.1007/s00468-021-02188-7>
- Schulte PJ (1992) The units of currency for plant water status. *Plant, Cell Environ* 15:7–10. <https://doi.org/10.1111/j.1365-3040.1992.tb01453.x>
- Silva M, Rubilar R, Espinoza J et al (2017) Respuesta en parámetros de intercambio gaseoso y supervivencia en plantas jóvenes de genotipos comerciales de *Eucalyptus spp* sometidas a déficit hídrico. *Bosque* 38(1):79–87. <https://doi.org/10.4067/S0717-92002017000100009>
- Souden S, Mustapha E, Ouledali S et al (2020) Water relations, photosynthesis, xylem embolism and accumulation of carbohydrates and cyclitols in two *Eucalyptus* species (*E. camaldulensis* and *E. torquata*) subjected to dehydration–rehydration cycle. *Trees* 34:1439–1452. <https://doi.org/10.1007/s00468-020-02016-4>
- Sperry JS, Saliendra NZ (1994) Intra- and inter-plant variation in xylem cavitation in *Betula occidentalis*. *Plant, Cell Environ* 17(11):1233–1244. <https://doi.org/10.1111/j.1365-3040.1994.tb02021.x>
- Sperry JS, Hacke UG, Oren R, Comstock JP (2002) Water deficits and hydraulic limits to leaf water supply. *Plant, Cell Environ* 25(2):251–263. <https://doi.org/10.1046/j.0016-8025.2001.00799.x>
- Steel RGD, Torrie JH (1980) Principles and procedures of statistics: a biometrical approach, 2nd edn. McGraw-Hill, New York
- Vander Willigen C, Pammenter NW (1998) Relationship between growth and xylem hydraulic characteristics of clones of *Eucalyptus* spp. at contrasting sites. *Tree Physiol* 18(8–9):595–600. <https://doi.org/10.1093/treephys/18.8-9.595>
- White DA, Turner NC, Galbraith JH (2000) Leaf water relations and stomatal behavior of four allopatric *Eucalyptus* species planted in 44 Mediterranean southwestern Australia. *Tree Physiol* 20(17):1157–1165. <https://doi.org/10.1093/treephys/20.17.1157>
- Whitehead D, Beadle CL (2004) Physiological regulation of productivity and water use in *Eucalyptus*: a review. *For Ecol Manage* 193(1–2):113–140. <https://doi.org/10.1016/j.foreco.2004.01.026>
- Xue LL, Anjum SA, Wang LC, Saleem MF, Liu XJ et al (2011) Influence of straw mulch on yield, chlorophyll contents, lipid

- peroxidation and antioxidant enzymes activities of soybean under drought stress. *J Food Agric Environ* 9:699–704
- Zhang Y, Wang X (2021) Geographical spatial distribution and productivity dynamic change of eucalyptus plantations in China. *Sci Rep* 11:19764. <https://doi.org/10.1038/s41598-021-97089-7>
- Zhang ZZ, Zhao P, Oren R, McCarthy HR et al (2015) Water use strategies of a young *Eucalyptus urophylla* forest in response to seasonal change of climatic factors in South China. *Biogeosci Discuss* 12(13):10469–10510. <https://doi.org/10.5194/bgd-12-104692015>
- Zhu S, Chen Y, Ye Q, He P, Liu H, Li R et al (2018) Leaf turgor loss point is correlated with drought tolerance and leaf carbon economics traits. *Tree Physiol* 38:658–663. <https://doi.org/10.1093/treephys/tpy013>

Publisher's Note Springer Nature remains neutral with regard to jurisdictional claims in published maps and institutional affiliations.

Springer Nature or its licensor (e.g. a society or other partner) holds exclusive rights to this article under a publishing agreement with the author(s) or other rightsholder(s); author self-archiving of the accepted manuscript version of this article is solely governed by the terms of such publishing agreement and applicable law.

3. Anatomía funcional del xilema en especies puras y clones híbridos interespecíficos de *Eucalyptus* con diferente resistencia a la sequía

3.1. Resumen

Los eventos climáticos extremos amenazan la resiliencia de las plantaciones de *Eucalyptus*; sin embargo, el cruzamiento con especies tolerantes a la sequía podría mejorar la resistencia al estrés. En este estudio se analizaron respuestas anatómicas y funcionales del xilema frente a la sequía en clones comerciales de *Eucalyptus grandis* (GG) y sus híbridos: *E. grandis* × *camaldulensis* (GC), *E. grandis* × *tereticornis* (GT) y *E. grandis* × *urophylla* (GU1, GU2). Se evaluaron características de los vasos (transporte de agua), fibras (soporte mecánico) y densidad de la madera (D) en tallos y ramas. También se estimó la conductividad hidráulica teórica del tallo (k_{Stheo}), la fracción de lúmenes (F), la composición de los vasos (S) y sus asociaciones con datos previos de hidráulica y crecimiento. Se observaron diferentes respuestas a la sequía entre genotipos. El clon GC presentó un perfil característico en los ajustes del xilema que explicaría su mayor desempeño bajo diferentes condiciones de riego. Los híbridos de eucalipto colorado (GC, GT) mantuvieron la k_{Stheo} durante la sequía, con un valor estable de F y vasos de menor diámetro promedio, particularmente en las ramas. En cambio, GG y GU2 mostraron una reducción de F y S. Además, la k_{Stheo} en los tallos disminuyó a pesar de mostrar valores similares de F, lo que indicaría una reconfiguración vascular que ajusta el xilema del tallo hacia una configuración más similar con el xilema de la rama. Casi todos los clones aumentaron la densidad de la madera bajo sequía, en ambos órganos, con el mayor incremento en los híbridos de eucalipto colorado. Estos resultados revelan la activación de distintos ajustes anatómicos frente a la sequía entre los clones, lo que explica parcialmente sus respuestas en crecimiento.

Palabras clave: *Eucalyptus grandis*, estrés hídrico, conductividad hidráulica, elementos xilemáticos, densidad de madera

Article

Xylem Functional Anatomy of Pure-Species and Interspecific Hybrid Clones of *Eucalyptus* Differing in Drought Resistance

José Gándara ^{1,2,*}, Matías Nión ¹, Silvia Ross ¹, Jaime González-Tálice ³, Paolo Tabeira ¹ and María Elena Fernández ^{4,5}

¹ Departamento de Biología Vegetal, Facultad de Agronomía, Universidad de La República, Av. Garzón 780, Montevideo 12900, Uruguay; mniion@fagro.edu.uy (M.N.); sross@fagro.edu.uy (S.R.); paolotabeira@gmail.com (P.T.)

² Unidad de Posgrados y Educación Permanente, Facultad de Agronomía, Universidad de La República, Av. Garzón 780, Montevideo 12900, Uruguay

³ Departamento Forestal, Facultad de Agronomía, Universidad de La República, Av. Garzón 780, Montevideo 12900, Uruguay; jgonzalez@fagro.edu.uy

⁴ CONICET, Consejo Nacional de Investigaciones Científicas y Técnicas, Godoy Cruz 2290, Buenos Aires, Argentina; ecologia_forestal@yahoo.com.ar

⁵ INTA, Instituto Nacional de Tecnología Agropecuaria, Ecología Forestal, UEDD INTA-CONICET IPADS, Tandil 7000, Buenos Aires, Argentina

* Correspondence: jgandara@fagro.edu.uy

Abstract

Climate extremes threaten the resilience of *Eucalyptus* plantations, yet hybridization with drought-tolerant species may enhance stress tolerance. This study analyzed xylem anatomical and functional drought responses in commercial *Eucalyptus grandis* (GG) clones and hybrids: *E. grandis* × *camaldulensis* (GC), *E. grandis* × *tereticornis* (GT), and *E. grandis* × *urophylla* (GU1, GU2). We evaluated vessel traits (water transport), fibers (mechanical support), and wood density (D) in stems and branches. Theoretical stem hydraulic conductivity (k_{Sttheo}), vessel lumen fraction (F), vessel composition (S), and associations with previous hydraulic and growth data were assessed. While general drought responses occurred, GC had the most distinct xylem profile. This may explain it having the highest performance in different irrigation conditions. Red gum hybrids (GC, GT) maintained k_{Sttheo} under drought, with stable F and a narrower vessel size, especially in branches. Conversely, GG and GU2 reduced F and S; and stem k_{Sttheo} declined for a similar F in these clones, indicating vascular reconfiguration aligning the stem with the branch xylem. Almost all clones increased D under drought in any organ, with the highest increase in red gum hybrids. These results reveal diverse anatomical adjustments to drought among clones, partially explaining their growth responses.

Keywords: *Eucalyptus grandis*; water stress; hydraulic conductivity; xylem elements; wood density



Academic Editor: Álvaro Rubio-Cuadrado

Received: 30 June 2025

Revised: 23 July 2025

Accepted: 1 August 2025

Published: 2 August 2025

Citation: Gándara, J.; Nión, M.; Ross, S.; González-Tálice, J.; Tabeira, P.; Fernández, M.E. Xylem Functional Anatomy of Pure-Species and Interspecific Hybrid Clones of *Eucalyptus* Differing in Drought Resistance. *Forests* **2025**, *16*, 1267. <https://doi.org/10.3390/f16081267>

Copyright: © 2025 by the authors. Licensee MDPI, Basel, Switzerland. This article is an open access article distributed under the terms and conditions of the Creative Commons Attribution (CC BY) license (<https://creativecommons.org/licenses/by/4.0/>).

1. Introduction

Eucalyptus species cover over 20 million hectares worldwide due to their high productivity and adaptability [1]. In the subtropical and warm-temperate regions of South America, *Eucalyptus grandis* is widely cultivated for its superior pulp and timber yields. However, an increasing occurrence of droughts, frosts, and heatwaves [2,3] threatens plantation resilience, particularly during early growth stages. Consequently, breeding programs

prioritize genotypes exhibiting traits linked to abiotic stress tolerance, such as efficient water use, sustained hydraulic function, and stable growth under adverse conditions. Within this context, hybridization with drought-tolerant red gums (*E. camaldulensis*, *E. tereticornis*) and *E. urophylla* is commonly used to enhance adaptability and productivity.

Balancing xylem hydraulic efficiency and safety is a fundamental physiological strategy that allows plants to maintain function, survive, and remain productive under drought conditions [4–6]. During water stress, increased xylem tension frequently induces cavitation and embolism, which reduce hydraulic conductivity and limit gas exchange and carbon assimilation. The potentially severe consequences of this process, including hydraulic failure and plant mortality, underscore the importance of understanding the trade-off between efficiency and safety in xylem function [4,7]. In angiosperms, susceptibility to hydraulic dysfunction is closely linked to anatomical features such as vessel diameter, vessel grouping, and pit membrane structure, which collectively influence both conductivity and resistance to cavitation [8,9]. Vessel wall reinforcement also plays a critical role in preserving conduit integrity under negative pressure [8], while fibers primarily provide mechanical support, although they may also contribute to sustaining hydraulic function under stress [10–12].

Overall, vessel wall reinforcement and thicker fiber walls contribute to increase wood density, a trait generally associated with enhanced xylem safety under negative pressure conditions [8]. In response to drought, many woody species exhibit anatomical adjustments that favor a safer xylem structure—such as a reduced vessel diameter or increased cell wall thickness—often at the cost of lower transport efficiency, typically quantified as specific hydraulic conductivity (k_s) [13–16]. This trade-off between hydraulic safety and efficiency is a central principle in plant hydraulic architecture [17], and elucidating its underlying mechanisms is essential for understanding species-specific responses to water stress [18–20]. In this context, structural traits such as the lumen fraction (F) and vessel composition (S) are particularly informative, as they influence both the water transport capacity and vulnerability to embolism. These integrative traits offer valuable insights into how plants coordinate hydraulic function in response to environmental variability [21].

The *Eucalyptus* genus, comprising over 700 species, exhibits a wide range of hydraulic strategies to cope with drought. In a comparative study of 31 species along an aridity gradient, Pfautsch et al. [22] reported that species native to drier environments tend to develop narrower vessels and denser wood. These traits are typically associated with lower theoretical specific hydraulic conductivity (i.e., maximum k_s based on vessel dimensions), reflecting a trade-off that favors hydraulic safety over transport efficiency. Such characteristics are largely genetically determined and exhibit limited plasticity. For example, *Eucalyptus grandis* displays high stem k_s values due to its large vessel diameters and high vessel area, features generally linked to a lower wood density and greater conductive capacity. However, under water-limited conditions, *E. grandis* adopts a water-conservative strategy, primarily through tight stomatal regulation and the maintenance of stable water potentials [23–25]. In contrast, red gums such as *E. camaldulensis* and *E. tereticornis* follow a water-spending strategy, maintaining higher rates of gas exchange and growth even under drought stress.

The hydraulic strategy employed by red gum species involves a greater degree of hydraulic risk. While relatively resistant to cavitation, these species often experience significant reductions in specific conductivity due to limited stomatal regulation and anisohydric behavior [26]. In branch wood, *E. camaldulensis* develops wider vessels than *E. grandis* [27], a trait generally linked to lower cavitation resistance via increased pit area, a pattern observed across several *Eucalyptus* species [28]. However, fast-growing commercial genotypes may deviate from this expected safety–efficiency trade-off. For

instance, although it possesses wider vessels, *E. camaldulensis* has been shown to be less vulnerable to cavitation than *E. grandis*, suggesting that organ-specific deviations from the expected trade-off may occur. Similarly, *E. tereticornis* combines wide vessels with high cavitation resistance [28]. In contrast, *E. urophylla*, a species native to humid tropical regions, exhibits steep conductivity losses under drought, triggering strong stomatal closure and reduced gas exchange [29]. This response reflects xylem vulnerability, comparable to that observed in the fast-growing *E. grandis*.

Interspecific hybrids can exhibit anatomical and physiological traits that are intermediate or even superior to those of their parental species [30]. In *E. grandis* and its hybrids, hydraulic performance shows considerable genotypic variation, which influences their capacity to tolerate drought. In South Africa, hybrid clones differed from *E. grandis* in growth efficiency and canopy dieback under severe drought, despite displaying only moderate differences in vulnerability to cavitation [31]. Similarly, a previous study conducted in Uruguay reported high in situ levels of cavitation in *Eucalyptus* hybrids with red gum parentage, with percent loss of conductivity (PLC) reaching up to 85%, despite their presumed lower vulnerability. This unexpected behavior was attributed to weak stomatal control, combined with osmotic and elastic adjustments that allowed continued growth under both well-watered and drought conditions [32]. Hybrids such as *E. grandis* × *E. camaldulensis* and *E. grandis* × *E. urophylla* may thus adopt high-risk hydraulic strategies under water deficit [33]. However, it has been shown that among hybrids sharing *E. urophylla* parentage, drought vulnerability can vary considerably, despite similar wood anatomical features [34], thus suggesting that hybridization can lead to rather unpredictable functional combinations. Moreover, although drought-induced xylem downsizing and increased tissue density have been observed in *E. grandis*, the functional significance of these responses in hybrid genotypes remains unclear [35].

Most studies on xylem hydraulics have focused on a single organ—leaves, branches, stems, or roots—despite substantial anatomical and functional variation along the plant axis. In addition to vessel tapering that facilitates vertical water transport, some *Eucalyptus* species, including *E. grandis*, exhibit hydraulic decoupling between stems and branches as an adaptive response to drought. In *E. grandis*, stems typically contain large-diameter vessels and exhibit high specific conductivity, supporting rapid water transport and growth. In contrast, the vessel diameter in branches declines markedly along the vertical axis, from approximately 250 µm at the base to 20 µm at the distant ends [36]. While narrower vessels generally confer greater resistance to cavitation [37], *E. grandis* branches possess anatomical features such as larger pits [27] and thinner pit membranes [36], which enhance hydraulic conductivity but increase vulnerability to embolism. As a result, *E. grandis* often sheds branches during severe drought, a response interpreted as a means of protecting the stem from embolism propagation. This branch abscission strategy was not observed in *E. globulus* or *E. camaldulensis*, which exhibited greater resistance to cavitation at the branch level [27]. These organ-specific differences in vulnerability highlight the importance of assessing the whole-plant hydraulic architecture when evaluating drought responses and tolerance strategies in *Eucalyptus* [38].

Given its dual role in mechanical support and water transport, the wood-specific density is another key trait linked to the hydraulic function and drought response. In *Eucalyptus* species, wood density ranges from 400 to 1000 kg m⁻³ and varies across plant organs [21,39], potentially influencing hydraulic efficiency and vulnerability. Although differences in wood density between stems and branches are commonly reported, their direction and magnitude remain inconsistent across studies [40–43], suggesting complex underlying mechanisms that may depend on species-specific strategies, developmental stage, or environmental condition. Overall, the relationships among clonal drought resis-

tance, xylem anatomical traits, wood density, and the coordination of hydraulic properties across different organs remain poorly understood [44–46].

The objective of this study was to investigate the anatomical and functional responses of xylem to drought in commercial clones of *Eucalyptus grandis* and interspecific hybrids of *E. grandis* × *camaldulensis*, *E. grandis* × *tereticornis*, and *E. grandis* × *urophylla* grown under controlled greenhouse conditions. Despite the ecological and commercial importance of these genotypes, there is a significant knowledge gap regarding how such anatomical and physiological traits diverge between *E. grandis* and its hybrids, particularly in the context of drought stress. In previous work, we characterized the different physiological strategies employed by these genotypes to cope with water deficit [32]. Here, we advance on the wood anatomical traits that may underlie or help explain the differential drought responses previously observed.

We hypothesized that clone-specific differences in the size and arrangement of conductive (vessels) and supportive (fibers) cells under drought would contribute to variations in hydraulic performance and wood density in stems and branches, thereby affecting water supply to the foliage and plant growth under varying water availability regimes. These anatomical differences may reflect distinct drought-response strategies among *Eucalyptus grandis* and its interspecific hybrids, with direct implications for water transport efficiency and growth under contrasting moisture regimes. Understanding hydraulic differentiation and xylem plasticity among genotypes is essential for elucidating drought adaptation and guiding the selection of resilient genotypes for water-limited environments.

2. Materials and Methods

2.1. Plant Material and Growth Conditions

This study was conducted at the Department of Plant Biology, Centro Universitario de Tacuarembó, Uruguay (31.73° S, 55.97° W), using *Eucalyptus* clones widely cultivated in Uruguay, South America. The plant material consisted of rooted cuttings of *Eucalyptus grandis* (GG), *E. grandis* × *camaldulensis* (GC), *E. grandis* × *E. tereticornis* (GT), and *E. grandis* × *E. urophylla* (GU1 and GU2), propagated in a clonal nursery operated by Lumin Forestry Company. Cuttings were initially grown in a controlled environment (20–22 °C; 90%–95% relative humidity) in 120 cm³ tubes filled with inert substrate and periodically watered with a Biorend[®] nutrient solution (10 cm³ L⁻¹) (Bioagro S.A., Tierra del Fuego, Chile). After five months, plants were transplanted into 3 L pots containing Carolina Soils[®] substrate (Carolina Soil do Brasil Ltda., Santa Cruz do Sul, RS, Brasil). At six months of age, the plants were transferred into 18 L plastic pots and moved to the experimental greenhouse for acclimation to its specific environmental conditions.

2.2. Experimental Design and Treatments

A split-plot experimental design was employed to evaluate drought responses across two cycles. The main plots consisted of two watering treatments—water restriction (drought) and well-watered control—both applied uniformly across the entire plot. Within each main plot, subplots consisted of five *Eucalyptus* clones (GG, GC, GT, GU1, GU2). The experiment comprised two drought cycles, each lasting 60 days and separated by a 15-day recovery period, conducted between 29 October 2019 (austral spring) and 22 March 2020 (early autumn). The first drought cycle (29 October 2019–2 January 2020) was followed by a recovery period, after which the second cycle was applied (18 January–22 March 2020).

Each treatment × clone combination included six individual plants, totaling 60 plants. These were randomly assigned within four rows of 15 plants each to minimize spatial variability. This design allows for the assessment of the main effect of watering treatment, the effect of clones, and their interaction.

Irrigation was supplied automatically via a drip system twice daily (6:30 and 19:30 h) for 15 min per session. The system employed two opposing emitters positioned 5 cm below the substrate surface, each with a flow rate of 8 mL min^{-1} . Plants classified as well-watered (WW) received enough irrigation to compensate for the losses caused by evapotranspiration entirely. In contrast, water-restricted (WR) plants were supplied with 30% of that amount, a previously validated level for applying drought stress in these genotypes.

Water loss was periodically measured for each pot using gravimetric assessments [32]. During the recovery period, all plants were irrigated at the WW rate. Substrate water content (θ , %, w/w) was measured biweekly during drought cycles using a time-domain reflectometry sensor (Decagon®, Pullman, WA, USA). Air temperature (T , °C) and relative humidity (RH, %) were measured at 15 min intervals throughout the experimental period using an RHT10 sensor (Extech Instruments Corp., Nashua, NH, USA) positioned 1 m above the ground. Data were used to calculate the air vapor pressure deficit (VPD, kPa) following the method described by [47]. Within each drought cycle, plant water status and physiological parameters were measured over a one-week period at the beginning and end of each cycle. More details are provided in [32]. The air vapor pressure deficit (VPD, kPa) during the experimental period presented mid-morning and midday averages ranging from 4 to 5.5 kPa. Soil moisture levels were maintained below 10% in all water-restricted plants and above 35% under well-watered conditions.

2.3. Sample Processing

For this study, anatomical analyses were conducted on stem and branch wood tissue collected at the end of the second drought cycle. From each plant, one stem segment (basal section) and one branch segment were sampled. The branch segment was taken from the proximal portion of a subapical branch—i.e., the section closest to the stem. Both segments measured 6–8 cm in length. In branches, all growth occurred during the water stress treatment. In stems, growth started before the experiment; however, the wood formed before and after treatment was not separated. Nevertheless, over two-thirds of stem growth occurred during the treatment (Section S4). As these are diffuse-porous species, distinguishing between pre- and post-treatment growth is technically challenging, which may reduce the precision of radial growth estimates (more details are provided in Section S4).

Cross-sections of each segment, 15–18 μm thick, were obtained using a manual microtome (Euromex® MT 5501, Euromex Microscopen BV, Duiven, The Netherlands) and stained with a 0.5% (v/v) safranin solution, followed by rinsing in distilled water. Images of the stained sections were captured to measure vessel dimensions, using an AmScope® MU853B digital camera (United Scope LLC, Irvine, CA, USA) mounted on an Olympus® CX21-9 light microscope (Olympus Corporation, Tokyo, Japan) (see Appendix A for examples of cross-section images).

Macerates were prepared to evaluate the anatomical traits related to fibers. Three wood samples (30 mg each) were taken longitudinally from stem and branch segments. The samples were placed in glass test tubes containing a 1:1 (v/v) mixture of acetic acid and hydrogen peroxide and incubated at 60 °C for 24 h to ensure complete fiber dissociation. After incubation, samples were rinsed three times with distilled water. A 1 mL aliquot was then taken from each tube and stained with a 0.5% (v/v) safranin solution. A drop of the stained suspension was mounted on a glass slide for light microscopy. Images of each sample were captured using the previously described digital camera mounted on the microscope (see Appendix A for examples of cross-section images).

2.4. Wood Basic Density

Basic density (D , g cm^{-3}) of each stem or branch segment was calculated as the ratio of oven-dry mass (m) to saturated volume, i.e., $D = m/V$, assuming a water density of 0.9983 g cm^{-3} at 20°C . Samples were first carefully debarked and immersed in distilled water for 72 h to ensure saturation. Saturated volume was determined by water displacement, with samples blotted before submersion. Subsequently, samples were oven-dried at $105 \pm 2^\circ\text{C}$ until a constant mass was reached and then weighed to determine their dry mass. Data were used to calculate the branch-to-stem density ratio (Dif_{bs} , %) as $[(D_{\text{branch}} - D_{\text{stem}}) / D_{\text{stem}}] \times 100$.

2.5. Xylem Anatomical Variables

Images captured from stained cross-sections were analyzed using ImagePro® Plus software, version 6.3 (Media Cybernetics, Rockville, MD, USA). Three images, each covering an area of 0.723 mm^2 , were taken from each sample to quantify the mean vessel diameter (V_d , μm), maximum vessel diameter ($V_{d_{\text{max}}}$, μm), minimum vessel diameter ($V_{d_{\text{min}}}$, μm), average vessel range ($V_{\text{dif}} = V_{d_{\text{max}}} - V_{d_{\text{min}}}$, μm), and mean vessel area (V_a , μm^2). The number of vessels per image was recorded to calculate the vessel density (N , $\text{n}^\circ \text{mm}^{-2}$). Using these measurements, the vessel lumen fraction ($F = V_a \times N$, unitless), which reflects the relative area available for water transport, and the vessel composition ($S = V_a/N$, mm^4), representing the average vessel size within that area, were calculated following the approach described in [21].

Theoretical hydraulic conductivity (k_{stheo}) was determined based on the Hagen–Poiseuille law as $k_{\text{stheo}} = (\pi \rho V_d^4) / (\eta \cdot 128 N)$ ($\text{kg m}^{-1} \text{MPa}^{-1} \text{s}^{-1}$), where V_d is the vessel diameter (m), η is the dynamic viscosity of water at 20°C ($1.002 \times 10^{-9} \text{ MPa}^{-1} \text{s}^{-1}$), ρ is the density of water at 20°C (998.3 kg m^{-3}), and N is the vessel density.

Images obtained from macerates were analyzed to assess fiber length (Fl , μm ; $n = 60$ per sample), fiber total diameter (F_{td} , μm ; $n = 60$ per sample), and fiber lumen diameter (F_{ld} , μm ; $n = 60$ per sample) using AmScope TouPView 3.7 version (2022) Data were used to calculate the fiber lumen fraction ($F_f = F_{ld}/F_{td}$, unitless), and fiber wall thickness (F_{wt} , μm), calculated as the difference between F_{td} and F_{ld} , divided by two (i.e., single wall thickness).

2.6. Hydraulic Conductivity

Stem hydraulic conductivity (k_h , $\text{kg s}^{-1} \text{m MPa}^{-1}$) was measured in 60 plants at the end of the second drought cycle. To minimize sampling-induced cavitation, plants were irrigated the evening before harvest. Subapical shoot segments were collected the following day, defoliated underwater, and trimmed 30 cm from the apex. Hydraulic conductivity (k_h) was determined using the pipette method [48], followed by maximum conductivity ($k_{h_{\text{max}}}$) after embolism removal via pressurized perfusion. Percent loss of conductivity (PLC) was calculated as $\text{PLC} = [(1 - k_h/k_{h_{\text{max}}})] \times 100$. Specific conductivity (k_s , $k_{s_{\text{max}}}$, $\text{kg s}^{-1} \text{m}^{-1} \text{MPa}^{-1}$) was normalized by cross-sectional area. Further methodological details are available in [32].

2.7. Plant Growth

Plant height (H_t , cm) and stem diameter at ground level (Φ , mm) were measured for all 60 plants. Relative growth (RG, %) was calculated as the percentage change in H_t and Φ from the beginning of the experiment and the end of the second drought cycle as $\text{RG} = [(G_n - G_{n-1}) / (G_{n-1})] \times 100$, where G represents the plant height (H_t) or diameter (Φ). For more details on the methodology, see [32].

2.8. Statistical Analyses

To test the hypothesis of differential clonal responses to drought, two-way ANOVA was performed for each variable, considering the effects of the clone, water regime, and their interaction. Assumptions of normality and homogeneity of variances were assessed using the Shapiro–Wilk and Levene’s tests, respectively. When significant main effects or interactions were detected, post hoc comparisons were conducted using Tukey’s test ($p < 0.05$). For variables violating ANOVA assumptions, the non-parametric Kruskal–Wallis test was applied, followed by Dunn’s test for pairwise comparisons. Proportional data was arcsine square-root transformed prior to ANOVA. All analyses were conducted using InfoStat® software version 2020 (InfoStat Group, Córdoba, Argentina) [49]. Relationships between anatomical variables and wood density were examined by multiple linear regression. The influence of the lumen fraction (F) and vessel spatial composition (S) on the theoretical specific conductivity (k_{Sttheo}) of branches and stems across clones and treatments was explored via linear or non-linear regression analyses.

To assess the relationship between multiple xylem traits and overall plant performance under well-watered and drought conditions, multivariate analyses were conducted. Due to missing data in some variables, only individuals with complete records across all measured traits (29 variables) were selected, retaining three to four individuals per clone and treatment. A small number of remaining missing values (29 out of 957) were imputed using the mean of the other individuals from the same clone and treatment. A correlation matrix was first computed to exclude variables with high correlations (Pearson’s $r \geq 0.7$), resulting in a final set of 22 variables. These were used to perform an exploratory cluster analysis based on standardized data, using the Euclidean distance and the Ward.D linkage method in Navure Professional Version 2.6.1 software [50], which was also used for the correlation analysis. Subsequently, a principal component analysis (PCA) was performed in RStudio version 2025.05.1+513 [51] using the FactoMineR package v2.11 [52], along with Factoextra v1.0.7, Factoinvestigate v1.9, and additional packages (ggplot2, v3.5., dplyr v1.1.4, tibble v3.2.1) for data handling and graphical representation.

3. Results

3.1. Wood Density

Wood density varied among genotypes and between plant organs. Red gum hybrids (GC and GT) exhibited a stem wood density approximately 20% higher than *Eucalyptus grandis* clones (GG) ($p < 0.0001$), with mean values of 0.500 and 0.401 g cm⁻³, respectively. The GC clone exhibited the highest wood density in both stem and branches. GU hybrids presented intermediate values, approximately 10%–12% lower than those of GC and GT. On average, branch wood was 25% denser than stem wood across genotypes. The largest proportional difference between stem and branch density was observed in the *E. grandis* clone (34%), calculated between stem wood density, which was not affected by the treatment, and branch wood density under drought conditions. In contrast, the smallest difference occurred in GC under the same treatment (13%) (Table 1).

Drought increased wood density—considering stems and branches combined—across all genotypes, with the greatest relative increase (30%) observed in the GG clone. When analyzing organs separately, branches showed a stronger response to water deficit, exhibiting an average wood density increase of 11% across the clones, compared to a 5% increase in stems. Only the red gum hybrids showed a significant stem wood density increase of approximately 10% under drought conditions. In contrast, branch wood density increased in all clones except for GC (Table 1).

Table 1. Mean stem and branch basic wood density (D , g cm^{-3}) in *E. grandis* (GG), *E. grandis* \times *camaldulensis* (GC), *E. grandis* \times *tereticornis* (GT), and *E. grandis* \times *urophylla* (GU1 and GU2) clones under well-watered (WW) and water-restricted (WR) conditions. The proportional difference between organs (Dif_{bs} , %) was calculated for each clone and treatment as $[(D_{\text{branch}} - D_{\text{stem}}) / D_{\text{stem}}] \times 100$. Data are presented as mean \pm standard error (SE). Different lowercase letters indicate statistically significant differences within each clone for a given treatment (ANOVA, $p < 0.05$).

Clone	Water Regime	Stem Wood Density	Branch Wood Density	Dif_{bs} (%)
GG	WW	0.391 \pm 0.013 a	0.499 \pm 0.044 b	27.62
	WR	0.412 \pm 0.013 a	0.603 \pm 0.040 a	46.36
GC	WW	0.465 \pm 0.028 b	0.620 \pm 0.025 a	33.33
	WR	0.516 \pm 0.032 a	0.624 \pm 0.043 a	21.32
GT	WW	0.481 \pm 0.020 b	0.543 \pm 0.029 b	12.89
	WR	0.525 \pm 0.017 a	0.627 \pm 0.024 a	19.43
GU1	WW	0.443 \pm 0.009 a	0.519 \pm 0.035 b	17.16
	WR	0.459 \pm 0.010 a	0.600 \pm 0.036 a	30.72
GU2	WW	0.416 \pm 0.014 a	0.524 \pm 0.026 a	25.96
	WR	0.440 \pm 0.013 a	0.528 \pm 0.027 a	20.00

3.2. Xylem Anatomical Traits

3.2.1. Variation in Vessel Characteristics

At the stem level, vessel density (N) increased under drought conditions ($p < 0.0001$) by an average of 60%, ranging from 50 to 64 vessels mm^{-2} in water-stressed plants. The greatest increase was observed in the red gum hybrids (reaching up to 75%), followed by the *E. grandis* clone (Table 2). Vessel diameter (Vd) was reduced ($p = 0.0007$) under water restriction in red gum hybrids (17%) and GG clones (12%), while the GU hybrids showed no response. As observed in Vd, vessel lumen area (Va) significantly decreased ($p = 0.0222$) in drought-stressed plants of GG and GC, with the most pronounced decrease (35%) found in GC. Additionally, the difference between maximum and minimum vessel diameter (Vdif), an indicator of lumen size uniformity, was reduced by 21% on average ($p = 0.0134$). The vessel composition within the sapwood (S) declined under drought ($H = 25.86$, $p = 0.0021$), except in the GU1 clone, where no change was observed. Notably, the drought-induced reduction in S was twice as large in red gum hybrids and GU1 compared to the *E. grandis* clone. The vessel lumen fraction (F) also declined under drought, particularly in GG ($p = 0.0088$) and GU clones ($p = 0.0248$), with an average decrease of 25%. F remained unchanged in the red gum hybrids (Table 2).

Drought affected branches differently than stems. Vessel density (N) increased under water restriction, but this response was limited to the GG clone ($p = 0.010$). Conversely, vessel diameter (Vd) was significantly reduced in the GG ($p = 0.0114$) and GU2 ($p = 0.0027$) clones. Unlike stems, Vd in the GT clone's branches remained unaffected by drought, and no significant changes in the vessel lumen area (Va) were detected in any clone. Vessel diameter variation (Vdif) also exhibited organ-specific patterns, decreasing in branches of GC (34%) and GT (30%) hybrids, whereas in stems, this reduction was restricted to GC only. Vessel composition (S) followed a similar organ-specific trend, showing an average 36% reduction in branches of both GU hybrids under drought ($p = 0.0409$; Table 3). In contrast, the reduction was only observed in stems for GU2 (Table 2).

Table 2. Mean stem vessel density (N, n° mm⁻²), vessel diameter (Vd, µm), difference between maximum and minimum vessel diameter (Vdif, µm), vessel lumen area (Va, µm²), lumen fraction (F), vessel size distribution (S, mm⁴), fiber length (µm), fiber diameter (Ftd, µm), fiber lumen diameter (Fld, µm), fiber lumen fraction (Ff), and fiber wall thickness (Fwt, µm) in *E. grandis* (GG), *E. grandis* × *camaldulensis* (GC), *E. grandis* × *tereticornis* (GT), and *E. grandis* × *urophylla* (GU1 and GU2) clones under well-watered (WW) and water-restricted (WR) conditions. Data are presented as mean ± standard error (SE) or median with interquartile range (IQR), according to data distribution. Lowercase letters denote significant differences between treatments within each clone (*p* < 0.05), determined by Tukey’s HSD test for parametric variables (N, Vd, Vdif, F, Ftd, Fld, Ff) and Dunn’s post hoc test for non-parametric variables (Va, S, Fl, Fwt).

Clone	Water Regime	Conductive Elements					Biomechanical Support					
		N (n° mm ⁻²)	Vd (µm)	Vdif (µm)	Va (µm ²)	F (Unitless)	S (mm ⁴)	Fl (µm)	Ftd (µm)	Fld (µm)	Ff (Unitless)	Fwt (µm)
GG	WW	35.03 b	141.40 a	133.82 a	19,099 a	0.19 a	4.5 × 10 ⁻⁴ a	728.27 a	22.14 a	14.05 a	0.63 a	4.05 b
	WR	61.37 a	116.36 b	123.37 a	14,498 b	0.15 b	1.9 × 10 ⁻⁴ b	647.39 b	16.32 b	5.80 b	0.36 b	5.26 a
GC	WW	36.17 b	140.32 a	154.24 a	18,281 a	0.18 a	3.8 × 10 ⁻⁴ a	797.31 a	19.43 a	9.28 a	0.48 a	5.08 a
	WR	63.75 a	115.47 b	127.24 b	12,361 b	0.15 a	1.5 × 10 ⁻⁴ b	804.62 a	14.88 b	4.64 b	0.32 b	5.12 a
GT	WW	34.25 b	137.18 a	136.29 a	21,635 a	0.21 a	4.8 × 10 ⁻⁴ a	796.97 a	15.83 a	7.43 a	0.47 a	4.23 a
	WR	53.60 a	117.56 b	135.75 a	17,650 a	0.18 a	2.9 × 10 ⁻⁴ b	754.49 a	12.38 b	5.53 b	0.45 a	4.29 a
GU1	WW	45.81 b	113.99 a	162.30 a	16,297 a	0.23 a	2.9 × 10 ⁻⁴ a	721.65 a	17.16 a	10.98 a	0.64 a	3.14 a
	WR	62.73 a	115.98 a	151.81 a	16,181 a	0.16 b	2.1 × 10 ⁻⁴ a	669.08 b	14.70 b	6.99 b	0.58 a	3.86 a
GU2	WW	34.97 b	130.94 a	152.82 a	17,705 a	0.22 a	4.2 × 10 ⁻⁴ a	705.04 a	17.48 a	10.35 a	0.60 a	3.47 a
	WR	55.60 a	113.39 a	147.44 a	15,602 a	0.18 b	2.3 × 10 ⁻⁴ b	593.60 b	14.24 b	6.98 b	0.49 a	3.63 a
SE		4.28	4.70	13.29	1409	0.015	0.50 × 10 ⁻⁴	25.12	0.43	0.67	0.03	0.40

Table 3. Mean branch vessel density (N, n° mm⁻²), vessel diameter (Vd, µm), difference between maximum and minimum vessel diameter (Vdif, µm), vessel lumen area (Va, µm²), lumen fraction (F), vessel size distribution (S, mm⁴), fiber length (µm), fiber diameter (Ftd, µm), fiber lumen diameter (Fld, µm), fiber lumen fraction (Ff), and fiber wall thickness (Fwt, µm) in *E. grandis* (GG), *E. grandis* × *camaldulensis*, *E. grandis* × *tereticornis*, and *E. grandis* × *urophylla* clones under well-watered (WW) and water-restricted (WR) conditions. Data are presented as mean values ± standard error (SE) or median with interquartile range (IQR), according to data distribution. Lowercase letters denote significant differences between treatments within each clone (*p* < 0.05), determined by Tukey’s HSD test for parametric variables (N, Vd, Vdif, F, Ftd, Fld, Ff) and Dunn’s post hoc test for non-parametric variables (Va, S, Fl, Fwt).

Clone	Water Regime	Conductive Elements					Biomechanical Support					
		N (n° m ⁻²)	Vd (µm)	Vdif (µm)	Va (µm ²)	F (Unitless)	S (mm ⁴)	Fl (µm)	Ftd (µm)	Fld (µm)	Ff (Unitless)	Fwt (µm)
GG	WW	80.36 b	101.36 a	92.03 a	9661 a	0.25 a	9.2 × 10 ⁻⁵ a	593.07 a	12.04 a	6.33 a	0.46 a	3.74 a
	WR	109.56 a	77.06 b	97.85 a	9335 a	0.15 a	9.6 × 10 ⁻⁵ a	477.07 b	12.52 a	5.50 a	0.46 a	3.25 a
GC	WW	89.93 a	87.40 a	83.78 a	7080 a	0.15 a	6.2 × 10 ⁻⁵ a	636.08 a	13.27 a	6.22 a	0.47 a	3.52 b
	WR	82.17 a	86.14 a	55.16 b	7526 a	0.15 a	6.5 × 10 ⁻⁵ a	590.76 a	13.28 a	5.36 a	0.41 b	3.96 a
GT	WW	83.17 a	98.21 a	99.99 a	9362 a	0.13 a	9.8 × 10 ⁻⁵ a	648.94 a	14.99 a	5.95 a	0.40 a	4.04 b
	WR	82.13 a	84.44 a	70.47 b	6698 b	0.17 a	6.3 × 10 ⁻⁵ a	616.59 a	12.66 b	4.59 b	0.36 b	4.52 a
GU1	WW	74.70 a	97.47 a	105.62 a	8876 a	0.17 a	9.3 × 10 ⁻⁵ a	597.67 a	12.04 a	4.78 a	0.40 a	3.63 a
	WR	85.93 a	90.15 a	96.21 a	8240 b	0.14 b	7.1 × 10 ⁻⁵ b	472.76 b	12.52 a	5.07 a	0.40 a	3.73 a
GU2	WW	81.17 a	97.70 a	80.12 a	9109 a	0.17 a	8.7 × 10 ⁻⁵ a	563.74 a	12.38 a	4.22 a	0.30 a	3.71 a
	WR	87.33 a	77.43 b	63.23 a	5843 b	0.12 b	5.7 × 10 ⁻⁵ b	434.04 b	13.45 a	4.50 a	0.34 a	4.04 a
SE		9.30	3.90	11.11	637	0.02	4.76 × 10 ⁻⁶	16.79	0.99	0.70	0.03	0.39

3.2.2. Anatomical Characteristics of Xylem Fibers

In stems, fiber length (Fl) varied significantly among clones ($p < 0.0001$) and between water regimes ($p = 0.024$). However, red gum hybrids, which exhibited the highest Fl, were not affected by the drought treatment in this variable (Table 2). Fiber diameter (Ftd) decreased markedly under drought conditions ($p < 0.0001$), with the most significant reductions observed in *E. grandis* (28%) and the GC clone (25%). The GC clone also had the highest Ftd ($19.23 \pm 0.82 \mu\text{m}$), whereas the lowest was recorded in GT ($14.11 \pm 0.82 \mu\text{m}$). A similar but more pronounced pattern was observed for fiber lumen diameter (Fld), with the GG clone showing a 50% reduction from $14.05 \mu\text{m}$ in well-watered plants to $5.80 \pm 0.70 \mu\text{m}$ under drought. The clones exhibited a reduction in the fiber lumen fraction (Ff) of varying degrees, with significant differences in GC and the most pronounced in the GG clone (Table 2). Additionally, GG was the only clone to show an increase in fiber cell wall thickness (Fwt) under drought, with a 30% rise (Table 2).

In branches, fiber length (Fl) was also highest in the red gum hybrids, averaging 15% greater length than in the other clones, and—as observed in stems—remained unaffected by water drought. In contrast, the remaining clones exhibited a 21% reduction in Fl ($p < 0.0001$). The GT hybrid was the only clone to exhibit significant reductions in fiber diameter (Ftd), fiber lumen diameter (Fld), and fiber lumen fraction (Ff), accompanied by a 12% increase in fiber wall thickness (Fwt) in response to drought. A similar increase in Fwt was also observed in the GC clone (Table 3).

Overall, drought caused greater anatomical variation in stems than in branches, particularly in terms of fiber traits. In stems, drought led to reductions in fiber diameter and fiber lumen size across clones, while an increase in cell wall thickness was exclusive to GG. In branches, fiber length remained stable in red gum hybrids, which also exhibited an increase in Fwt. In contrast, reductions in Ftd and Fld under drought were detected only in the GT hybrid.

3.3. Relationship Between Anatomical Traits and Wood Density

The models developed to predict wood basic density using stem and branch data identified stem fiber length (Fl) and total fiber diameter (Ftd) as significant predictors of stem wood density in the studied clones. These variables had the highest associated t -values, indicating a stronger contribution to the model. Both showed a positive linear relationship with wood density (Table 4). In contrast, the model for branch wood density did not yield statistically significant coefficients ($p > 0.05$).

Table 4. Coefficients and associated statistics from multiple linear regression models predicting stem wood density based on anatomical variables in stems of *E. grandis* (GG), *E. grandis* \times *camaldulensis*, *E. grandis* \times *tereticornis*, and *E. grandis* \times *urophylla* clones under well-watered (WW) and water-restricted (WR) conditions.

Predictor Variable	Coef	SE	LI (95%)	LS (95%)	t	p -Value	R^2
const	422.11	6.55	287.60	556.61	6.44	<0.0001	
Fwt	9.53	5.61	−1.98	21.05	1.70	0.1009	
Fl	0.17	0.07	0.02	0.32	2.37	0.0254	0.58
Ftd	−11.15	2.21	−15.67	−6.62	−5.06	<0.0001	
Vd	0.37	0.33	−0.31	1.05	1.12	0.2733	

3.4. Theoretical Hydraulic Conductivity

Under drought conditions, the theoretical specific hydraulic conductivity (ks_{theo}) decreased significantly in both stems ($H = 29.45$, $p = 0.00054$) and branches ($H = 24.89$, $p = 0.0031$). However, the magnitude and significance of this reduction varied between

plant organs and among clones. In stems, significant decreases were observed in the clones GG, GC, and GU2, with GU2 showing the most pronounced decline (up to 64%). In branches, significant reductions in $k_{s_{theo}}$ occurred in water-stressed plants of the GG, GU1, and GU2 clones. It is worth noting that the *E. grandis* clone (GG) exhibited the most severe decline overall, with a 67% reduction in branches (Table 5).

Table 5. Mean theoretical hydraulic specific conductivity ($k_{s_{theo}}$, $\text{kg s}^{-1} \text{m}^{-1} \text{MPa}^{-1}$) in stems and branches of *E. grandis* (GG), *E. grandis* × *canaldulensis* (GC), *E. grandis* × *tereticornis* (GT), and *E. grandis* × *urophylla* (GU1 and GU2) clones under well-watered (WW) and water-restricted (WR) conditions. Values are presented as mean ± standard error (SE). Different lowercase letters indicate significant differences between treatments within each clone (ANOVA, $p < 0.05$).

Clone	Water Regime	Stem Theoretical k_s ($\text{kg s}^{-1} \text{m}^{-1} \text{MPa}^{-1}$)	Branch Theoretical k_s ($\text{kg s}^{-1} \text{m}^{-1} \text{MPa}^{-1}$)
GG	WW	7.42 ± 0.84 a	2.14 ± 0.39 a
	WR	3.46 ± 0.92 b	0.71 ± 0.16 b
GC	WW	7.20 ± 1.03 a	1.07 ± 0.11 a
	WR	3.32 ± 0.51 b	1.10 ± 0.11 a
GT	WW	6.54 ± 0.93 a	1.06 ± 0.48 a
	WR	4.59 ± 0.58 a	1.80 ± 0.21 a
GU1	WW	6.00 ± 1.13 a	1.68 ± 0.26 a
	WR	3.60 ± 0.82 a	1.33 ± 0.07 b
GU2	WW	8.66 ± 1.28 a	1.66 ± 0.11 a
	WR	3.13 ± 0.64 b	0.75 ± 0.15 b

In the same plants, the maximum specific hydraulic conductivity ($k_{s_{max}}$) was measured in apical stem segments after embolism removal, as previously reported by [32]. A significant correlation (Pearson's r) was found between measured stem $k_{s_{max}}$ and theoretical k_s across all clones and treatments ($r = 0.60$; $p = 6.8 \times 10^{-5}$). Clone-specific analyses revealed the strongest correlation in GU1 ($r = 0.86$; $p = 0.010$) and GU2 ($r = 0.76$; $p = 0.015$). In contrast, the GC clone showed the weakest but still highly significant correlation ($r = 0.51$; $p = 0.024$), suggesting a weaker relationship between hydraulic conductivity and the studied vessel traits. Intermediate correlation values were observed in clones GG ($r = 0.63$; $p = 0.009$) and GT ($r = 0.67$; $p = 0.007$). Similar correlations were observed between $k_{s_{max}}$ and $k_{s_{theo}}$ within each water regime, with $r = 0.70$ ($p < 0.0001$) under drought conditions and $r = 0.65$ ($p < 0.0001$) in well-watered plants.

Additionally, the regression slopes of these parameters versus the vessel-related parameter F , which quantifies the lumen fraction at the tissue level, were consistently lower in branches than in stems across all clones (Figure 1A). Although F values were similar between organs within each clone (x -axis of Figure 1; mean values in Tables 2 and 3), the $k_{s_{theo}}$ was higher in stems than in branches for a given F (Figure 1) across WW and WR plants. However, in clones GG and GU2, the relationship between $k_{s_{theo}}$ and F differed between stems developed under drought and control conditions. For a given lumen fraction and comparable variability, drought-stressed stems exhibited lower $k_{s_{theo}}$ values, as indicated by reduced regression slopes (red lines in Figure 1). Despite F remaining relatively stable or even increasing under drought, $k_{s_{theo}}$ decreased substantially, leading to functional convergence between stressed stems and branches in these clones (Figure 1).

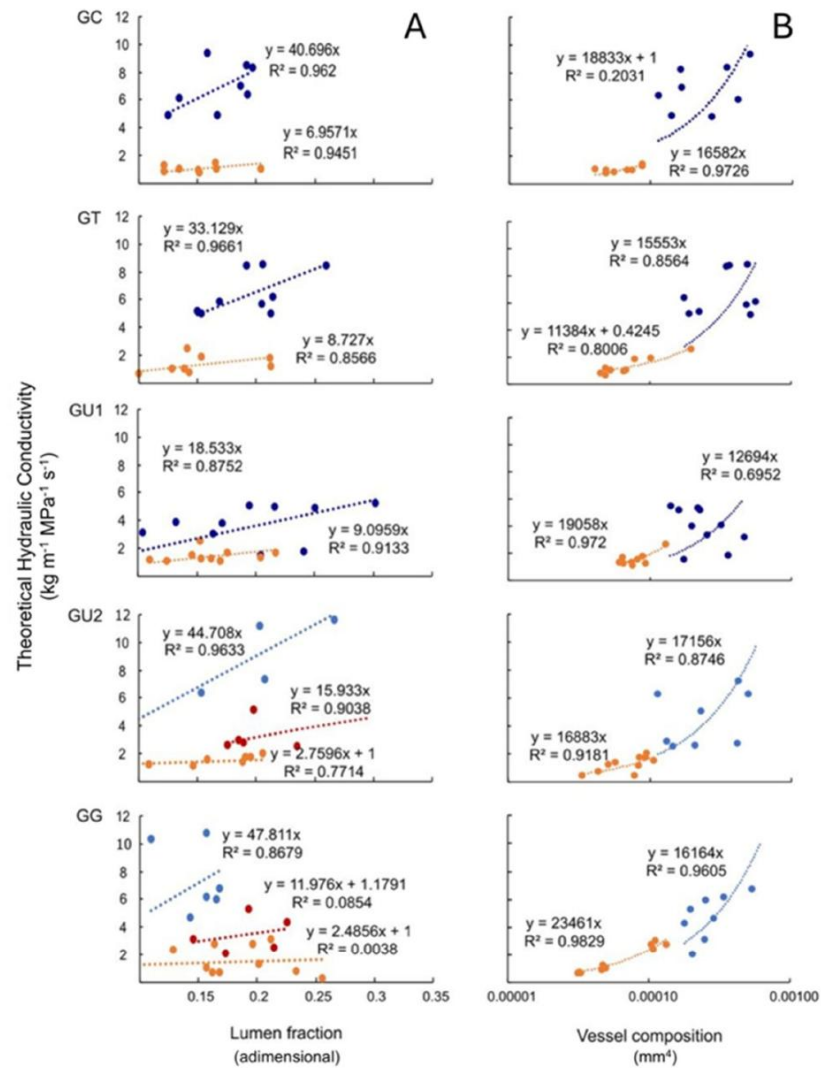


Figure 1. Relationship between theoretical specific conductivity ($k_{s,theo}$, $\text{kg s}^{-1} \text{m}^{-1} \text{MPa}^{-1}$) and vessel lumen fraction (F , unitless), and vessel composition (S , mm^4) in stems (dark blue) and branches (orange) of five *Eucalyptus* clones: *E. grandis* (GG), *E. grandis* \times 528 *camaldulensis* (GC), *E. grandis* \times *tereticornis* (GT), and *E. grandis* \times *urophylla* (GU1 and GU2). Each row corresponds to a different clone; panels A and B within each row show the respective relationships for that genotype. Regressions lines include both well-watered and water-restricted treatments, due to consistent patterns, except for stems of GG and GU2, which are shown separately. In these cases, light blue symbols represent stems from well-watered plants and red symbols represent stems from water-restricted plants. Note that S is plotted on a log₁₀ scale to account for magnitude differences between stems and branches.

In contrast to F , which presents similar ranges in stem and branches, S , which quantifies the size distribution or composition of vessels, was consistently lower in branches than stems within each clone. Theoretical k_S increased with the logarithm of S across both organs and irrigation treatments in all clones (Figure 1B). As a whole, these results indicate that the total amount of lumen space is not the most important determinant of conductivity but rather how that space is distributed across different vessel sizes and numbers.

3.5. Multivariate Analyses

Exploratory cluster analysis distinguished two main groups, consisting of WW and WR individuals of all clones. Within each group, the GC clone appeared as the most differentiated, while the remaining clones clustered differently depending on the irrigation treatment (Section S1). The PCA explained a relatively low percentage of variability, with the first three principal components (PC1, PC2, and PC3) accounting for 48.1% of the total variance (Figure 2). When irrigation treatments were not considered, the GC clone was separated from the GG clone, being more closely associated with a higher $k_{S_{max}}$, height growth, stem and branch wood density, and fiber wall thickness. The confidence intervals of both GU clones overlapped with those of the GG clone, and GT was not differentiated from the GC clone (Section S2). When irrigation treatments were taken into account, as in the cluster analysis, two distinct groups were separated along the x -axis: all the clones grown under well-watered conditions clustered on the center-right, while those subjected to water-restricted conditions were grouped on the left (Figure 2). PC1 (Dim1 in right panel of Figure 2 and Section S2), which explained the highest percentage of the variance and most effectively separated the two groups, was primarily associated with vessel number (VN), vessel diameter (Vd), vessel composition (S), and fiber diameter (Ftd) in one or both organs (stems and/or branches). Vessel number was higher in drought-stressed plants, whereas fiber diameter was greater in well-watered individuals.

Within these general groupings, however, some clones were further differentiated, mainly along the y -axis of the first biplot (PC1 and PC2). Among WR plants, the GC clone (upper left) was clearly separated from the others (lower left). In addition, within this group of four clones, the GG clone (orange in Figure 2) was distinguished from GT (green). The WR-GC clone was associated with a higher maximum hydraulic conductivity ($k_{S_{max}}$), stem wood density (WD_{st}), and fiber wall thickness (Fwt_{st}), traits that reflect a combination of high hydraulic efficiency and safety. In contrast, the WR-GG and WR-GU clones were associated with a higher vessel number (VN) and lumen fraction (VF) in stem tissues. Notably, in these WR clones, higher lumen fractions did not correspond to higher theoretical k_S values (Figure 1, red dots and lines).

On the other hand, among WW plants, the red gum clones (GC and GT) occupied a similar region in the biplot and were associated with a greater diameter growth (RGd) and longer fiber length (Fl) in both stems and branches. In contrast, the GG and both GU clones grouped together and were associated with a broader range of vessel diameter (Vdrange) (Figure 2). The second biplot (Dim1 and Dim3) did not distinguish clones within each irrigation treatment; however, the two main groups remain separated along the x -axis.

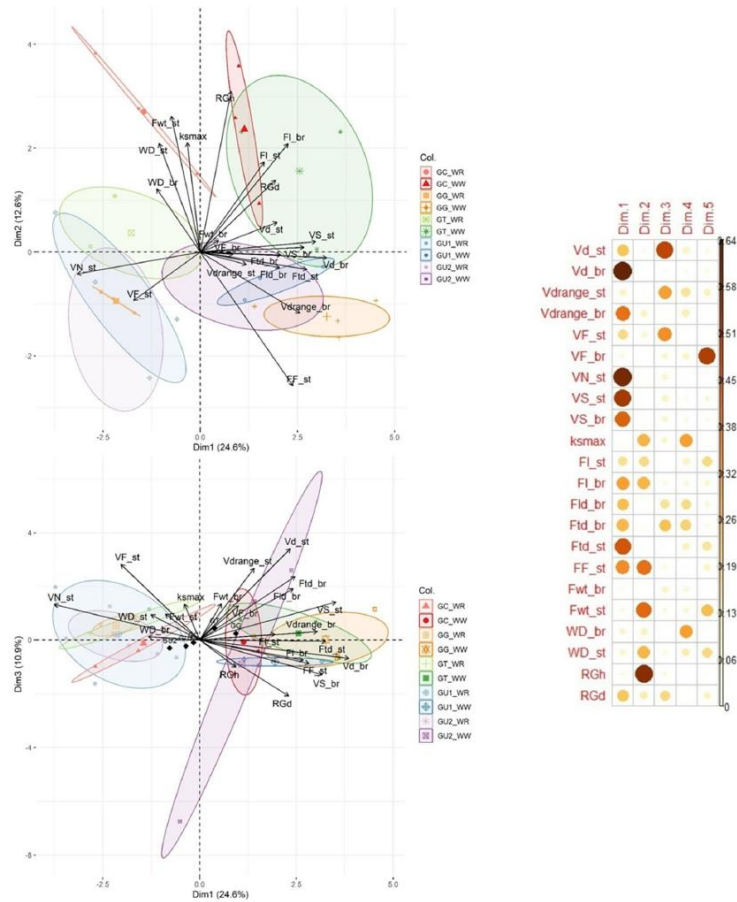


Figure 2. Principal component analysis. Left panels show biplots of PC1 (Dim1) vs. PC2 (Dim2), and PC1 (Dim1) vs. PC3 (Dim3). Right panels display the relative contribution (larger circles and darker color indicate larger contribution) of each trait to the first three principal components (percentages of each contribution are provided in Sections S1–S3). Points represent clone means, with confidence intervals, under well-watered (WW) and water-restricted (WR) conditions. Colors indicate clones: *E. grandis* (GG), *E. grandis* × *camaldulensis* (GC), *E. grandis* × *tereticornis* (GT), and *E. grandis* × *urophylla* (GU1, GU2). Black diamonds represent the average of each clone irrespective of the irrigation treatment. Vd_st: stem vessel diameter, Vd_br: branch vessel diameter, Vdrange_st: stem vessel diameter range, Vdrange_br: branch vessel diameter range, VF_st: stem vessel lumen fraction, VF_br: branch vessel lumen fraction, VN_st: stem vessel frequency, VS_st: stem hydraulic space index, VS_br: branch hydraulic space index, ksmax: stem specific hydraulic conductivity after embolism removal, FL_st: stem fiber length, FL_br: branch fiber length, Fld_br: branch fiber lumen diameter, Fld_st: stem fiber diameter, Ffd_st: stem fiber diameter, FF_st: stem Fld/Fdt ratio, Fwt_br: branch fiber cell wall thickness, Fwt_st: stem fiber cell wall thickness, WD: branch wood basic density, WD_st: stem wood basic density, RGh: plant height relative growth, RGd: stem diameter relative growth.

4. Discussion

In this study, we investigated the effects of drought on anatomical and functional variation in xylem traits across commercial *E. grandis* (GG) clones and their hybrids *E. grandis* × *camaldulensis* (GC), *E. grandis* × *tereticornis* (GT), and *E. grandis* × *urophylla* (GU). We assessed changes in conductive and supportive xylem elements of stems and branches to gain a better picture of whole-plant hydraulic responses to drought. By quantifying vessel and fiber traits, theoretical hydraulic conductivity, and wood density, we identified structural adjustments with potential hydraulic consequences, highlighting xylem plasticity under drought stress. These results were then analyzed in light of other functional and performance traits of the exact clones previously reported by [32].

In that earlier work, red gum hybrids (GC and GT) exhibited higher transpiration rates, osmotic or elastic adjustments in foliar tissues, and a greater percentage loss of conductivity (PLC), likely due to their water-spending strategy. Despite their common physiological patterns, superior stem growth under drought conditions was only observed in the GC clone. In contrast, the GG clone exhibited a more drought-avoidant strategy, characterized by tighter stomatal regulation, resulting in low in situ cavitation, as indicated by the lowest PLC, and lower growth. GU hybrids displayed conservative water-use traits similar to those of the GG clone. However, they achieved greater stem growth under drought, specially GU1, suggesting a more favorable trade-off between hydraulic safety and growth [32]. In the present study, we observed that, although all the clones showed relatively common general responses to drought at the xylem level, differing in the magnitude rather than the direction of the changes, xylem traits of the GC clone were the most differentiated, with values suggesting both high efficiency (high theoretical ks) and safety (high wood density and fiber wall reinforcement). In the following sections, we discuss the observed trends of the studied traits in the different clones and their potential implications to explain their performance under well-watered and drought conditions.

4.1. Response of Xylem Traits to Drought

As revealed by the individual traits integrated through the multivariate analyses, the main variation observed in the xylem traits across clones and water availability treatments was primarily associated with the latter: all clones clustered according to the irrigation treatment. However, we identified some differences within them, which are discussed in Section 4.1.1. Overall, well-watered conditions were associated with larger vessels, longer and wider fibers, a broader range of vessel sizes (Vdif), and a higher vessel composition (S). In contrast, drought conditions resulted in a higher wood density, thickness of fiber walls, vessel frequency, and vessel lumen fraction (F). This general pattern was expected, as traits associated with hydraulic efficiency were primarily expressed in clones under well-watered conditions.

Conversely, traits associated with xylem safety were linked to clones grown under drought conditions. This suggests that plasticity at the xylem level (both the size and distribution of vessels and fibers and wood density) tends to maximize safety under drought, probably resulting in a general trade-off between efficiency and safety when considering all clones together. The significant drought-induced plasticity observed in several traits, at least within some clones, contrasts with the lack of wood anatomical variation between sites with contrasting aridity reported by [22], who compared seven eucalypt species growing both in wet and dry native forest sites. However, our findings are consistent with studies on *Eucalyptus* commercial genotypes, which have revealed relatively high xylem sensitivity to water availability, particularly in vessel traits, fiber characteristics, and wood density [53,54].

4.1.1. Differential Responses at Clone Level

Anatomical differences among clones help explain their divergent hydraulic strategies. In GC and GT hybrids, stem wood density was the highest, approximately 25% greater than that of the GG clone, which exhibited the lowest values. Moreover, stem wood density increased in response to drought in these two clones, whereas it remained unchanged in the other three (Table 1). This increase in density was likely associated with thicker cell walls and smaller lumen areas in conductive and/or supportive xylem elements. Such anatomical changes likely improved mechanical strength and enhanced resistance to cavitation under low water potential [8,10]. Red gum hybrids, differentiated from other clones, also maintain a relatively constant vessel lumen fraction (F) under drought, even when presenting a reduced vessel diameter (Vd), as seen in the GG clone (Table 2). Besides the mean vessel diameter, in GT, this adjustment occurred without changing the vessel diameter range (Vdif), which, in turn, was reduced in the GC clone, as well as in all the other clones. In eucalypts, it has been shown that a larger amplitude in vessel sizes is correlated with both higher ks and resistance to cavitation [27,55]. The implications of the observed maintenance in stem lumen fraction on theoretical ks are discussed below.

In contrast, the GG clone exhibited substantial changes in fiber traits in response to drought, including a 65% reduction in fiber lumen diameter (Fld) and a 30% increase in fiber wall thickness (Fwt), as well as adjustments in vessel lumen mean size and distribution. Besides the functional implications of those changes, the marked sensitivity of fiber characteristics—although not reflected in whole-stem wood density—may have important implications for the wood industrial properties of *E. grandis*, as suggested for *E. globulus* [54].

GU hybrids exhibited an intermediate behavior between red gum hybrids and the GG clone (Tables 1 and 2), with no changes in stem wood density and a decrease in vessel lumen fraction—similar to the GG clone—; an increase in vessel frequency, as observed in all the clones; and a uniquely stable mean and range of vessel sizes (diameter and area) and composition (S). In terms of stem fiber plasticity, some traits varied similarly to the GG clone (i.e., reduced fiber length) and others similar to the red gums (no change in fiber fraction and wall thickness). It is important to note, however, that although the GU clones behaved somewhat similarly (i.e., they were grouped in the PCA), their xylem (this study) and growth [32] responses to drought were not identical (i.e., in addition to some differences at the univariate level, the cluster analyses grouped them in the control conditions but not under drought). This finding is in agreement with previous studies on hybrids of *E. grandis* with *E. urophylla* in South Africa, which showed a large variation in drought responses among hybrids related in a variable way to the xylem anatomy of the clones [34].

In summary, some clones exhibited significant variation in wood density in response to drought (red gums), while others varied in their fiber sizes, lumen diameter, or wall thickness. Overall, these shifts resulted in a greater proportion of cell wall material per unit volume, probably increasing the mechanical strength of the wood but also allowing higher internal tensions due to drought in all the clones. It is probable that these changes are accompanied by other compensatory anatomical strategies focused on vessel size modulation and pit architecture to minimize the cavitation risk, as has been described for other taxa [56,57]. However, the implications of the observed changes in functional terms (xylem safety) require measurements of vulnerability to cavitation that are still lacking in the studied clones.

4.1.2. Differential Responses at Organ Level

Most of the previous analysis was focused on the observed changes at the stem level. However, our results reveal organ-specific adjustments in xylem anatomy under drought conditions, adding an extra layer of complexity to understanding the plastic changes that

a plant can display in response to water availability. These changes varied among clones, reflecting genotype-specific strategies that influenced wood anatomy and basic density in both stems and branches, ultimately leading to differences in hydraulic function.

Wood density was, on average, 25% higher in branches than in stems. This higher density in distal organs likely reflects an adaptive strategy to enhance hydraulic safety where the risk is greater due to higher tension during water flux [58]. However, the degree of differentiation between organs varied among the clones and the water availability treatments, with the highest differentiation between stem and branch in the GC clone under well-water conditions and in the GG clone under drought stress. A large difference in wood density between the stem and branches has been described for adult trees in *E. grandis*, larger than in *E. viminalis* and *E. globulus*, suggesting a high degree of hydraulic segmentation in this species [12].

As discussed in the previous section, the observed changes in xylem traits indicate a greater investment in mechanical reinforcement under drought [59]. However, they may also imply a reduced capacity for hydraulic compensation [60]. Although we did not directly compare xylem traits between organs, our findings suggest potential functional differentiation: stems appear to prioritize hydraulic conductivity, while branches may emphasize hydraulic safety. In this regard, under drought, wood density increased in both organs, but with a more pronounced rise in branches (11%), doubling the response observed in stems across clones. To validate this hypothesis, further studies focusing on detailed anatomical traits, especially vessel pit structure and distribution, are needed. These traits are crucial in mediating the trade-off between hydraulic efficiency and safety under drought conditions [27,61].

One limitation of this study is the exclusion of root development parameters. This decision was based on the inherent constraints of pot cultivation under greenhouse conditions, which often induce atypical root architectures, such as root circling and limited lateral expansion, which do not accurately reflect the conditions experienced by field-grown trees. These artificial constraints may mask genuine genotypic differences in root traits between *Eucalyptus* hybrids and *E. grandis* [62,63]. Furthermore, pot size can significantly influence water and nutrient availability, introducing additional variability that complicates the interpretation of belowground responses [64]. Since the main objective of this study was to evaluate aboveground growth and physiological performance, root traits were intentionally excluded to avoid confounding effects associated with artificial root restriction. Future studies conducted under field conditions or using root observation systems may help clarify potential genotype-specific differences in root development.

4.2. Vessel Architecture and Hydraulic Efficiency of the Studied Clones

The response of theoretical specific conductivity ($k_{S_{theo}}$) to vessel composition (S) was consistent across clones and organs, indicating a stable functional relationship. However, S values were ten times higher in stems than in branches, reflecting significant anatomical differences despite this conserved pattern. As noted by [21], the size distribution of vessels influences the trade-off between hydraulic efficiency and safety by affecting both redundancy and the risk of embolism spread. Higher S values typically indicate fewer, wider, and more interconnected vessels, which enhances conductivity but increases vulnerability to cavitation. In contrast, lower S values reflect narrower, more numerous, and less connected vessels, which favor safety by limiting the propagation of embolism.

Under drought, S declined by an average of 35% in GU hybrid branches and in stems of all clones except GU1, with a notable 60% reduction in GC. These changes suggest a shift toward greater safety at the cost of efficiency. While these patterns are broadly applicable to angiosperms, interpretation in eucalypts must consider their predominance of solitary

vessels. *Eucalyptus* xylem anatomy is complex [65], with cell types such as vasicentric tracheids and fiber-tracheids playing functional roles [27,55]. Further research is needed on these components.

Regarding the relationship between $k_{S_{theo}}$ and the lumen fraction (F), in contrast to common patterns across stems and branches about S, $k_{S_{theo}}$ was consistently higher in stems than in branches for a given F value in all clones. This suggests that the distribution of vessel sizes (quantified in S) rather than the total amount of lumen space may be crucial to understanding the variation in xylem efficiency across clones and organs. Therefore, a plastic change in S could imply an important change in hydraulic conductivity, even if a similar lumen fraction is maintained. In this regard, in a study of stems of adult trees of three *Eucalyptus* species, Barotto et al. [12] found a higher relative impact of F than S on their $k_{S_{theo}}$. However, the degree of variation among and within species was much larger in S than in F, suggesting that the last is a more conservative feature within eucalypts xylem. In this study, GG and GU2 clones modified both F and S under drought. Red gum hybrids changed only S, while GU1 adjusted only F. These contrasting patterns highlight the diversity of anatomical responses among clones.

On the other hand, clones GG and GU2 exhibited an additional behavior in response to drought compared to the other three clones. In these clones, for a given stem F value, $k_{S_{theo}}$ was significantly lower in drought-stressed than in well-irrigated plants, as shown by reduced regression slopes. This suggests high plasticity in stem hydraulic function, with greater efficiency loss than in other clones. Notably, the lumen fraction remained stable or increased under drought, yet $k_{S_{theo}}$ declined, indicating a decoupling between anatomical investment and hydraulic performance. This response suggests that stems of these two clones under drought adopt xylem traits more similar to those of branches, indicating an adaptive vascular reconfiguration. Comparable patterns of organ-specific plasticity have been reported in *Cunninghamia* sp., where xylem shifts mediated hydraulic variation across organs under water stress [16].

In stems, $k_{S_{theo}}$ showed a moderate-to-strong correlation ($r = 0.58$) with measured $k_{S_{max}}$ from our previous study. In xylem research, this magnitude is considered a strong correlation [66], with vessel lumen size alone explaining ~60% of the $k_{S_{max}}$ variation. The remaining ~40% may be attributed to traits such as pit type and density, perforation plates, and the presence of non-functional vessels, which affect overall conductivity beyond vessel dimensions. In addition to these vessel characteristics, it is important to consider that other cell types participate in water (and air) movement in eucalypts. As previously noted, vasicentric tracheids may enhance both hydraulic efficiency and safety in eucalypts, acting as conductive bridges for water and barriers to the spread of embolism [55].

4.3. Relationship Between Xylem Traits and Clones' Performance

Clone performance, measured by height and basal diameter growth, varied among genotypes under both control and drought conditions [32]. All hybrids outperformed the GG clone in height growth across both irrigation treatments. Under well-watered conditions, stem diameter growth was relatively uniform among clones; however, under drought, the GC clone outperformed the others. GU1 also performed relatively well under drought, though still below GC. Several morpho-physiological traits related to this performance were discussed in [32]. In the present complementary study, we explored associations with functional wood anatomy and density, demonstrating that xylem traits also play a critical role in explaining clone responses to drought.

Multivariate analyses identified the GC clone as the most differentiated, consistent with its superior growth under both water regimes. This strong performance challenges the commonly reported trade-off between high growth potential and stress resistance [64].

In this study, GC exhibited xylem characteristics and plasticity indicative of both high hydraulic efficiency and safety, likely supporting sustained water flux to leaves under tension, despite high conductivity losses, as previously shown for this clone and its parental species *E. camaldulensis* [61]. Notably, PCA grouped both red gum hybrids under well-watered conditions but not under drought conditions, aligning with the poor drought performance of the GT clone despite its physiological similarities with GC [32].

The shared anisohydric behavior of red gums hybrids supports a fast-growth strategy under water-limited conditions [4]. However, GT's stem diameter growth under drought did not match that of GC, likely reflecting differences in biomass allocation patterns. In terms of xylem traits, GT exhibited lower vessel plasticity compared to GC, as indicated by a narrower range of vessel diameters and areas, which allowed it to maintain theoretical stem-level hydraulic conductivity ($k_{s,theo}$) under drought. Although elevated $k_{s,theo}$ may favor efficient water transport, it may not offset the risk-prone stomatal behavior characteristic of red gum hybrids. Further investigation into the plasticity of vulnerability to cavitation is needed to determine whether GT's limited vessel adjustment also reflects constrained plasticity in hydraulic safety. While restricted cavitation plasticity has been documented in *Eucalyptus* branches [31] and *E. obliqua* leaves [6], few studies have addressed this trait across a range of pure and hybrid *Eucalyptus* clones. Additional evidence is needed to clarify whether vulnerability to cavitation represents a conservative trait across these genotypes.

The GG clone exhibited several anatomical adjustments indicative of marked plasticity in response to drought. Previous studies have reported high anatomical variability in adult plants of other *E. grandis* clones, suggesting considerable xylem plasticity under environmental stress [12]. However, in GG, these adjustments, while likely enhance xylem safety, did not prevent the strong stomatal control observed, in contrast to the looser regulation in red gum hybrids [32]. Water-restricted GG plants exhibited the lowest percent loss of conductivity (PLC) among all clones, even lower than their well-irrigated counterparts [32], suggesting that xylem modifications facilitated efficient dehydration avoidance. Nonetheless, this conservative strategy came at the cost of the lowest growth.

Although GU1 and GU2 shared several xylem traits and clustered together in the PCA, the clone exhibiting superior diameter growth under drought (GU1) showed a distinct pattern of stem-level vessel plasticity, as evidenced by the relationship between the theoretical k_s and vessel lumen fraction (Figure 1). Moreover, GU1 increased branch wood density in response to drought, whereas GU2 did not exhibit any change. While these traits alone may not fully account for GU1's enhanced performance under water-limited conditions, they clearly distinguish it from GU2. Comparable variation among GU hybrids has previously been reported [34], highlighting the importance of evaluating each new commercial clone independently to assess its adaptive potential under contrasting water availability.

In conclusion, this study reveals a range of xylem strategies exhibited by the studied clones that partially resemble their growth responses to drought. Inherent values and differential plasticity of xylem traits in branches and stems contribute to understanding the complex mechanisms involved in the drought performance of pure vs. hybrid clones.

5. Conclusions

This study demonstrates that drought elicits anatomically and functionally distinct responses among five commercially relevant *Eucalyptus* clones, reflecting divergent hydraulic strategies under water-limited conditions. In particular, red gum hybrids (*E. grandis* × *camaldulensis* and *E. grandis* × *tereticornis*) sustained the theoretical specific hydraulic conductivity during drought by maintaining the vessel lumen fraction while reducing the vessel diameter, especially in branch xylem. This combination, along with increased wood density, indicates a conservative hydraulic strategy that balances conductivity and

safety. Among the tested genotypes, the *E. grandis* × *camaldulensis* clone exhibited the most distinct xylem profile, characterized by a high theoretical conductivity co-occurring with an elevated wood density, suggesting a potential for both efficient water transport and resistance to hydraulic failure. These characteristics are in agreement with its better growth performance under different water availabilities, as previously reported.

In contrast, the pure species (*E. grandis*) and certain hybrids (e.g., *E. grandis* × *urophylla*) exhibited signs of vascular adjustment under drought, marked by reductions in both vessel lumen fraction (F) and composition (S), despite a stable or even increased individual vessel area. These anatomical shifts were associated with significant declines in theoretical hydraulic conductivity. Such patterns underscore the role of hybridization with drought-adapted species in enhancing xylem resilience and maintaining the water transport capacity under stress. By integrating organ-level anatomical and functional analyses, this study advances the understanding of wood formation dynamics in response to drought and offers valuable criteria for the selection of drought-adaptive genotypes suited to future climate scenarios.

Future research should further explore the contrasting patterns of hydraulic regulation between stems and branches to determine inherent differences in hydraulic architecture among *Eucalyptus* clones. A deeper understanding of this axial variation, together with the genotype-specific plasticity observed in xylem traits, will be essential for elucidating the mechanisms underlying drought adaptation and for refining selection criteria in breeding programs targeting water-limited environments.

Supplementary Materials: The following supporting information can be downloaded at <https://www.mdpi.com/article/10.3390/f16081267/s1>, Figure S1: Cluster analysis of clones based on Euclidean distance and dissimilarity; Figure S2: Principal component analysis results; Figure S3: Relative contributions of measured variables to the first three principal components (PC1, PC2, and PC3) based on PCA; Table S1: Mean stem basal area (BA) increment, calculated from the difference in the diameter between the start of the treatment and the end of the study. Standard deviation (SD) is also shown.

Author Contributions: Conceptualization, J.G., M.E.F. and J.G.-T.; data curation: J.G.; formal analysis: J.G., M.E.F. and M.N.; methodology: J.G., M.E.F. and J.G.-T.; funding acquisition: J.G.; investigation: J.G., M.N. and P.T.; writing—original draft preparation, J.G. and M.E.F.; writing—review and editing, J.G., M.E.F., S.R. and J.G.-T.; software: M.E.F. and M.N.; validation: J.G.; visualization, J.G. and M.N.; supervision, M.E.F. and J.G.; project administration, J.G. All authors have read and agreed to the published version of the manuscript.

Funding: This research was funded by the Comisión Sectorial de Investigación Científica, Universidad de la República (Uruguay), through the Programa Iniciación a la Investigación 2017, grant ID233.

Data Availability Statement: The datasets generated and/or analyzed during the current study are available from the corresponding author on reasonable request.

Acknowledgments: Plant material was kindly provided by Lumin Forest Products Company (Tacuarembó, Uruguay). We thank Roberto Scoz and INIA (Instituto Nacional de Investigación Agropecuaria) for their technical support throughout this study, as well as the Unidad de Posgrados y Educación Permanente of the Facultad de Agronomía for its continuous academic support. We would also like to acknowledge Silvia Monteoliva (CONICET, Universidad Nacional de La Plata, Argentina) for her expert and valuable advice on xylem anatomical methodologies and analysis and Lucía Delgado Vázquez for her selfless help with the multivariate analyses carried out using R software. The authors used ChatGPT (OpenAI version 2024) and Grammarly Premium (Grammarly Inc., version 2023) solely for language editing and text improvement, with all suggestions being supervised and carefully evaluated.

Conflicts of Interest: The authors declare no conflicts of interest. The funders had no role in the design of this study; in the collection, analyses, or interpretation of data; in the writing of the manuscript; or in the decision to publish the results.

Appendix A

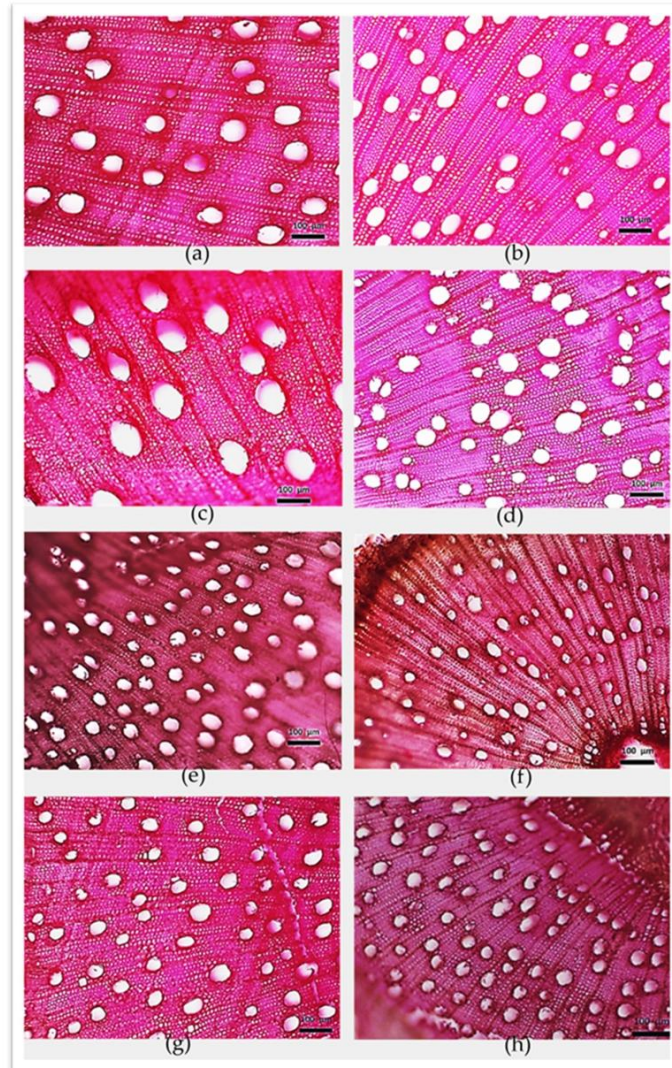


Figure A1. Cross-sectional images illustrating conduits, fibers, and rays in (a,b) stems of *E. grandis* (GG), (c,d) *E. grandis* × *urophylla* (GU2), and branches of (e,f) *E. grandis* × *tereticornis* (GT) and (g,h) *E. grandis* (GG) clones. (Left) panels show well-watered conditions, and (Right) panels depict drought conditions.

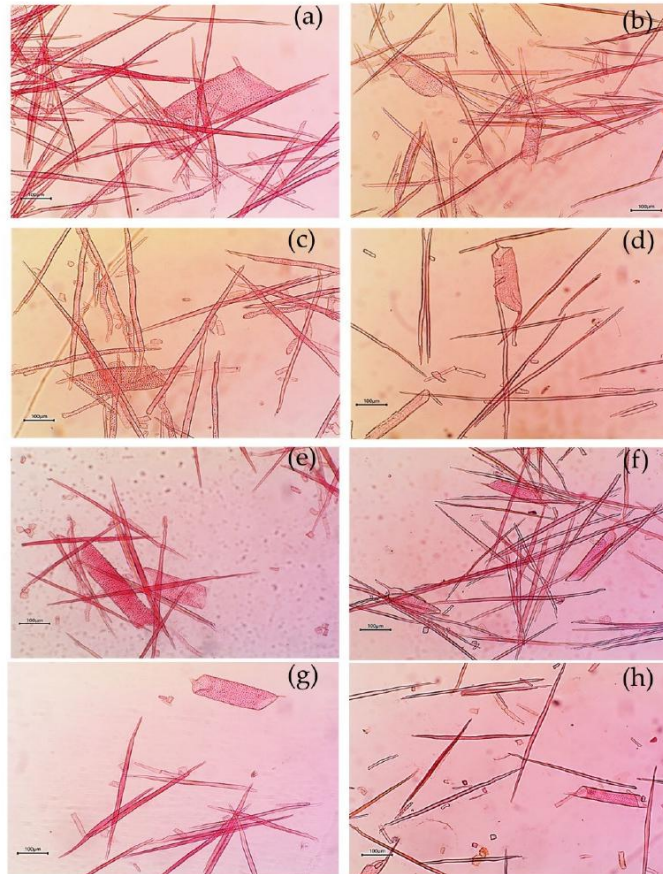


Figure A2. Images of macerates illustrating fibers and vessels in (a,b) stems of *E. grandis* × *urophylla* (GU2) and (c,d) *E. grandis* (GG), and in branches of (e,f) *E. grandis* × *E. camaldulensis* (GC) and (g,h) *E. grandis* × *urophylla* (GU1). (Left) panels show well-watered conditions, and (Right) panels depict drought conditions.

References

1. Zhang, Y.; Wang, X. Geographical spatial distribution and productivity dynamic change of *Eucalyptus* plantations in China. *Sci. Rep.* **2021**, *11*, 19764. [CrossRef]
2. Linderman, T.; Plata, V.; Sancho, D.; Oyhantcabal, W. *Clima de Cambios*; Oyhantcabal, W., Sancho, D., Galván, M., Eds.; FAO, Ministerio de Ganadería, Agricultura y Pesca, República Oriental del Uruguay: Montevideo, Uruguay, 2013; Available online: <https://www.fao.org/4/as256s/as256s.pdf> (accessed on 9 June 2025).
3. IPCC. *Climate Change 2023: Synthesis Report. Contribution of Working Groups I, II and III to the Sixth Assessment Report of the Intergovernmental Panel on Climate Change*; Core Writing Team, Lee, H., Romero, J., Eds.; IPCC: Geneva, Switzerland, 2023. [CrossRef]
4. Tyree, M.T.; Zimmermann, M.H. *Xylem Structure and the Ascent of Sap*, 2nd ed.; Springer: Berlin, Germany, 2002; ISBN 978-3-642-07768-5. [CrossRef]

5. Choat, B.; Jansen, S.; Brodribb, T.J.; Cochard, H.; Delzon, S.; Bhaskar, R.; Bucci, S.J.; Feild, T.S.; Gleason, S.M.; Hacke, U.G.; et al. Global convergence in the vulnerability of forests to drought. *Nature* **2012**, *491*, 752–755. [[CrossRef](#)]
6. Pritzkow, C.; Williamson, V.; Szota, C.; Trouvé, R.; Arndt, S.K. Phenotypic plasticity and genetic adaptation of functional traits influences intra-specific variation in hydraulic efficiency and safety. *Tree Physiol.* **2019**, *40*, 215–229. [[CrossRef](#)]
7. McDowell, N.; Pockman, W.T.; Allen, C.D.; Breshears, D.D.; Cobb, N.; Kolb, T.; Plaut, J.; Sperry, J.; West, A.; Williams, D.G.; et al. Mechanisms of plant survival and mortality during drought: Why do some plants survive while others succumb to drought? *New Phytol.* **2008**, *178*, 719–739. [[CrossRef](#)] [[PubMed](#)]
8. Hacke, U.G.; Sperry, J.S.; Pockman, W.T.; Davis, S.D.; McCulloh, K.A. Trends in wood density and structure are linked to prevention of xylem implosion by negative pressure. *Oecologia* **2001**, *126*, 457–461. [[CrossRef](#)]
9. Lens, F.; Sperry, J.S.; Christman, M.A.; Choat, B.; Rabaey, D.; Jansen, S. Testing hypotheses that link wood anatomy to cavitation resistance and hydraulic conductivity in the genus *Acer*. *New Phytol.* **2011**, *190*, 709–723. [[CrossRef](#)] [[PubMed](#)]
10. Jacobsen, A.L.; Ewers, F.W.; Pratt, R.B.; Paddock III, W.A.; Davis, S.D. Do xylem fibers affect vessel cavitation resistance? *Plant Physiol.* **2005**, *139*, 546–556. [[CrossRef](#)]
11. Pratt, R.B.; Jacobsen, A.L.; Ewers, F.W.; Davis, S.D. Relationships among xylem transport efficiency, vulnerability to embolism, and wood density of nine Rhamnaceae of the California chaparral. *New Phytol.* **2007**, *173*, 217–225. [[CrossRef](#)]
12. Barotto, A.J.; Monteoliva, S.; Gyenge, J.; Martínez-Meier, A.; Moreno, K.; Tesón, N.; Fernández, M.E. Wood density and anatomy of three *Eucalyptus* species: Implications for hydraulic conductivity. *For. Syst.* **2017**, *26*, e010. [[CrossRef](#)]
13. Martínez-Vilalta, J.; Prat, E.; Oliveras, I.; Piñol, J. Xylem hydraulic properties of roots and stems of nine Mediterranean woody species. *Oecologia* **2002**, *133*, 19–29. [[CrossRef](#)] [[PubMed](#)]
14. Zimmermann, J.; Link, R.M.; Hauck, M.; Leuschner, C.; Schuldt, B. 60-year record of stem xylem anatomy and related hydraulic modification under increased summer drought in ring- and diffuse-porous temperate broad-leaved tree species. *Trees* **2021**, *35*, 919–937. [[CrossRef](#)]
15. Soro, A.; Lenz, P.; Roussel, J.R.; Nadeau, S.; Pothier, D.; Bousquet, J.; Achim, A. The phenotypic and genetic effects of drought-induced stress on wood specific conductivity and anatomical properties in white spruce seedlings, and relationships with growth and wood density. *Front. Plant Sci.* **2023**, *14*, 1297314. [[CrossRef](#)]
16. Li, Y.; Huang, Y.; Zheng, Y.; Zhang, J.; Zou, Y.; Heal, K.R.; Zhou, Y. Xylem plasticity of root, stem, and branch in *Cunninghamia lanceolata* under drought stress: Implications for whole-plant hydraulic integrity. *Front. Plant Sci.* **2024**, *15*, 10910014. [[CrossRef](#)]
17. Liu, H.; Ye, Q.; Gleason, S.M.; He, P.; Yin, D. Weak trade-off between xylem hydraulic efficiency and safety: Climatic seasonality matters. *New Phytol.* **2021**, *229*, 1440–1452. [[CrossRef](#)]
18. Anderegg, W.R.L.; Klein, T.; Bartlett, M.; Sack, L.; Pellegrini, A.F.A.; Choat, B.; Jansen, S. Meta-analysis reveals that hydraulic traits explain cross-species patterns of drought-induced tree mortality across the globe. *Proc. Natl. Acad. Sci. USA* **2016**, *113*, 5024–5029. [[CrossRef](#)]
19. Johnson, D.M.; Katul, G.; Domec, J.C. Catastrophic hydraulic failure and tipping points in plants. *Plant Cell Environ.* **2022**, *45*, 2073–2084. [[CrossRef](#)] [[PubMed](#)]
20. Li, S.; Wang, J.; Lu, S.; Salmon, Y.; Liu, P.; Guo, J. Trade-off between hydraulic safety and efficiency in plant xylem and its influencing factors. *Forests* **2023**, *14*, 1817. [[CrossRef](#)]
21. Zanne, A.E.; Westoby, M.; Falster, D.S.; Ackerly, D.D.; Loarie, S.R.; Arnold, S.E.J.; Coomes, D.A. Angiosperm wood structure: Global patterns in vessel anatomy and their relation to wood density and potential conductivity. *Am. J. Bot.* **2010**, *97*, 207–215. [[CrossRef](#)]
22. Pfautsch, S. Hydraulic anatomy and function of trees—Basics and critical developments. *Curr. For.* **2016**, *2*, 236–248. [[CrossRef](#)]
23. White, D.A.; Turner, N.C.; Galbraith, J.H. Leaf water relations and stomatal behavior of four allopatric *Eucalyptus* species planted in Mediterranean southwestern Australia. *Tree Physiol.* **2000**, *20*, 1157–1165. [[CrossRef](#)]
24. Searson, M.J.; Thomas, D.S.; Montagu, K.D.; Conroy, J.P. Leaf water use efficiency differs between *Eucalyptus* seedlings from contrasting rainfall environments. *Funct. Plant Biol.* **2004**, *31*, 441–450. [[CrossRef](#)]
25. Whitehead, D.; Beadle, C.L. Physiological regulation of productivity and water use in *Eucalyptus*: A review. *For. Ecol. Manag.* **2004**, *193*, 113–140. [[CrossRef](#)]
26. Trifiló, P.; Nardini, A.; Lo Gullo, M.A.; Barbera, P.; Savi, T.; Raimondo, F. Diurnal changes in embolism rate in nine dry forest trees: Relationships with species-specific xylem vulnerability, hydraulic strategy and wood traits. *Tree Physiol.* **2015**, *35*, 694–705. [[CrossRef](#)]
27. Fernández, M.E.; Barotto, A.J.; Martínez-Meier, A.; Monteoliva, S. New insights into wood anatomy and function relationships: How *Eucalyptus* challenges what we already know. *For. Ecol. Manag.* **2019**, *454*, 117638. [[CrossRef](#)]
28. Peters, J.M.R.; López, R.; Nolf, M.; Hutley, L.B.; Wardlaw, T.; Cernusak, L.A.; Choat, B. Living on the edge: A continental-scale assessment of forest vulnerability to drought. *Glob. Change Biol.* **2021**, *27*, 3620–3641. [[CrossRef](#)] [[PubMed](#)]

29. Zhang, Z.Z.; Zhao, P.; Oren, R.; McCarthy, H.R.; Niu, J.F.; Zhu, L.W.; Ni, G.Y.; Huang, Y.Q. Water use strategies of a young *Eucalyptus urophylla* forest in response to seasonal change of climatic factors in South China. *Biogeosci. Discuss.* **2015**, *12*, 10469–10510.
30. López Lauenstein, D.A.; Fernández, M.E.; Verga, A.R. Drought stress tolerance of *Prosopis chilensis* and *Prosopis flexuosa* species and their hybrids. *Trees Struct. Funct.* **2013**, *27*, 285–296. [CrossRef]
31. Van der Willigen, C.; Pammenter, N.W. Relationship between growth and xylem hydraulic characteristics of clones of *Eucalyptus* spp. at contrasting sites. *Tree Physiol.* **1998**, *18*, 595–600. [CrossRef] [PubMed]
32. Gándara, J.; Ni6n, M.; González-Tálice, J.; Ross, S.; Villar, J.; Fernández, M.E. Similar but unique: Physiological response to drought and growth of pure species and interspecific hybrid clones of *Eucalyptus*. *Trees* **2025**, *39*, 36. [CrossRef]
33. Saunders, A.; Drew, D.M. Measurements done on excised stems indicate that hydraulic recovery can be an important strategy used by *Eucalyptus* hybrids in response to drought. *Trees* **2022**, *36*, 139–151. [CrossRef]
34. Crous, C.J.; Greyling, I.; Wingfield, M. Dissimilar stem and leaf hydraulic traits suggest varying drought tolerance among co-occurring *Eucalyptus grandis* × *E. urophylla* clones. *South. For.* **2018**, *80*, 175–184. [CrossRef]
35. Keret, R.; Drew, D.M.; Hills, P.N. Xylem Cell Size Regulation Is a Key Adaptive Response to Water Deficit in *Eucalyptus grandis*. *Tree Physiol.* **2024**, *44*, tpa108. [CrossRef]
36. Pfautsch, S.; Aspinwall, M.; Drake, J.; Chacon-Doria, L.; Langelaan, R.J.A.; Tissue, D.T.; Tjoelker, M.G.; Lens, F. Traits and trade-offs in whole-tree hydraulic architecture along the vertical axis of *Eucalyptus grandis*. *Ann. Bot.* **2018**, *121*, 129–141. [CrossRef]
37. Wheeler, J.K.; Sperry, J.S.; Hacke, U.G.; Hoang, N. Inter-vessel pitting and cavitation in woody Rosaceae and other vesselless plants: A basis for a safety versus efficiency trade-off in xylem transport. *Plant Cell Environ.* **2005**, *28*, 800–812. [CrossRef]
38. Lamy, J.B.; Delzon, S.; Bouche, P.S.; Alia, R.; Vendramin, G.G.; Cochard, H.; Plomion, C. Limited genetic variability and phenotypic plasticity detected for cavitation resistance in a Mediterranean pine. *New Phytol.* **2014**, *201*, 874–886. [CrossRef]
39. Momo, S.T.; Libalah, M.B.; Rossi, V.; Fonton, N.; Mofack, G.I.; Kamdem, N.G.; Nguetsop, V.F.; Sonké, B.; Ploton, P.; Barbier, N. Using volume-weighted average wood specific gravity of trees reduces bias in aboveground biomass predictions from forest volume data. *For. Ecol. Manag.* **2018**, *424*, 519–528. [CrossRef]
40. Swenson, N.G.; Enquist, B.J. The relationship between stem and branch wood specific gravity and the ability of each measure to predict leaf area. *Am. J. Bot.* **2008**, *95*, 516–519. [CrossRef] [PubMed]
41. Williamson, G.B.; Wiemann, M.C. Measuring wood specific gravity correctly. *Am. J. Bot.* **2010**, *97*, 519–524. [CrossRef]
42. Dadzie, P.K.; Amoah, M.; Frimpong-Mensah, K.; Shi, S.Q. Comparison of density and selected microscopic characteristics of stem and branch wood of two commercial trees in Ghana. *Wood Sci. Technol.* **2016**, *50*, 91–104. [CrossRef]
43. Monteoliva, S.; Barotto, A.J.; Alarc6n, P.; Tes6n, N.; Fern6ndez, M.E. Wood density as an integrating variable of wood anatomy: Analysis of branches and stem in four species of *Eucalyptus*. *Rev. Fac. Agron.* **2017**, *116*, 1–11.
44. Olson, M.E.; Rossell, J.A. Vessel diameter-stem diameter scaling across woody angiosperms and the ecological causes of xylem vessel diameter variation. *New Phytol.* **2012**, *197*, 1204–1213. [CrossRef]
45. Arnaud, C.; Brancheriau, L.; Sabatier, S.-A.; Heinz, C.; Chaix, G.; Tomazello Filho, M. Interactions between the mechanical and hydraulic properties of *Eucalyptus* trees under different environmental conditions of fertilization and water availability. *BioResources* **2019**, *14*, 7157–7168. [CrossRef]
46. Pulido-Rodr6guez, E.; L6pez-Camacho, R.; Torres, J.; Velasco, E.; Negret, B.S. Traits and trade-offs of wood anatomy between trunks and branches in tropical dry forest species. *Trees* **2020**, *34*, 497–505. [CrossRef]
47. Allen, R.G.; Pereira, L.S.; Raes, D.; Smith, M. *Crop Evapotranspiration: Guidelines for Computing Crop Water Requirements*; FAO Irrigation and Drainage Paper No. 56; FAO: Rome, Italy, 1998; 300p.
48. Sperry, J.S.; Hacke, U.G.; Oren, R.; Comstock, J.P. Water deficits and hydraulic limits to leaf water supply. *Plant Cell Environ.* **2002**, *25*, 251–263. [CrossRef] [PubMed]
49. Di Rienzo, J.A.; Casanoves, F.; Balzarini, M.G.; Gonzalez, L.; Tablada, M.; Robledo, C.W. *InfoStat Versi6n 2020*; Grupo InfoStat, FCA, Universidad Nacional de C6rdoba: C6rdoba, Argentina, 2020.
50. Navure Team. Navure (v2.6.1): A Data-Science-Statistic Oriented Application for Making Evidence-Based Decisions. 2023. Available online: <http://www.navure.com> (accessed on 5 June 2025).
51. RStudio Team. *R Studio: Integrated Development Environment for R*; RStudio, PBC: Boston, MA, USA, 2022; Available online: <https://posit.co/products/open-source/rstudio> (accessed on 20 May 2025).
52. Husson, F.; Josse, J.; L6, S.; Mazet, J. FactoMineR: Factor Analysis and Data Mining with R.; R Package Version 1.04; 2007. Available online: <http://CRAN.R-project.org/package=FactoMineR> (accessed on 26 May 2025).
53. Drew, D.M.; Pammenter, N.W. Vessel frequency, size and arrangement in two eucalypt clones growing at sites differing in water availability. *N. Z. J. For.* **2006**, *51*, 23–28.
54. Drew, D.M.; Downes, G.M.; O’Grady, A.P.; Read, J.; Worledge, D. High-resolution temporal variation in wood properties in irrigated and non-irrigated *Eucalyptus globulus*. *Ann. For. Sci.* **2009**, *66*, 406. [CrossRef]

55. Barotto, A.J.; Fernandez, M.E.; Gyenge, J. First insights into the functional role of vasicentric tracheids and parenchyma in *Eucalyptus* species with solitary vessels: Do they contribute to xylem efficiency or safety? *Tree Physiol.* **2016**, *36*, 1485–1497. [[CrossRef](#)]
56. Schreiber, S.G.; Hacke, U.G.; Hamann, A. Intraspecific Variation in Xylem Vessel Diameter in *Populus tremuloides* across a Climate Gradient. *Funct. Ecol.* **2015**, *29*, 1278–1289. [[CrossRef](#)]
57. Lourenço, J., Jr.; Enquist, B.J.; von Arx, G.; Sonsin-Oliveira, J.; Morino, K.; Thomaz, L.D.; Milanez, C.R.D. Hydraulic Trade-Offs Underlie Local Variation in Tropical Forest Functional Diversity and Sensitivity to Drought. *New Phytol.* **2022**, *235*, 1815–1830. [[CrossRef](#)]
58. Ziemirńska, K.; Westoby, M.; Wright, I.J. Broad anatomical variation within a narrow wood density range—A study of twig wood across 69 Australian angiosperms. *Plants* **2015**, *4*, 325–347. [[CrossRef](#)]
59. Longui, E.; Rajput, K.S.; Galvão de Melo, A.C.; de Araújo Alves, L.; do Nascimento, C.B. Root to branch wood anatomical fvariation and its influence on hydraulic conductivity in five Brazilian Cerrado species. *Bosque* **2017**, *38*, 183–193. [[CrossRef](#)]
60. MacFarlane, D. W. Functional Relationships Between Branch and Stem Wood Density for Temperate Tree Species in North America. *Front. For. Glob. Change* **2020**, *3*, 63. [[CrossRef](#)]
61. Barigah, T.S.; Gyenge, J.E.; Barreto, F.; Rozenberg, P.; Fernández, M.E. Narrow vessels cavitate first during a simulated drought in *Eucalyptus camaldulensis*. *Physiol. Plant.* **2021**, *173*, 2081–2090. [[CrossRef](#)] [[PubMed](#)]
62. Poorter, H.; Bühler, J.; van Dusschoten, D.; Climent, J.; Postma, J.A. Pot size matters: A meta-analysis of the effects of rooting volume on plant growth. *Funct. Plant Biol.* **2012**, *39*, 839–850. [[CrossRef](#)]
63. Kharkina, T.G.; Ottosen, C.-O.; Rosenqvist, E. Effects of root restriction on the growth and physiology of cucumber plants. *Physiol. Plant.* **1999**, *105*, 434–441. [[CrossRef](#)]
64. NeSmith, D.S.; Duval, J.R. The effect of container size. *HortTechnology* **1998**, *8*, 495–498. [[CrossRef](#)]
65. Dadswell, H.E. *The Anatomy of Eucalypt Wood*; Technical Paper No. 66; Forest Products Laboratory, Division of Applied Chemistry, CSIRO: Melbourne, Australia, 1972; p. 36.
66. Gleason, S.M.; Butler, D.W.; Ziemirńska, K.; Waryszak, P.; Westoby, M. Stem xylem conductivity is key to plant water balance across Australian angiosperm species. *Funct. Ecol.* **2012**, *26*, 343–352. [[CrossRef](#)]

Disclaimer/Publisher's Note: The statements, opinions and data contained in all publications are solely those of the individual author(s) and contributor(s) and not of MDPI and/or the editor(s). MDPI and/or the editor(s) disclaim responsibility for any injury to people or property resulting from any ideas, methods, instructions or products referred to in the content.

4. Diferencias en el estado hídrico, eficiencia del uso del agua y crecimiento en híbridos clonales de *Eucalyptus grandis*, durante temporadas de crecimiento con distinto régimen de precipitaciones

4.1. Resumen

Objetivo del estudio: Analizar el estado hídrico foliar y la eficiencia en el uso del agua en clones comerciales de *E. grandis* e híbridos interespecíficos durante dos temporadas de crecimiento consecutivas con diferente régimen de precipitaciones.

Área de estudio: El trabajo se llevó a cabo en el norte de Uruguay.

Métodos: Se instaló un ensayo de bloques al azar con clones de *E. grandis*, *E. grandis* × *camaldulensis*, *E. grandis* × *tereticornis* (híbridos con eucaliptos colorados), y *E. grandis* × *urophylla*. Se midió el potencial hídrico foliar en prealba (Ψ_{pd}) y al mediodía (Ψ_{md}) cada seis semanas, desde los dieciséis meses de edad de los árboles y durante dos temporadas de crecimiento (2013-2014 y 2014-2015) con un régimen de precipitaciones contrastante. Se midieron la conductancia estomática (g_s), la tasa de fotosíntesis neta (A) y la transpiración en hojas (E) una vez en cada estación de crecimiento, junto con la discriminación isotópica de carbono ($\Delta^{13}C$) y el crecimiento de los árboles. También se analizaron la densidad y distribución estomáticas.

Resultados: Los clones de *E. grandis* y *E. grandis* × *urophylla* presentaron la menor fluctuación diaria del potencial hídrico foliar ($\Delta\Psi = \Psi_{pd} - \Psi_{md}$) y una mayor regulación estomática. Además, fueron hipostomáticos, con estomas inmaduros exclusivamente en cara abaxial de las hojas. Los híbridos con eucaliptos colorados transpiraron de manera más intensa, según lo indicado por el $\Delta\Psi$, y fueron anfiestomáticos. Además, estos clones fueron menos eficientes en el uso del agua, tanto instantánea (EUA) como a integrada en el tiempo (EUAI), y mostraron un crecimiento más rápido durante la temporada de mayor precipitación (2014-2015).

Aspectos destacados de la investigación: Los híbridos con eucaliptos colorados mostraron menor regulación estomática y un patrón de distribución estomática diferente al resto de los clones. Estas características reforzaron el crecimiento diamétrico, especialmente durante la temporada de crecimiento más húmeda.

Palabras clave: híbridos de eucaliptos, conductancia estomática, eficiencia en el uso del agua, transpiración



Differential water-use efficiency and growth among *Eucalyptus grandis* hybrids under two different rainfall conditions

José Gándara (Gándara, J.)*, Silvia Ross (Ross, S.), Gastón Quero (Quero, G.), Pablo Dellacassa (Dellacassa, P.), Joaquín Dellepiane (Dellepiane, J.), Gonzalo Figarola (Figarola, G.), Luis Viega (Viega, L.)

Plant Physiology Section, Department of Plant Biology, Faculty of Agronomy, University of the Republic, Avda. Eugenio Garzón 809, Montevideo 12900 (Uruguay)

Abstract

Aim of study: To analyze the course of leaf water status, water-use efficiency and growth in *Eucalyptus grandis* and hybrids throughout seasons with different rainfall.

Area of study: The study was conducted in northern Uruguay.

Material and methods: A randomized block trial was established containing *E. grandis* (ABH17), *E. grandis* × *Eucalyptus camaldulensis* (GC172), *E. grandis* × *Eucalyptus tereticornis* (GT529), and *E. grandis* × *Eucalyptus urophylla* (GU08). Predawn leaf water potential (Ψ_{pd}) and midday leaf water potential (Ψ_{md}) were measured every six weeks from the age of 16 months, throughout two growing seasons. Stomatal conductance (g_s), net photosynthetic rate (A), and leaf-level transpiration (E) were measured once in each growing season, along with leaf carbon isotope discrimination ($\Delta^{13}C$) and tree growth. Stomatal density and distribution were studied.

Main results: ABH17 and GU08 had the lowest daily fluctuation of leaf water potential and showed stronger stomatal regulation; they were hypostomatic, and stomata on the adaxial leaf surfaces remained immature. GC172 and GT529 (Red-Gum hybrids) were amphistomatic and transpired more intensively; they were less efficient in instantaneous and intrinsic water use and grew faster under high soil moisture (inferred from rainfall). Under such conditions, GC172 reached the highest gas-exchange rate due to an increase in tree hydraulic conductance. ABH17 and GU08 were hypostomatic and used water more efficiently because of stronger stomatal regulation.

Research highlights: Red-Gum hybrids evidenced less water use efficiency due to lower stomatal regulation, different stomatal features, and distinct growth patterns as a function of soil moisture (inferred from rainfall).

Keywords: Eucalypt hybrids; stomatal conductance; water-use efficiency; transpiration.

Abbreviations used: Ψ_{pd} : predawn leaf water potential; Ψ_{md} : midday leaf water potential; $\Delta\Psi$: daily fluctuation of leaf water potential ($\Delta\Psi = \Psi_{pd} - \Psi_{md}$); A : net photosynthetic rate, E : leaf transpiration rate, g_s : stomatal conductance, WUE: instantaneous water-use efficiency; WUEi: integrated water-use efficiency; A/E : leaf photosynthesis-to-leaf transpiration ratio; $\Delta^{13}C$: leaf carbon isotope discrimination; K : tree hydraulic conductance; $E/\Delta\Psi$: ratio between leaf transpiration and daily fluctuation of leaf water potential; $\delta^{13}C$: natural abundance of ^{13}C .

Authors' contributions: JG conceived and designed the experiment, performed the analysis, collected the data and wrote the manuscript. SR, LV and GQ collected the data and reviewed the manuscript. PD, JD and GF helped to collect the data. LV supervised the work. Citation by JG, SR, GQ, PD, D, GF and LV.

Citation: Gándara, J., Ross, S., Quero, G., Dellacassa, P., Dellepiane, J., Figarola, G., Viega, L. (2020). Differential water-use efficiency and growth among *Eucalyptus grandis* hybrids under two different rainfall conditions. *Forest Systems*, Volume 29, Issue 2, e006. <https://doi.org/10.5424/fs/2020292-16011>.

Received: 10 Nov 2019 **Accepted:** 08 Jul 2020

Copyright © 2020 INIA. This is an open access article distributed under the terms of the Creative Commons Attribution 4.0 International (CC-by 4.0) License.

Funding agencies/institutions
Lumin (formerly Weyerhaeuser Uruguay S.A.)
INIA (National Agricultural Research Institute of Uruguay)
Facultad de Agronomía (Faculty of Agronomy, University of the Republic, Uruguay).

Competing interests: The authors declare no conflict of interest. The funders had no role in the design of the study; in the collection, analyses, or interpretation of data; in the writing of the manuscript, or in the decision to publish the results".

Correspondence should be addressed to José Gándara: jgandara@fagro.edu.uy

Introduction

Eucalyptus afforestation occupies 22 million hectares in more than 90 countries, being one of the most

popular woody crops in the world (Dharhi *et al.*, 2018). In Uruguay, eucalypt plantations for hardwood timber or pulpwood supply cover 70% of the Uruguayan afforested area (one million hectares) (Martin, 2018), and

in the last few years, the increase of climate variability (Linderman *et al.*, 2013) led to the selection of promising clones by crossing *Eucalyptus grandis* with *Eucalyptus urophylla* and Red-Gum species (*Eucalyptus camaldulensis* and *Eucalyptus tereticornis*). Since there is a positive correlation between carbon fixation and water loss, breeders face the challenge of selecting genotypes for high plant growth and high water-use efficiency (WUE) (Morris *et al.*, 1998; Dye, 2000; Mokotedi, 2013). However, information regarding several commercial genotypes is still lacking.

To avoid further embolism and xylem dysfunction (Tyree & Ewers, 1991; Brodrigg *et al.*, 2003; McDowell *et al.*, 2008; Sperry *et al.*, 2016), many woody species can keep leaf water potential (Ψ) relatively constant through a complex relationship between stomatal conductance (g_s), tree hydraulic conductivity and Ψ (Sperry *et al.*, 1998; Martínez-Vilalta *et al.*, 2004; Lambers *et al.*, 2008). Unlike Red-Gum species (such as *E. camaldulensis* and *E. tereticornis*), *E. grandis* displays stronger stomata control (Kallarackal & Somen, 2008), which means a higher water potential threshold for stomatal closure (~ -2.0 MPa). On the other hand, Red-Gum species are thought to grow faster and transpire more intensively than other related species (Pohjonen & Pukkala, 1990; Kallarackal & Somen, 1997; Drake *et al.*, 2012). *E. grandis* \times *E. urophylla* genotypes show stronger stomata regulation than Red-Gum hybrids and seem to be more sensitive to water stress (Eksteen *et al.*, 2013).

Generally, eucalypts exhibit high transpiration rates to enhance carbon fixation and growth, even under severe drought conditions (Lewis *et al.*, 2011). Such behavior is commonly known as anisohydric and reflects the occurrence of high transpiration rates all year round (Meinzer *et al.*, 2014). On the other hand, isohydric plants close stomata to reduce gas exchange and maintain high Ψ (Mc Dowell *et al.*, 2008). These patterns represent the two ends of the stomatal regulation sensitivity spectrum (Sade & Moshelion, 2014). Gas exchange can be inferred from leaf water potential fluctuation ($\Delta\Psi$), that is, the difference between predawn and midday bulk leaf water potential (Ψ_{pd} and Ψ_{mid} , respectively) (Choné *et al.*, 2001; Franks *et al.*, 2007), which varied as a function of soil water content and atmospheric demand (vapor pressure deficit, VPD).

Leaf-level water-use efficiency is frequently estimated by instantaneous and integrated methodologies (WUE and WUE_i, respectively). The former is the ratio of leaf photosynthesis to leaf-transpiration rate, while the latter is related to leaf carbon isotope discrimination ($\Delta^{13}\text{C}$) during gas diffusion and Rubisco-dependent reactions. In C_3 species, such as eucalypts, $\Delta^{13}\text{C}$ is negatively correlated with the ratio of transpiration efficiency and whole-plant dry-mass accumulation (Farquhar *et al.*, 1989), and a significant correlation was observed between foliar $\Delta^{13}\text{C}$ and

WUE_i in *E. grandis* (Olbrich *et al.*, 1993), *E. globulus* (Osório and Pereira, 1994), *E. camaldulensis* (Akhter *et al.*, 2005) and *E. grandis* \times *E. camaldulensis* (Le Roux *et al.*, 1996). However, $\Delta^{13}\text{C}$ may change when scaling up to stems, shoots, and whole trees (Olbrich *et al.*, 1993), and so may WUE. Moreover, WUE_i can be inferred from different plant organs, and it can be estimated as the whole-plant WUE (Seib *et al.*, 2008). Although $\Delta^{13}\text{C}$ may not be an indicator of WUE, it may be useful as a screening tool (Le Roux *et al.*, 1996). A significant relationship between foliar ^{13}C signature ($\delta^{13}\text{C}$) and instantaneous WUE in *E. grandis* was found, which could be used as a proxy for WUE (Casparus *et al.*, 2018). Water-use efficiency can also be studied from wood rings (from the trunk or branch cores), although in many species ring growth may be caused by carbon synthesized in previous growing seasons (Mc Farlane & Adams, 1998; Skomarkova *et al.*, 2006).

Stem biomass can increase without modifying WUE, as previously found by Battie-Laclau *et al.* (2016) in *E. grandis* plantations. Leaf transpiration also depends upon stomatal traits such as density and distribution, both of them varying not only among eucalypt species (David *et al.*, 1997; Morris *et al.*, 1998; Héroult *et al.*, 2013) but also between related hybrids (Eksteen *et al.*, 2013). However, little research has been done in commercial genotypes so far.

The present study was designed to analyze the course of leaf water status and leaf-level WUE in *E. grandis*, *E. grandis* \times *E. camaldulensis*, *E. grandis* \times *E. tereticornis*, and *E. grandis* \times *E. urophylla* clones, during two consecutive growing seasons with different rainfall. We hypothesized the following: (a) these genotypes differ in stem growth capacity, transpiration activity ($\Delta\Psi$), stomatal traits and leaf-level water use efficiency (WUE), as inferred either from their instantaneous WUE or leaf carbon isotope discrimination ($\Delta^{13}\text{C}$); b) that this behavior is related to different regulation of stomatal opening (g_s) and carbon fixation (A); c) this regulation modifies stem growth and varies between growing seasons as a function of soil water moisture (inferred from effective rainfall).

Materials and methods

Plant material and experiment design

Cuttings from three months old sprouts of each clone were collected in April 2012 and rooted in the clonal nursery of Lumin (formerly Weyerhaeuser Uruguay) with controlled humidity (90 to 95%). They were irrigated from May to August with a Biorend® solution (10 cm³ L⁻¹) and then transplanted into 3 L plastic pots containing Carolina Soils® substrate, a mix of sphagnum peat

(58%), vermiculite (40%), and trace minerals (2%). They were fertilized three times a week with 18-18-18 (NPK) for two months.

At the age of four months (September 2012), the plants were planted in a field trial in Tacuarembó (Uruguay; 31° 38' 15" S, 55° 54' 17" W), where the regional climate is humid subtropical (Cfa, Köppen classification system) with a mean annual rainfall of 1484 mm and an average temperature of 10.3 °C in July and 22.3 °C in January. Soils are sandy to loamy (Typic Hapludult, USDA classification system) with a poorly drained B horizon (0.35 to 0.60 m) and Fe-Mn concretions down to 1.50 m deep.

A randomized complete block design with three blocks was used. Within each of the three blocks, ten trees per clone of *E. grandis* (ABH17), *E. grandis* × *camaldulensis* (GC172), *E. grandis* × *tereticornis* (GT529), and *E. grandis* × *urophylla* (GU08) were planted in rows, at a spacing of 4.75 m × 5 m. Each row was a plot. Two trees per plot were randomly selected to assess ecophysiological variables. From the age of 16 months (December 2013), Ψ was measured every six weeks throughout two consecutive growing seasons (2013-14 and 2014-15). Diameter at breast height and tree height were measured for all trees of the trial (n=72) at the beginning and end of each growing season. Leaf gas-exchange measurements were performed once a season, as well as foliar sampling for carbon isotope analyses.

Bulk leaf water potential (Ψ_{pd} , Ψ_{md})

Leaf water potential (predawn and midday) was measured with a Schölander pressure chamber (Soil Moisture Equipment®, Santa Barbara, CA) on three current-year branchlets of each selected tree. Predawn leaf water potential (MPa) was recorded before sunrise (4:30 to 06:00 a.m.) on the lower branches. Midday leaf water potential (MPa) was measured from 12:00 to 03:00 p.m. (one hour per block) on the sunlit foliage of the upper tree crown. Average clone Ψ was calculated from three measurements of each selected tree, and the daily fluctuation of Ψ was calculated as $\Delta\Psi = \Psi_{pd} - \Psi_{md}$. We checked for block effect when analyzing the data. Atmospheric demand was used as a covariate (Faustino *et al.*, 2013) when analyzing the data effect.

Gas exchange (A , E)

Net photosynthetic rate A ($\mu\text{mol m}^{-2} \text{s}^{-1}$), stomatal conductance g_s ($\text{mmol m}^{-2} \text{s}^{-1}$), and leaf transpiration rate E ($\text{mmol m}^{-2} \text{s}^{-1}$) were measured on three current-year leaves at the top of the crown, between 11:00 a.m. and 03:00 p.m., using a portable gas-exchange device (LiCor 6400,

LiCor®, Lincoln, NE) at a photon flux density of $900.78 \pm 1.20 \mu\text{mol m}^{-2} \text{s}^{-1}$ and an airflow rate of $500.16 \pm 0.64 \text{ mL min}^{-1}$. For *E. grandis*, this irradiance is saturating (Whitehead and Beadle 2004). Measurements within each block lasted a maximum of one hour and 15 minutes, and we checked for block effect when analyzing the data. Air temperature, CO_2 level, and VPD inside the chamber matched the outside air condition. The purpose was to study gas exchange under water deficits. However, soil moisture (inferred from Ψ_{pd} value) began to decrease in autumn of the second growing season. Measurements were taken on 02/26/2014 (summer) and 05/08/2015 (autumn). The maximum air temperature during measurements was $29.25 \pm 1.84 \text{ }^\circ\text{C}$ in the first growing season and $23.90 \pm 0.95 \text{ }^\circ\text{C}$ in the second. Data were used to calculate instantaneous water-use efficiency (WUE) as the A/E ratio, and K as $E/\Delta\Psi$ ratio.

^{13}C abundance and carbon isotope discrimination

Nine leaves per tree were collected to obtain the ^{13}C signature ($\delta^{13}\text{C}$), from the same branchlets selected for gas-exchange measurements, and located on the northern (sunny) side of the trees' upper crown. Total carbon concentration and relative abundance of ^{13}C and ^{12}C were measured by mass spectrometry using a Delta Plus® spectrometer (Finnigan MAT, Bremen, Germany). Each sample was analyzed with an elemental Flash EA 112. The standard deviation of total carbon and ^{13}C were calculated from leucine as a reference. The natural abundance of ^{13}C ($\delta^{13}\text{C}$, ‰) was expressed in relation to international standard PDB as $[(R_{\text{sample}} / R_{\text{standard}}) - 1]$ (Craig, 1957), where R is the $^{13}\text{C}/^{12}\text{C}$ ratio. Data were used to calculate $\Delta^{13}\text{C}$ (‰) as $(\delta^{13}\text{C}_{\text{air}} - \delta^{13}\text{C}_{\text{leaf}}) / (1 + \delta^{13}\text{C}_{\text{leaf}} / 1000)$, being $\delta^{13}\text{C}_{\text{air}}$ the atmospheric $\delta^{13}\text{C}$ abundance and $\delta^{13}\text{C}_{\text{leaf}}$ the sample ^{13}C content (Farquhar *et al.*, 1989).

Stomatal density and distribution

The observation of these traits was not part of the original work and was considered only for the second growing season. Three one-year-old leaves per tree of similar leaf age were collected to study stomatal density (No. mm^{-2}) and distribution. Three epidermal impressions of adaxial and abaxial leaf surfaces were prepared with nail varnish; dried layers were peeled off with tweezers (modified from D'Ambrogio, 1986). Stomatal density was calculated from images taken with a Dino Eye 2.0 digital camera added to a Nikon E100 light microscope (10X). Five fields (0.15 mm^2) on each leaf surface were analyzed using DinoCapture® software.

Tree growth

Tree height (Ht, m) and diameter at breast height (Dbh, m) of all the trees in a plot were measured at the beginning of each growing season. Data were used to calculate diameter and height relative growth as $RG = (G_n - G_{n-1}) / G_{n-1}$, being G the tree Dbh or Ht, and standing tree volume (V, m³) as $V = Dbh^2 \times \pi / 4 \times Ht \times FF$, being FF the form factor. An average form factor of 0.5 was used (Da Silva *et al.*, 1999).

Statistical analysis

The effect of the differences and interactions between clone and date on the variances was tested using a two-way analysis of variance (ANOVA). Data were analyzed for homoscedasticity and normality (Shapiro Wilks, $p > 0.05$), and when these conditions were met, the ANOVA was performed using InfoStat® software (UNC, Córdoba, Argentina). Mean comparison was performed by Tukey's post hoc test ($p < 0.05$). Clone-date interaction was studied for Ψ within each growing season using VPD as a covariate. The proposed model was the following:

$$y_{ijk} = \mu + \alpha_i + \beta_j + \tau_k + (\alpha\tau)_{ik} + \gamma_l + \varepsilon_{ijkl}$$

where y_{ijk} is the response variable, μ is the overall mean, α_i is the effect of the i^{th} clone, β_j is the effect of the j^{th} block, τ_k is the effect of the k^{th} date, $(\alpha\tau)_{ik}$ is the effect of the i^{th} clone and k^{th} date, γ_l is the effect of the covariate, and ε_{ijkl} is the residual error with $\varepsilon_{ij} \sim N(0, \sigma^2\varepsilon)$.

Results

Bulk leaf water potential and rainfall

Effective rainfall was higher during the second growing season (2014-15) (Fig. 1), and Ψ_{pd} reflected such variation (Tables 1 and 2). In that season, Ψ_{pd} attained the highest average (-0.21 ± 0.01 MPa) and no clonal effect was observed. However, differences between clones appeared in the first growing season (the driest one), as *E. grandis* (ABH17) averaged the lowest value ($\Psi_{pd} = -0.66 \pm 0.03$ MPa) ($p < 0.0149$).

Unlike Ψ_{pd} , Ψ_{md} did show the clone effect ($p < 0.0001$) in both seasons, and Red-Gum hybrids had the lowest average. GT529 showed this behavior throughout both growing seasons ($\Psi_{md} = -1.96 \pm 0.08$ in the first season, and -2.45 ± 0.05 MPa in the second), whereas GC172 showed it during the wettest one ($\Psi_{md} = -2.34 \pm 0.05$ MPa). ABH17 and GU08 behaved similarly, except at the beginning of

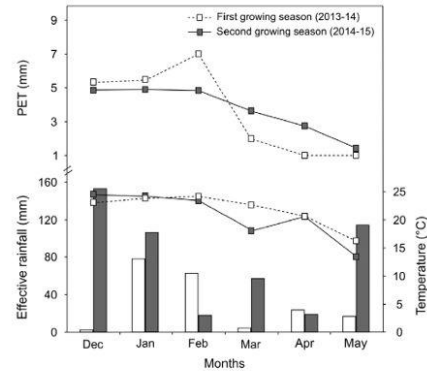


Figure 1. Environmental parameters of water supply and atmospheric demand in the experimental assay; potential evapotranspiration (PET, mm) and monthly average temperature (°C) (lines), effective rainfall (mm) recorded in the first growing season (2013-14) (white bars) and second growing season (2014-15) (gray bars) at INIA Tacuarembó Station (W 55° 58' 43"; S 31° 44' 18").

the wettest season (2013-14), when GU08 averaged the minimum value.

Clone-date interaction was significant for Ψ_{md} in both growing seasons ($p < 0.0001$), although for Ψ_{pd} , this interaction appeared during the driest season ($p < 0.0001$) (Tables 1 and 2). The daily fluctuation of leaf water potential varied among genotypes ($p < 0.0001$) and was lowest in the Red-Gum hybrids (Fig. 2). During summertime, it was 30 to 50% higher than that of the other clones.

Gas exchange and instantaneous water-use efficiency

Net photosynthetic rate (A) differed among hybrids in both growing seasons ($p < 0.0068$ and $p < 0.0001$), with the GU08 clone showing the lowest A in both study periods (12.80 and 11.91 $\mu\text{mol m}^{-2} \text{s}^{-1}$, first and second season respectively). Despite being variable, carbon fixation was similar among the other genotypes (Table 3). Stomatal conductance (g_s) also varied among clones across both growing seasons ($p < 0.0001$), when Red-Gum hybrids displayed the highest average and, therefore transpired more intensively (higher E) (Table 3). These results revealed a stronger relationship between A and g_s for the ABH17 clone during both growing seasons ($r^2 = 0.76$ in the first growing season and 0.8 in the second), and for GU08 during the first growing season ($r^2 = 0.83$) (Fig. 3). Unlike Red-Gum hybrids, these genotypes attained higher carbon fixation under low stomatal conductance (Fig. 3),

Table 1. Mean leaf predawn (Ψ_{pd}) and midday water potential (Ψ_{md}) (MPa) of *Eucalyptus grandis* (ABH17), *E. grandis* \times *E. camaldulensis* (GC172), *E. grandis* \times *E. tereticornis* (GT529) and *E. grandis* \times *E. urophylla* (GU08) clones throughout the first growing season (2013-2014), considering clones as main factor and mid-morning air vapor pressure deficit (VPD) as covariate Means within columns followed by different letters are significantly different (Tukey, $p < 0.05$), p_{VPD} and r_{VPD} for VPD covariance also shown

Clone	Second growing season (2014-15)							
	Ψ_{pd} (MPa)				Ψ_{md} (MPa)			
	Dec	Feb	Mar	May	Dec	Feb	Mar	May
ABH17	-0.53 a	-0.64 b	-0.58 a	-0.82 a	-2.01 a	-1.66 a	-1.81 a	-0.92 a
GC172	-0.67 a	-0.38 a	-0.49 a	-0.69 a	-2.30 b	-1.59 a	-2.31 b	-0.75 a
GT529	-0.69 a	-0.36 a	-0.46 a	-0.69 a	-2.29 b	-2.30 b	-2.60 b	-0.66 a
GU08	-0.68 a	-0.36 a	-0.48 a	-0.70 a	-1.92 a	-1.48 a	-1.74 a	-0.92 b
<i>p</i> -value	0.1316	<0.0001	0.2098	0.0093	0.0004	<0.0001	<0.0001	0.0005
SE	0.05	0.04	0.04	0.05	0.07	0.09	0.11	0.04
p_{VPD}	0.052				<0.0001			
r_{VPD}	0.06				-0.93			

Means within columns followed by different letters are significantly different (Tukey, $p < 0.05$), p_{VPD} and r_{VPD} for VPD covariance also shown

Table 2. Mean leaf predawn water potential (Ψ_{pd}) and midday water potential (Ψ_{md}) (MPa) of *E. grandis* (ABH17), *E. grandis* \times *E. camaldulensis* (GC172), *E. grandis* \times *E. tereticornis* (GT529) and *E. grandis* \times *E. urophylla* (GU08) clones throughout the second growing season (2014-2015), considering clones as main factor and mid-morning air vapor pressure deficit (VPD) as covariate

Clone	Second growing season (2014-15)							
	Ψ_{pd} (MPa)				Ψ_{md} (MPa)			
	Dec	Feb	Mar	May	Dec	Feb	Mar	May
ABH17	-0.22 a	-0.19 a	-0.19 a	-0.15 a	-2.33 ab	-2.05 ab	-2.16 ab	-1.94 a
GC172	-0.22 a	-0.20 a	-0.19 a	-0.17 a	-2.42 a	-2.09 ab	-2.17 ab	-2.20 a
GT529	-0.21 a	-0.19 a	-0.22 a	-0.16 a	-2.50 a	-2.36 b	-2.45 b	-2.52 a
GU08	-0.23 a	-0.21 a	-0.21 a	-0.18 a	-2.95 b	-1.72 a	-2.09 a	-2.24 a
<i>p</i> -value	0.8534	0.3835	0.3811	0.5641	<0.0001	0.0009	0.0147	0.1829
SE	0.02	0.01	0.01	0.01	0.06	0.10	0.08	0.10
p_{VPD}	0.04				<0.0001			
r_{VPD}	0.07				0.50			

Means within columns followed by different letters are significantly different (Tukey, $p < 0.05$), p_{VPD} and r_{VPD} for VPD covariance also shown

therefore showing higher instantaneous WUE (A/E ratio). In addition, there was no relationship between overall instantaneous WUE and Ψ_{md} , so WUE remained relatively constant for a wide range of Ψ_{md} .

Tree hydraulic conductance (K) ($p < 0.0001$) varied among clones only during the wettest season. In that period, GC172 had the highest average (2.02 ± 0.14 mmol m⁻² s⁻¹ MPa⁻¹) (Table 4). When comparing K between seasons, we found a higher K in the less rainy first

season (2.8 ± 0.11 vs. 1.49 ± 0.10 mmol m⁻² s⁻¹ MPa⁻¹) ($p < 0.0001$).

Carbon isotope discrimination and water-use efficiency

Red-Gum hybrids showed higher $\Delta^{13}C$ ($p < 0.0001$), suggesting less efficiency in leaf-level intrinsic water use (A/E integrated over time). In contrast, ABH17 and

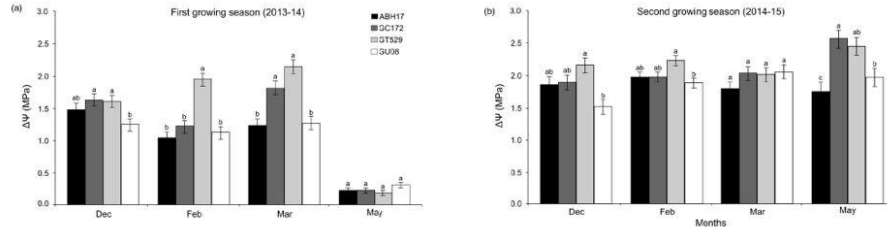


Figure 2. Mean leaf water potential gradient ($\Delta\Psi_w$, MPa) of *E. grandis* (ABH17), *E. grandis* \times *E. camaldulensis* (GC172), *E. grandis* \times *E. tereticornis* (GT529) and *E. grandis* \times *E. urophylla* (GU08) clones during the first (a) and second (b) growing season; bars topped with different letters differ statistically within the same date (Tukey, $p < 0.05$).

GU08 showed the opposite behavior, as inferred either from their higher instantaneous WUE or their lower foliar $\Delta^{13}C$ (Table 3).

Stomatal density and distribution

Stomatal density showed no clonal difference and ranged between 428 ± 82 and 340 ± 56 stomata mm^{-2} (Fig. 4). The stomatal distribution pattern did vary among clones, since Red-Gum hybrids were amphistomatous, whereas ABH17 and GU08 were hypostomatic and stomata on their upper epidermis remained entirely immature (Fig. 5).

Tree growth

Clonal difference ($p < 0.0001$) in diametric relative growth was observed in the second year of the study

(*i.e.*, during the wettest growing season). By then, the *E. grandis* \times *camaldulensis* (GC172) clone had the highest diametric relative increment (0.23 ± 0.01), whereas *E. grandis* \times *urophylla* (GU08) showed the lowest one (0.07 ± 0.01). On the other hand, differences in height growth appeared during the driest year of the study (the first growing season), but they did not affect volumetric tree growth (all clones averaged $0.065 \pm 5.8 \times 10^{-3} \text{ m}^3$; data not shown). However, differences in stem volume were observed at the end of the study, when GU08 averaged the lowest value (Tables 5 and 6).

Discussion

Leaf water potential and transpiration

Leaf bulk water potential and transpiration reflected the differences in soil moisture (inferred from the effective

Table 3. Mean net photosynthetic rate (A , $\mu\text{molCO}_2 \text{ m}^{-2} \text{ s}^{-1}$), stomatal conductance (g_s , $\text{molH}_2\text{O m}^{-2} \text{ s}^{-1}$), transpiration rate (E , $\text{molH}_2\text{O m}^{-2} \text{ s}^{-1}$), instantaneous water-use efficiency ($\mu\text{molCO}_2 \text{ m}^{-2} \text{ s}^{-1} / \text{molH}_2\text{O m}^{-2} \text{ s}^{-1}$) and foliar carbon isotope discrimination ($\Delta^{13}C$, ‰) of *E. grandis* (ABH17), *E. grandis* \times *E. camaldulensis* (GC172), *E. grandis* \times *E. tereticornis* (GT529) and *E. grandis* \times *E. urophylla* (GU08) clones

Clone	n	First growing season (2013-14)					Second growing season (2014-15)				
		A	g_s	E	WUE	$\Delta^{13}C$	A	g_s	E	WUE	$\Delta^{13}C$
ABH17	10	17.49 a	0.13 b	3.51 bc	4.98 a	21.77 b	13.89 ab	0.11 c	2.20 c	6.31 a	20.93 b
GC172	17	17.18 ab	0.18 a	4.13 ab	4.14 ab	23.42 a	15.94 a	0.30 a	4.85 a	3.28 c	22.25 a
GT529	17	18.28 a	0.17 a	4.67 a	3.91 b	23.30 a	15.27 a	0.18 b	3.40 b	4.49 b	21.88 a
GU08	14	12.80 b	0.09 b	2.84 c	4.51 ab	20.32 c	11.91 b	0.10 c	2.05 c	5.81 a	20.47 b
p -value		0.0068	<0.0001	<0.0001	0.02	<0.0001	<0.0001	<0.0001	<0.0001	<0.0001	<0.0001
SE		1.07	0.01	0.24	0.22	0.16	0.60	0.01	0.13	0.22	0.16

Means within columns followed by different letters are significantly different (Tukey, $p < 0.05$), standard error of the mean (SE) also shown

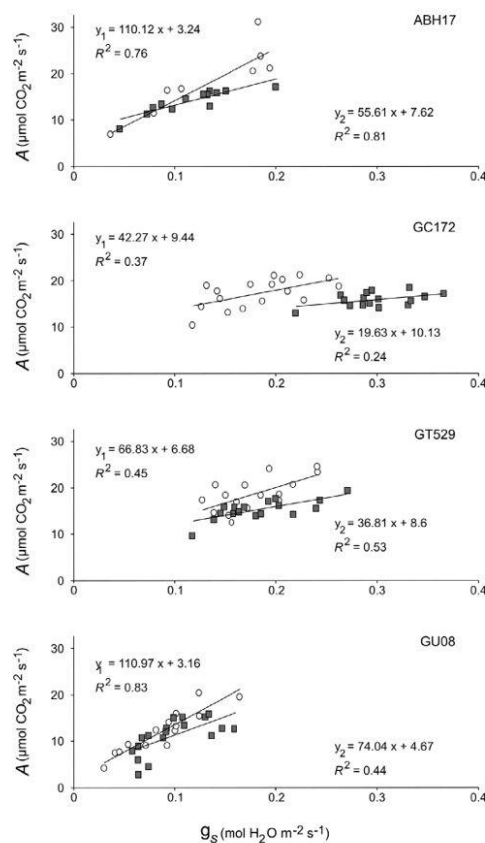


Figure 3. Relationship between net photosynthetic rate (A) and stomatal conductance (g_s) of (a) *E. grandis* (ABH17), (b) *E. grandis* \times *E. camaldulensis* (GC172), (c) *E. grandis* \times *E. tereticornis* (GT529) and (d) *E. grandis* \times *E. urophylla* (GU08) clones in the first and second growing season (circles and squares, respectively); regression equations for both growing seasons also shown (y_1 and y_2 , first and second respectively)

rainfall). During the wettest growing season, Ψ_{pd} showed a three-fold increase in comparison to the first seasons, and all genotypes averaged a similar value. In addition, $\Delta\Psi$ was 1.88 times larger, which suggests a higher leaf-level water loss. Red-Gum hybrids (GC172 and GT529) transpired more intensively in both growing seasons, with an increase of 67% in their $\Delta\Psi$ under well-watered conditions (2014-15).

Stomatal opening can be quite sensitive to atmospheric demand in some eucalypt species (White *et al.*, 2000). However, soil moisture modifies the relationship between

g_s and VPD (Leuning *et al.*, 1991). Under well-watered conditions, as in the second growing season, the magnitude of the increase in water loss (E) depends on the sensitivity of decreasing g_s with increased VPD. We observed an increase of E in Red-Gum hybrids during the summer (high $\Delta\Psi$), and higher g_s when measuring instantaneous gas exchange (measured once a season). Therefore, midday leaf water potential decreased more steeply because of transpiration (Tables 1 and 2), which reveals a lower stomatal sensitivity in these clones. *E. camaldulensis* and *E. tereticornis* seem to display higher

Table 4. Mean (\pm SE) tree hydraulic conductance (K , $\text{mmol m}^{-2} \text{s}^{-1} \text{MPa}^{-1}$) of *E. grandis* (ABH17), *E. grandis* \times *E. camaldulensis* (GC172), *E. grandis* \times *E. tereticornis* (GT529) and *E. grandis* \times *E. urophylla* (GU08) clones

	Tree hydraulic conductance (K)	
	First growing season	Second growing season
	(February 2104)	(May 2015)
ABH17	3.10 \pm 0.32 a	1.19 \pm 0.16 b
GC172	3.24 \pm 0.24 a	2.02 \pm 0.14 a
GT529	2.47 \pm 0.22 a	1.53 \pm 0.16 ab
GU08	2.66 \pm 0.24 a	1.14 \pm 0.15 b
<i>p</i> -value	0.094	0.0002

Means within columns followed by different letters are significantly different (Tukey, $p < 0.05$)

Table 5. Mean (\pm SE) tree height (m) and height relative growth (RG, unitless) of *E. grandis* (ABH17), *E. grandis* \times *E. camaldulensis* (GC172), *E. grandis* \times *E. tereticornis* (GT529) and *E. grandis* \times *E. urophylla* (GU08) clones

Clone	Tree height (H, m)			Height relative growth	
	Dec 2013	Dec 2014	Dec 2015	Dec 2013- Dec 2014	Dec 2014- Dec 2015
	ABH17	6.33 \pm 0.18 a	10.52 \pm 0.6 a	13.54 \pm 0.53 a	0.40 \pm 0.02 b
GC172	5.80 \pm ab	9.49 \pm 0.22 ab	12.73 \pm 0.33 ab	0.39 \pm 0.01 b	0.35 \pm 0.003 a
GT529	5.59 \pm b	9.86 \pm 0.30 ab	13.6 \pm 0.47 a	0.43 \pm 0.01 ab	0.38 \pm 0.004 a
GU08	4.73 \pm 0.13 c	8.84 \pm 0.26 b	11.47 \pm 0.47 b	0.46 \pm 0.01 a	0.31 \pm 0.04 a
<i>p</i> -value	<0.0001	0.0033	0.0168	0.0004	0.4197

Means within columns followed by different letters are significantly different (Tukey, $p < 0.05$)

Table 6. Mean (\pm SE) diameter at breast height (Dbh, m), diametric relative growth (RG, unitless) and stem volume (V , m^3) of *E. grandis* (ABH17), *E. grandis* \times *E. camaldulensis* (GC172), *E. grandis* \times *E. tereticornis* (GT529) and *E. grandis* \times *E. urophylla* (GU08) clones

	Diameter at breast height			Diametric relative growth		Stem volume
	Dec 2013	Dec 2014	Dec 2015	2013-14	2014-15	Dec 2015
ABH17	0.07 \pm 3.1* a	0.13 \pm 4.2* a	0.16 \pm 4.7* b	0.48 \pm 0.01 a	0.17 \pm 0.02 b	0.13 \pm 0.01 a
GC172	0.07 \pm 2.0* a	0.14 \pm 2.6* a	0.17 \pm 3.0* a	0.49 \pm 0.01 a	0.23 \pm 0.01 a	0.14 \pm 0.01 a
GT529	0.06 \pm 2.0* b	0.12 \pm 3.5* b	0.14 \pm 4.2* b	0.50 \pm 0.01 a	0.20 \pm 0.01 ab	0.11 \pm 0.01 ab
GU08	0.07 \pm 3.1* a	0.14 \pm 3.1* a	0.14 \pm 4.2* b	0.49 \pm 0.01 a	0.07 \pm 0.01 c	0.09 \pm 0.01 b
<i>p</i> -value	0.0130	0.0012	<0.0001	0.7397	<0.0001	0.0013

* Dbh $\times 10^{-3}$

Means within columns followed by different letters are significantly different (Tukey, $p < 0.05$)

g_s at saturating irradiance (Whitehead & Beadle, 2004), similarly to GC172 and GT529 in the present work.

Although Red-Gum hybrids had the highest E (and $\Delta\Psi$) during the summer, GC172 was more sensitive to soil water content and displayed stronger regulation of stomata opening (Table 3). In addition, gas exchange

results for this clone revealed a 40% reduction in g_s during that period. Stomatal conductance in *E. camaldulensis* decreases steeply as a function of soil water status (White, 2000), the same behaviour recorded for the GC hybrid. However, transpiration also depends on K (Tyree & Ewers, 1991; Bond & Kavanagh, 1999). Our

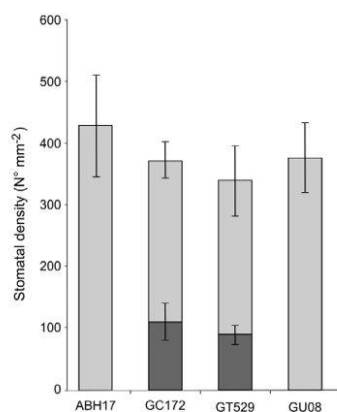


Figure 4. Stomatal density on adaxial and abaxial leaf surfaces (dark and gray bars, respectively) of *E. grandis* (ABH17), *E. grandis* × *E. camaldulensis* (GC172), *E. grandis* × *E. teteretincornis* (GT529) and *E. grandis* × *E. urophylla* (GU08) clones; error bars indicate the standard deviation of the mean.

results suggest that all genotypes increased their K under low soil moisture (first growing season) to sustain gas exchange and, consequently, carbon gain. In well-watered conditions, GC172 had the highest K , which confirms the findings of White (2000) in *E. camaldulensis*. In addition, GC172 displayed a lower control of stomatal opening under high soil moisture (second growing season) (Table 3), mainly due to an increase in K (Table 4) to deal with rising xylem tension (lower Ψ_{md}). Under such conditions, this species is known to produce extensive adventitious roots, to display stem hypertrophy (increased stem diameter), and to increase root porosity to sustain higher g , and K , which modify tree growth (Argus *et al.*, 2015). Some of these features could explain the behavior of the GC clone in the wettest season, mainly if stem growth is considered (Tables 5 and 6).

In recent work, we studied the clonal variation of hydraulic traits and wood anatomy of one-and-a-half-year specimens of GC172, GT529, and ABH17, grown without water limitations under greenhouse conditions. We found that GC172 had the highest leaf-specific hydraulic conductivity without embolism ($k_s \text{ max} = 7.53 \pm 0.53 \text{ kg m}^{-1} \text{ MPa}^{-1} \text{ s}^{-1}$) and wider xylem vessels ($0.04 \pm 0.001 \text{ mm}$). This clone showed the highest $\Delta\Psi$ and was also the most vulnerable to cavitation (higher percentage loss of hydraulic conductivity; unpublished data). These results are consistent with the high transpiration of Red-Gum hybrids in the present study, and the higher hydraulic conductance of GC172 under well-watered conditions.

Water-use efficiency and growth

The analysis of instantaneous WUE (A/E) and $\Delta^{13}C$ led to similar conclusions. Red-Gum hybrids were the least efficient in intrinsic leaf-level water use, most likely due to lower stomatal regulation over time (long term A/E ratio) (Table 3, Fig. 3). This outcome confirms the information provided by leaf water potential and suggests that Red-Gum hybrids adjust $\Delta\Psi$ to sustain carbon gain (Le Roux *et al.*, 1996). Conversely, ABH17 and GU08 seemed to be more VPD sensitive and would therefore be more suitable for withstanding drought conditions by reducing leaf gas exchange. These clones were highly efficient in carbon fixation (high A), although GU08 was more water-use efficient in during the driest period (as inferred by $\Delta^{13}C$ data) (Table 3). This behavior could have led to higher WUE by decoupling stomatal conductance and carbon gain (A), as previously reported for humid-zone eucalypt species (Hérault *et al.*, 2013).

To our knowledge, hybrids with *E. urophylla* appear to be highly sensitive to VPD, which implies a reduction of carbon gain under high VPD. However, WUE is not a constant characteristic of a given genotype, and it varies according to a combination of site conditions, weather and tree age. The frequency and duration of soil water deficits are crucial in determining WUE, which is sensitive to annual variations in rainfall amount as well as to rainfall distribution throughout the year (Dye, 2000). Under soil water deficits, *E. urophylla* is known to show higher WUE (lower $\Delta^{13}C$) due to stable stomatal

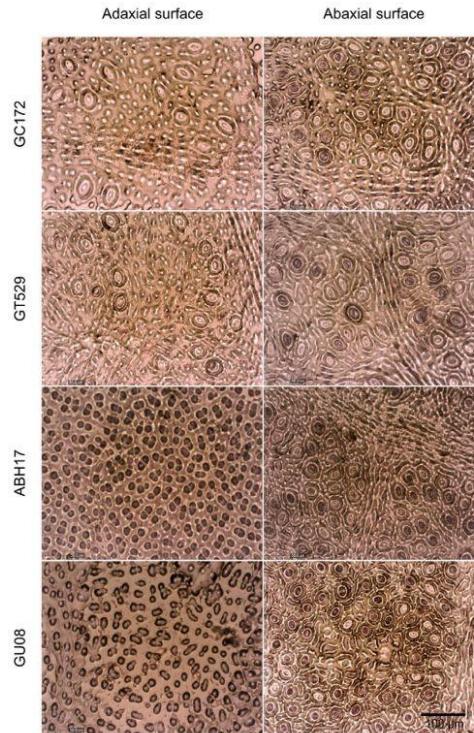


Figure 5. Photomicrographs of adaxial and abaxial leaf epidermis (columns) of *E. grandis* (ABH17), *E. grandis* × *E. camaldulensis* (GC172), *E. grandis* × *E. tereticornis* (GT529) and *E. grandis* × *E. urophylla* (GU08) clones (files); images (10X) were obtained on 0.15-mm² fields.

conductance as leaf water potential decreases (Zhang *et al.*, 2016). In our work, this mechanism was displayed by GU08 throughout the less rainy season (2013-14), as inferred from WUE_i (Table 3).

All genotypes had similar diametric relative growth and volumetric stem growth during the first year of the study (the less rainy one). During the wettest year, the GC clone attained the highest diametric relative growth (0.23 ± 0.01), whereas GU averaged the lowest (0.07 ± 0.01). The latter also showed the lowest stem volume at the end of the study (Table 6) and was the most efficient in water use (lower $\Delta^{13}C$) during the driest growing season. This behavior is consistent with the so-called “hare strategy,” which means that growth increases rapidly with soil water availability, as observed for diameter growth in 2014-15 (Table 6). Drew *et al.* (2009) reported this pattern for some GU clones in South

Africa. These authors found *E. grandis* × *camaldulensis* hybrids to keep growing even under severe drought conditions, referred to as the “tortoise” growing pattern. In our study, this hybrid grew faster than other clones in the driest season (Table 6), mainly due to a higher gas exchange (as inferred by $\Delta\Psi$, WUE, and WUE_i), which promoted carbon fixation.

Stomatal traits and water status

Transpiration was influenced by stomatal density and distribution. ABH17 and GU08 had hypostomatous leaves and showed stronger stomatal control that reduced gas exchange. In GU clones, Eksteen *et al.* (2013) reported that stomatal sensitivity to drought could be a consequence of both stomatal closure and the absence of stomata on

adaxial leaf surfaces. These traits are highly variable among closely related clones, and we did not study stomata development or their functionality. Leaves were sampled at the end of the second growing season on the same branchlets used for gas-exchange measurements, therefore reflecting the effect of environmental conditions on stomatal anatomy during this time (the preceding days or even weeks).

On the other hand, Red-Gum hybrids transpired more intensively and were amphistomatic. *E. grandis* × *camaldulensis* hybrid seems to have higher K under well-watered conditions to sustain carbon gain, which is consistent with gas-exchange results. Conversely, ABH17 and GU08 enhanced their net carbon fixation. Eksteen *et al.* (2013) observed that GC hybrids had higher growth than GU clones after 12 months of chronic water stress. This behavior was related to a higher gas exchange and different stomata density and distribution.

A noteworthy observation was that stomata on adaxial surfaces of ABH17 and GU08 remained entirely immature, similarly to some tropical herbs (Kagan & Sachs, 1991). England & Attiwill (2011) studied stomata development in *Eucalyptus regnans* and reported that they evolved progressively from margin to midrib in juvenile leaves. However, in the current study, stomata remained immature on the whole adaxial surface of adult leaves. This pattern could have reduced leaf gas exchange and it probably prevented leaf water potential from falling (*i.e.*, from being more negative). Hydraulic isolation in amphistomatic leaves can induce surface-specific stomatal closure in *E. globulus* (Richardson *et al.*, 2017), and this could explain why Red-Gum hybrids attained the highest gas exchange in our work, even in the driest growing season. Nevertheless, further research is needed to study leaf hydraulics and the functionality of such immature stomata.

Conclusions

We found differences in gas-exchange regulation, water status, and growth among genotypes as a function of soil water moisture (inferred from rainfall) in two growing seasons. Red-Gum hybrids (*E. grandis* × *E. camaldulensis*, GC172, and *E. grandis* × *E. tereticornis*, GT529) transpired more intensively (higher daily $\Delta\Psi$), and were therefore less water-use efficient as confirmed either by instantaneous (A/E) or intrinsic ($\Delta^{13}C$) WUE. These clones were amphistomatic and displayed lower stomatal control over time (higher $\Delta^{13}C$). The *E. grandis* × *E. camaldulensis* hybrid showed the highest gas exchange under well-watered conditions (wettest growing season), mainly due to an increase in tree hydraulic conductance (K). This behavior granted this hybrid constant g_s , therefore promoting carbon gain and stem growth. Conversely, *E.*

grandis (ABH17) and *E. grandis* × *E. urophylla* (GU08) genotypes were more water-use efficient over time because of stronger stomatal regulation that increased the A/E ratio. Therefore, they were more VPD sensitive across both growing seasons (and therefore in different soil water moisture conditions). These clones were hypostomatic, and stomata on their adaxial leaf epidermis remained entirely immature.

Acknowledgments

We would like to thank Lumin (formerly Weyerhaeuser S. A.) for funding support and technical assistance, as well as INIA Tacuarembó for providing meteorological data.

References

- Akhter J, Mahmood K, Tasneem M, Malik K, Naqvi M, Hussain F, Serraj R, 2005. Water-use efficiency and carbon isotope discrimination of *Acacia ampliceps* and *Eucalyptus camaldulensis* at different soil moisture regimes under semi-arid conditions. *Biol Plantarum* 49 (2): 269-272. <https://doi.org/10.1007/s10535-005-0272-6>
- Allen R, Pereira L, Raes D, Smith M.,1998. Crop evapotranspiration. Guidelines for computing crop water requirements. FAO Irrigation and drainage paper 56. FAO, Rome, Italy.
- Argus RE, Comer TD, Grierson PF, 2015. Early physiological flood tolerance is followed by slow post-flooding root recovery in the dryland riparian tree *Eucalyptus camaldulensis* subsp. *refulgens*. *Plant Cell Environ* 38: 1189-1199. <https://doi.org/10.1111/pce.12473>
- Battie-Laclau P, Delgado-Rojas JS, Christina M, Nouvellon Y, Bouillet JP, Piccolo MC, Moreira MZ, Gonçalves JL, Rousar O, Laclau JP, 2016. Potassium fertilization increases water-use efficiency for stem biomass production without affecting intrinsic water-use efficiency in *Eucalyptus grandis* plantations. *For Ecol Manag* 364: 77-89. <https://doi.org/10.1016/j.foreco.2016.01.004>
- Brodribb T, Holbrook N, Edwards E, Gutierrez MV, 2003. Relations between stomatal closure, leaf turgor and xylem vulnerability in eight tropical dry forest trees. *Plant Cell Environ* (26) 3: 443-450. <https://doi.org/10.1046/j.1365-3040.2003.00975.x>
- Casparus C, Greyling I, Wingfield MJ, 2018. Dissimilar stem and leaf hydraulic traits suggest varying drought tolerance among co-occurring *Eucalyptus grandis* × *E. urophylla* clones. *South For* 80 (2): 175-184. <https://doi.org/10.2989/20702620.2017.1315546>

- Choné X, Van Leeuwen C, Dubourdieu D, Gaudillère JP. 2001. Stem water potential is a sensitive indicator of grapevine water status. *Ann Bot* 87(4): 477-483.
- Craig H. 1957. Isotopic standards for carbon and oxygen and correction factors for mass-spectrometric analysis of carbon dioxide. *Geochim Cosmochim Acta* 12 (1-2): 133-149. [https://doi.org/10.1016/0016-7037\(57\)90024-8](https://doi.org/10.1016/0016-7037(57)90024-8)
- Comstock JP. 1998. Control of stomatal conductance by leaf water potential in *Hymenoclea salsola* (T. and G.), a desert subshrub. *Plant Cell Environ* 21(10): 1029-1038. <https://doi.org/10.1046/j.1365-3040.1998.00353.x>
- Da Silva JT, Hellmeister JT, Simoes JW, Tomazello M. 1999. Caracterização da madeira de sete espécies de eucaliptos para a construção civil: avaliações dendrométricas das árvores. *Sci For* 56: 113-124.
- D'Ambrogio A. 1986. Manual de Técnicas en histología vegetal. Hemisferio Sur, Montevideo, Uruguay.
- David TS, Ferreira MI, David JS, Pereira JS. 1997. Transpiration from a mature *Eucalyptus globulus* plantation in Portugal during a spring-summer period of progressively higher water deficit. *Oecologia* 110 (2): 153-159. <https://doi.org/10.1007/PL00008812>
- Dharhi S, Khouja ML, Ben Jamaa ML, Ben Yahia K, Saadaoui E. 2018. An overview of adaptative responses to drought stress in *Eucalyptus* spp. *For Stud* 67 (1): 86-96. <https://doi.org/10.1515/fsmu-2017-0014>
- Drake PL, Mendham DS, White DA, Ogden GN, Dell B. 2012. Water use and water-use efficiency of coppice and seedling *Eucalyptus globulus* Labill.: A comparison of stand-scale water balance components. *Plant Soil* 350: 221-235. <https://doi.org/10.1007/s11104-011-0897-5>
- Drew DM, Downes GM, Grzeskowiak V, Naidoo T. 2009. Differences in daily stem size variation and growth in two-hybrid eucalypt clones. *Trees* 23: 585-595. <https://doi.org/10.1007/s00468-008-0303-y>
- Dye P. 2000. Water use efficiency in South African *Eucalyptus* plantations: A review. *South Afr For J* 189: 17-26. <https://doi.org/10.1080/10295925.2000.9631276>
- Eksteen AB, Grzeskowiak V, Jones NB, Pammenter NW. 2013. Stomatal characteristics of *Eucalyptus grandis* clonal hybrids in response to water stress. *South For* 75 (3): 105-111. <https://doi.org/10.2989/20702620.2013.804310>
- England JR, Attiwill PM. 2011. Changes in stomatal frequency, stomatal conductance, and cuticle thickness during leaf expansion in the broad-leaved evergreen species, *Eucalyptus regnans*. *Trees Struct Funct* 25 (6): 987-996. <https://doi.org/10.1007/s00468-011-0573-7>
- Farquhar GD, Ehleringer R, Hubick KT. 1989. Carbon Isotope Discrimination and Photosynthesis. *Annu Rev Plant Physiol Plant Mol Biol* 40: 503-537. <https://doi.org/10.1146/annurev.pp.40.060189.002443>
- Faustino L, Bulfe N, Pinazo M, Monteoliva S, Graciano C. 2013. Dry weight partitioning and hydraulic traits in young *Pinus taeda* trees fertilized with nitrogen and phosphorus in a subtropical area. *Tree Physiol* 32: 241-251. <https://doi.org/10.1093/treephys/tps129>
- Franks PJ, Drake PL, Froend RH. 2007. Anisohydric but isohydrodynamic: Seasonally constant plant water potential gradient explained by a stomatal control mechanism incorporating variable plant hydraulic conductance. *Plant Cell Environ* 30 (1): 19-30. <https://doi.org/10.1111/j.1365-3040.2006.01600.x>
- Hérout A, Lin YS, Bourne A, Medlyn BE, Ellsworth DS. 2013. Optimal stomatal conductance in relation to photosynthesis in climatically contrasting *Eucalyptus* species under drought. *Plant Cell Environ* 36 (2): 262-274. <https://doi.org/10.1111/j.1365-3040.2012.02570.x>
- Kagan ML, Sachs T. 1991. Development of immature stomata: Evidence for epigenetic selection of a spacing pattern. *Dev Biol* 146 (1): 100-105. [https://doi.org/10.1016/0012-1606\(91\)90450-H](https://doi.org/10.1016/0012-1606(91)90450-H)
- Kallarackal J, Somen CK. 1997. An ecophysiological evaluation of the suitability of *Eucalyptus grandis* for planting in the tropics. *For Ecol Manag* 95 (1): 53-61. [https://doi.org/10.1016/S0378-1127\(97\)00004-2](https://doi.org/10.1016/S0378-1127(97)00004-2)
- Kallarackal J, Somen CK. 2008. Water Loss from Trees Plantations in the Tropics. *Curr Sci* 94 (2): 201-210.
- Lambers H, Chapin F S, Pons T L. 2008. *Plant Physiological Ecology*. Springer, New York. <https://doi.org/10.1007/978-0-387-78341-3>
- Le Roux D, Stock WD, Bond WJ, Maphanga D. 1996. Dry mass allocation, water use efficiency, and $\delta^{13}C$ in clones of *Eucalyptus grandis*, *E. grandis* × *camaldulensis* and *E. grandis* × *nitens* grown under two irrigation regimes. *Tree Physiol* (16): 497-502. <https://doi.org/10.1093/treephys/16.5.497>
- Leuning R, Kriedemann PE, McMurtrie RE. 1991. Simulation of evapotranspiration by trees. *Agric Water Manage* 19: 205-221. [https://doi.org/10.1016/0378-3774\(91\)90042-H](https://doi.org/10.1016/0378-3774(91)90042-H)
- Lewis JD, Phillips NG, Logan BA, Hricko CR, Tissue DT. 2011. Leaf photosynthesis, respiration and stomatal conductance in six *Eucalyptus* species native to mesic and xeric environments growing in a common garden. *Tree Physiol* 31 (9): 997-1006. <https://doi.org/10.1093/treephys/tpr087>
- Linderman T, Plata V, Sancho D, Oyhantcabel W. 2013. *Clima de cambios*. FAO, MGAP Uruguay. <http://www.fao.org/climatechange/84982/es/>.
- MacFarlane C, Adams MA. 1998. $\delta^{13}C$ of wood in growth-rings indicates cambial activity of drought stressed trees of *Eucalyptus globulus*. *Func Ecol* 12: 655-664. <https://doi.org/10.1046/j.1365-2435.1998.00230.x>

- Martin D, 2017. Producción vegetal: forsetación. Anuario estadístico agropecuario. DIEA 2017: 177-121. <https://descargas.mgap.gub.uy/DIEA/Anuarios/Anuario2017/DIEA-Anuario2017.pdf>
- Martínez-Vilalta J, Sala A, Piñol J, 2004. The hydraulic architecture of Pinaceae: a review. *Plant Ecol* (171) 1: 3-13. <https://doi.org/10.1023/B:VEGE.0000029378.87169.b1>
- McDowell N, Pockman WT, Allen CD, Breshears DD, Cobb N, Kolb T, Plaut J, Sperry J, West A, Williams DG *et al.*, 2008. Mechanisms of plant survival and mortality during drought: why do some plants survive while others succumb to drought? *New Phytol* 178: 719-739. <https://doi.org/10.1111/j.1469-8137.2008.02436.x>
- Meinzer FC, Woodruff DR, Marias DE, McCulloh KA, Sevanto S, 2014. Dynamics of leaf water relations components in co-occurring iso- and anisohydric conifer species. *Plant Cell Environ* 37 (11): 2577-2586. <https://doi.org/10.1111/pce.12327>
- Mokotedi O, 2013. Water relations of *Eucalyptus nitens* x *Eucalyptus grandis*: is there interclonal variation in response to experimentally imposed water stress? *South For: J For Sci* 75 (4): 213-220. <https://doi.org/10.2989/20702620.2013.858212>
- Morris J, Mann L, Collopy J, 1998. Transpiration and canopy conductance in a eucalypt plantation using shallow saline groundwater. *Tree Physiol* 18 (8-9): 547-555. <https://doi.org/10.1093/treephys/18.8-9.547>
- Olbrich BW, Le Roux D, Poulter AG, Bond WJ, Stock WD, 1993. Variation in water use efficiency and $\Delta^{13}C$ levels in *Eucalyptus grandis* clones. *J Hydro* 150 (2-4): 615-633. [https://doi.org/10.1016/0022-1694\(93\)90128-V](https://doi.org/10.1016/0022-1694(93)90128-V)
- Osório J, Pereira JS, 1994. Genotypic differences in water use efficiency and ^{13}C discrimination in *Eucalyptus globulus*. *Tree Physiol* 14 (7-9): 871-882. <https://doi.org/10.1093/treephys/14.7-8-9.871>
- Pohjonen V, Pukkala T, 1990. *Eucalyptus globulus* in Ethiopian forestry. *For Ecol Manag* 36 (1), 19-31. [https://doi.org/10.1016/0378-1127\(90\)90061-F](https://doi.org/10.1016/0378-1127(90)90061-F)
- Richardson F, Brodribb T, Jordan G, 2017. Amphistomatic leaf surfaces independently regulate gas exchange in response to variations in evaporative demand. *Tree Physiol* 37 (7): 869-878. <https://doi.org/10.1093/treephys/tpx073>
- Sade M, Moshelion M, 2014. The dynamic isohydric-anisohydric behavior of plants upon fruit development: taking a risk for the next generation. *Tree Phys* 34: 1199-1202. <https://doi.org/10.1093/treephys/tpu070>
- Seibt U, Rajabi A, Griffiths H, Berry J, 2008. Carbon isotopes and water use efficiency: sense and sensitivity. *Oecol* 155: 441-454. <https://doi.org/10.1007/s00442-007-0932-7>
- Skomarkova MV, Vaganov EA, Mund M, Knohl A, Linke P, Boerner A, Schulze ED, 2006. Interannual and seasonal variability of radial growth, wood density and carbon isotope ratios in tree rings of beech (*Fagus sylvatica*) growing in Germany and Italy. *Trees* 20: 571-586. <https://doi.org/10.1007/s00468-006-0072-4>
- Sperry JS, Adler FR, Campbell GS, Comstock JP, 1998. Limitation of plant water use by rhizosphere and xylem conductance: results from a model. *Plant Cell Environ* 21 (1): 347-359. <https://doi.org/10.1046/j.1365-3040.1998.00287.x>
- Sperry JS, Wang Y, Wolfe BT, Mackay DS, Anderegg WR, McDowell NG, Pockman WT, 2016. Pragmatic hydraulic theory predicts stomatal responses to climatic water deficits. *New Phytol* 212 (3): 577-589. <https://doi.org/10.1111/nph.14059>
- Tyree M, Ewers F, 1991. The hydraulic architecture of trees and other woody plants. *New Phytol* 119: 345-360. <https://doi.org/10.1111/j.1469-8137.1991.tb00035.x>
- Whitehead D, Beadle CL, 2004. Physiological regulation of productivity and water use in *Eucalyptus*: A review. *For Ecol Manag* 193 (1-2): 113-140. <https://doi.org/10.1016/j.foreco.2004.01.026>
- Zang Z, Zhao P, McCarthy H, Ouyang L, Niu J, Zhu L, Ni G, Huang Y. Hydraulic balance of a *Eucalyptus urophylla* plantation in response to periodic drought in low subtropical China. 2016. *Front Plant Sci* 7: 1-12. <https://doi.org/10.3389/fpls.2016.01346>

5. Resultados y discusión

En el presente trabajo se estudió la respuesta al déficit hídrico en clones comerciales de *E. grandis* (clon GG) y en híbridos con eucaliptos colorados, *E. grandis* × *camaldulensis* (clon GC) y *E. grandis* × *tereticornis* (clon GT), así como también en híbridos con el eucalipto de Timor, *E. grandis* × *urophylla* (clones GU1 y GU2). Se realizaron ensayos en condiciones de crecimiento controladas (invernáculo), con riego restringido y en árboles a campo durante dos temporadas con diferente disponibilidad hídrica en el suelo. Se identificaron diferentes mecanismos de respuesta a la sequía que involucraron ajustes en variables fisiológicas —estado hídrico, intercambio gaseoso y regulación de la turgencia—, atributos anatómicos de la madera y variables asociadas a la función hidráulica. A partir del análisis de dichas respuestas, se logró identificar distintas estrategias de regulación del estado hídrico que implicaron diferencias en la eficiencia en el uso del agua, seguridad hidráulica y fijación de carbono de los distintos genotipos. Estas se relacionaron con diferentes patrones de crecimiento ante distintas disponibilidades hídricas, tanto en los plantines creciendo en condiciones controladas (invernáculo) como en árboles juveniles creciendo a campo.

La presente discusión se organiza de la siguiente manera: en un primer apartado se retoman los objetivos específicos y se indica en qué artículos publicados, expuestos en capítulos anteriores, se encuentran los resultados correspondientes. A continuación, se incluye un apartado de integración de todos los resultados, los cuales se discuten a la luz del objetivo general e hipótesis de la tesis. Finalmente, se presentan las conclusiones generales del trabajo.

5.1. Contribuciones a los objetivos específicos

En el artículo titulado «Similar but unique: physiological response to drought and growth of pure species and interspecific hybrid clones of *Eucalyptus*» (Gándara et al., 2025a) se brindan resultados que responden a los objetivos a) caracterizar y comparar variables asociadas a las relaciones hídricas y al intercambio gaseoso en los diferentes clones durante la estación de crecimiento, en el estado de plantín y c)

cuantificar el grado de plasticidad fenotípica en caracteres funcionales (anatómicos, fisiológicos, morfológicos, de asignación de biomasa) en función de la disponibilidad hídrica del sustrato.

El artículo titulado «Xylem functional anatomy of pure-species and interspecific hybrid clones of *Eucalyptus* differing in drought resistance» (Gándara et al., 2025b) reúne los principales resultados relacionados con el objetivo *b*) cuantificar variables anatómico-funcionales del xilema y de la planta entera, relacionados con la arquitectura hidráulica de los diferentes genotipos, y contribuyen al objetivo *c*) en la dimensión de caracteres anatómicos del xilema.

En conjunto, ambos artículos y la discusión integral del próximo apartado, contribuyen al cumplimiento del objetivo específico *d*) identificar relaciones entre mecanismos fisiológicos y características anatómico-funcionales (objetivos *a* y *b*), así como grado de plasticidad fenotípica (objetivo *c*), con diferentes desempeños de clones puros e híbridos ante condiciones variables de disponibilidad hídrica (condiciones de alta disponibilidad o años húmedos vs. condiciones de baja disponibilidad o años secos).

Finalmente, el artículo «Differential water-use efficiency and growth among *Eucalyptus grandis* hybrids under two different rainfall conditions» (Gándara et al., 2020) presenta los resultados correspondientes al objetivo *e*) estudiar las relaciones hídricas y la fijación de carbono en individuos juveniles (2-4,5 años) de los diferentes taxones, creciendo a campo con distinta disponibilidad hídrica del suelo (condiciones medias del sitio o la disponibilidad hídrica estacional), e interpretar los patrones de crecimiento, comparándolos con los observados en el estado de plantín (objetivos anteriores), completándose la última parte del objetivo en la discusión integral de la presente tesis.

5.2. Integración de resultados a la luz del objetivo general

El objetivo general de esta tesis fue identificar mecanismos morfofisiológicos involucrados en la respuesta al déficit hídrico en clones comerciales de *Eucalyptus grandis* e híbridos con eucaliptos colorados (*E. camaldulensis* y *E. tereticornis*) y con *E. urophylla*, para contribuir al desarrollo de criterios de selección de genotipos más

tolerantes. Se planteó como hipótesis que los genotipos híbridos tendrían un mejor desempeño frente a la sequía que el clon de *E. grandis*, aunque no bajo condiciones de alta disponibilidad hídrica. Sin embargo, se esperaba una variación de respuestas entre genotipos, con alguna combinación que presentara un desempeño aceptable en todas las condiciones de disponibilidad hídrica, es decir, que minimizara el compromiso entre productividad y resistencia a estrés. Asimismo, se esperaba que esto se debiera tanto a variaciones en las estrategias y valores de los distintos rasgos como a una mayor plasticidad fenotípica de los clones híbridos (*i. e.*, mayor diferencia de la expresión de los caracteres entre tratamientos).

El análisis de las respuestas fisiológicas (Gándara et al., 2025a) reveló dos patrones generales de respuesta al déficit hídrico. Los híbridos con eucaliptos colorados (GC y GT) mostraron un comportamiento de tipo anisohídrico en comparación con el resto de los clones, lo que sugiere una estrategia más derrochadora de agua, asociada con un menor control estomático durante el estrés (relativamente alta g_s) que condujo a una elevada actividad transpiratoria y a un mayor $\Delta\Psi$ entre suelo y hoja. Esta estrategia hizo posible sostener la fijación de carbono y la capacidad de crecimiento de las plantas, aunque con altos porcentajes de pérdida de conductividad hidráulica. En consecuencia, estos genotipos presentaron menor eficiencia en el uso del agua —menor EUA—, consistente con observaciones reportadas en eucaliptos colorados en su zona de origen (Whitehead y Beadle, 2004). Nió n et al. (2024) encontraron un patrón similar en un híbrido GT bajo estrés severo en invernáculo. En los árboles creciendo a campo (Gándara et al., 2020), esta tendencia se observó tanto a partir de mediciones instantáneas (*i. e.*, EUA instantánea, $EUA = A / E$) como del análisis de isótopos estables de carbono (*i. e.*, EUA integrada, $EUA_i = A_i / g_s$). El curso estacional del $\Delta\Psi$ en los árboles siguió un patrón similar al isohidrodinámico definido por Franks et al. (2007) en *Eucalyptus gomphocephala*, con valores relativamente estables durante ciclos estacionales de contenido de humedad del suelo. Los híbridos GC y GT presentaron mayor actividad transpiratoria durante ambas temporadas de crecimiento, lo que sugiere que los patrones de uso del agua son similares entre genotipos, tanto en plantas creciendo en condiciones controladas como en los árboles

a campo. Esto sugiere que es posible realizar selecciones tempranas con base en el comportamiento de las plantas en etapas iniciales del desarrollo.

La evolución del potencial hídrico foliar se relacionó con diferencias en la anatomía y distribución de los estomas. En los árboles juveniles de los híbridos GC y GT, las hojas adultas fueron anfiestomáticas, lo que es consistente con su mayor actividad transpiratoria. Por el contrario, en los demás clones ensayados a campo (GG y GU1) se observó un patrón hipoestomático y la presencia de estomas inmaduros (protoestomas) en la cara adaxial de las láminas foliares, similar a lo reportado por England y Atwill (2011) en herbáceas tropicales. Pero, a diferencia de estos autores, en el presente estudio todos los estomas del haz permanecieron inmaduros, lo cual podría explicar, en alguna medida, las menores tasas de intercambio gaseoso de estos clones (Gándara et al., 2020). En este sentido, Eksteen et al. (2013) señalaron que la sensibilidad estomática puede deberse al control estomático y a la ausencia de estomas en el haz de las hojas. En cuanto a la actividad fotosintética, los híbridos con eucalipto colorado mantuvieron un elevado contenido de clorofila durante el estrés, lo que indicaría una aclimatación del proceso fotosintético al déficit hídrico, sumado al mantenimiento relativamente constante del área foliar específica (Gándara et al., 2025a). Este comportamiento no se observó en los otros clones y concuerda con lo que distintos autores definen como *respuesta hormética*, es decir, una activación del proceso fotosintético luego de un estrés moderado que desencadena respuestas adaptativas ante exposiciones futuras a la condición de estrés (Agathokleous et al., 2020; Mattson, 2008). Este patrón se ha reportado en híbridos GT bajo estrés hídrico severo en invernáculo (Nión et al., 2024).

Aunque los híbridos GC y GT presentaron una mayor pérdida de conductividad hidráulica (PLC), cercana a valores que generan daño irreversible, lograron activar mecanismos compensatorios que permitieron sostener la turgencia (CRA elevado) y el crecimiento (Gándara et al., 2025a). Entre los mecanismos más importantes se identificaron el ajuste elástico —reducción del módulo de elasticidad de pared, ϵ — y el ajuste osmótico. En el caso de GC, este último mecanismo se observó sobre el final del tratamiento de estrés, es decir, más tardíamente en la estación de crecimiento, con diferencias entre Ψ_{TLP} y Ψ_{sat} que triplicaron a lo reportado por Lemcoff et al. (2002) en

E. camaldulensis. La reducción de ϵ conlleva la generación de células con paredes más delgadas y mayor espacio intercelular, lo que produce cambios en las microfibrillas de celulosa y en los polisacáridos estructurales (Niinemets, 2001). En el caso de GC, se generó follaje con estas características durante la primavera, al comienzo del tratamiento de estrés hídrico, lo que sugiere que el ajuste elástico es una respuesta plástica que se desencadena antes en el tiempo que el ajuste osmótico en este clon. Probablemente, estos mecanismos de respuesta contribuyeron a mantener el balance hídrico y la apertura estomática y, quizás, también presentaron una mayor capacidad de almacenamiento de agua (capacitancia) en hojas y órganos leñosos. De esta manera, fue posible generar el gradiente de potencial hídrico necesario entre la planta y el suelo para sostener la absorción de agua (Lenz et al., 2006), a pesar del riesgo de cavitación. Por otro lado, estos clones presentaron una mayor eficiencia del sistema conductivo (k_h) en tallos, a pesar de una mayor reducción de la conductividad hidráulica.

En contraste con lo observado en plantines y árboles juveniles de los clones híbridos GC y GT, el clon de *E. grandis* (GG) adoptó una estrategia más conservadora del uso del agua, asociada con un patrón más isohídrico, tanto en los ensayos con plantines en invernáculo (Gándara et al., 2025a) como en los árboles a campo (Gándara et al., 2020). El comportamiento se debió principalmente a un estricto control estomático en condiciones de estrés —baja g_s — que minimizó la pérdida de agua y evitó una caída abrupta de la conductividad hidráulica. Como resultado, el PLC fue menor que en los clones con comportamiento anisohídrico. Esta estrategia prioriza la integridad del sistema hidráulico por encima de la eficiencia para evitar el embolismo y asegurar la funcionalidad del xilema (Li et al., 2024; Martínez-Vilalta et al., 2002; Zimmermann et al., 2021). En el clon GG también se observó ajuste osmótico, que —a diferencia de lo observado en GC y GT— se activó desde el inicio del período de estrés en primavera. Sin embargo, esta pronta respuesta de aclimatación no sería suficiente para permitir la apertura estomática de manera sostenida durante el período con déficit hídrico. Los resultados sugieren que *E. grandis* fue el clon más vulnerable a la cavitación, en concordancia con otros autores en estudios comparativos con *E. camaldulensis* (Barotto et al., 2016; Fernández et al., 2019), lo que obligó a un cierre estomático temprano y, paradójicamente, resultó en menores pérdidas de

conductividad debido a su comportamiento altamente conservativo. Estos dos elementos —el ajuste osmótico y la baja pérdida de cavitación asociada a un cierre estomático temprano— que actúan en hojas y tallos, contribuyeron a la retención de agua en los tejidos y a la resiliencia tras la sequía. Ambas características son propias de una estrategia evitadora y se tradujeron en mayores pérdidas relativas de crecimiento en el clon de *E. grandis* respecto de los genotipos híbridos (Gándara et al., 2025a).

Los híbridos GU1 y GU2 mostraron un comportamiento intermedio entre los híbridos con eucaliptos colorados y el clon de *E. grandis*, caracterizado por una regulación estomática y una tolerancia al estrés más moderadas, particularmente en los ensayos con plantas en invernáculo (Gándara et al., 2025a). La información obtenida a partir de las variables hidráulicas indica una relación más balanceada entre seguridad y eficiencia del sistema conductivo respecto al resto de los clones. Estas características favorecieron, en parte, el crecimiento de las plantas durante el período de estrés, y uno de los dos clones (GU1) presentó cierta superioridad de desempeño con respecto a *E. grandis*. Sin embargo, en árboles a campo, el clon GU1 presentó un patrón de crecimiento y de estado hídrico similar a GG, con el que compartió el mismo patrón de distribución y frecuencia estomáticas. En este sentido, el desempeño de los plantines no fue idéntico al observado en árboles juveniles a campo y planteó interrogantes acerca del comportamiento de los clones GU. Por un lado, respecto a las razones de sus diferentes desempeños ante el estrés —aun cuando su comportamiento fisiológico fue similar entre ambos— y, por otro, en relación con la variación de respuestas en distintos estadios ontogenéticos.

El estrés hídrico provocó ajustes en caracteres anatómicos del xilema, ya sea en ramas, tallos o en ambos órganos (Gándara et al., 2025b). En términos generales, todos los clones respondieron al déficit hídrico mediante la reducción del diámetro de vasos y el incremento de su frecuencia, junto con un aumento del espesor de la pared de las fibras y una disminución en su longitud. El déficit hídrico también promovió un descenso de la fracción ocupada por lúmenes de vasos (F) y una disminución de su composición (distribución de tamaños) en la albura (S). Estos cambios, en su conjunto, resultaron en un aumento en la densidad de la madera y reflejan la plasticidad que

presentan los rasgos del xilema en respuesta a la sequía. En condiciones de estrés, se favoreció la seguridad hidráulica en detrimento de la eficiencia, aunque existieron diferencias significativas entre clones.

GC y GT fueron los únicos clones que incrementaron la densidad de la madera de tallo bajo la sequía. Este aumento se debió, principalmente, a paredes celulares con mayor grosor y menor área individual de lúmenes en los elementos de conducción (vasos) y de sostén (fibras). Resulta interesante que estos híbridos mantuvieran constante la fracción de lúmenes (F), a pesar de reducir el diámetro medio de los vasos, hecho fundamental para explicar los altos de valores de conductividad hidráulica teórica ($k_{S_{theo}}$), particularmente en las ramas del clon GT. Los ajustes anatómicos probablemente aumentaron la resistencia a la cavitación y permitieron desplazar el umbral hacia valores más bajos de potencial hídrico. Es probable que estas modificaciones estén acompañadas por otras respuestas anatómicas compensatorias que apuntan a la regulación del tamaño de los vasos y a la estructura y dimensión de las puntuaciones intervasculares. Estas últimas reducen el riesgo de cavitación, tal como se ha descrito en otros taxones del género (Fernández et al., 2019). Por esta razón, es importante estudiar la vulnerabilidad a la cavitación con el objetivo de conocer las implicancias funcionales de los ajustes observados.

E. grandis mostró los ajustes más notables en las fibras —reducción de largo, aumento en el espesor de paredes y reducción de S —, aunque sin cambios significativos en la densidad de la madera. Los híbridos GU1 y GU2 exhibieron un comportamiento intermedio entre los híbridos con eucaliptos colorados y el clon de *E. grandis*. En términos de plasticidad, algunos rasgos de las fibras en estos híbridos variaron de manera similar a GG —reducción de longitud—, mientras que otros se comportaron como en GC y GT —fracción de lúmenes (F_f) y espesor de pared— y permanecieron relativamente constantes bajo el estrés.

Al comparar distintos órganos dentro de las plantas, se observaron diferencias en las respuestas entre tallo y rama, lo que sugiere una regulación diferencial del estado hídrico entre órganos (Gándara et al., 2025b). Por ejemplo, la densidad de la madera fue 25 % mayor en ramas que en tallos de las mismas plantas, lo que evidencia el compromiso entre seguridad y eficiencia en órganos distales, ya que están sometidos

a mayor tensión y riesgo de cavitación. Si bien en este trabajo no se compararon estadísticamente los atributos del xilema entre órganos, los resultados sugieren que en los tallos se prioriza la eficiencia hidráulica (mayor conductividad), y en las ramas, la seguridad del sistema conductivo. En este sentido, hubo diferencias entre clones y condición hídrica. El clon GG fue el que mostró mayores cambios en los rasgos anatómicos de rama debido al estrés, resultado consistente con la mayor sensibilidad al estrés de este clon que reportaron diversos autores, incluyendo los resultados de esta tesis.

El estudio de la eficiencia hidráulica, inferida por los rasgos anatómicos del xilema, reveló diferencias entre clones y órganos en respuesta al estrés. Esta se analizó a través de la $k_{St\text{theo}}$, calculada a partir de la cantidad y distribución de tamaño de los vasos. Todos los clones redujeron el valor de S (composición de vasos) en tallos durante el déficit hídrico y, al mismo tiempo, generaron vasos más pequeños y más homogéneamente distribuidos en términos de los extremos de tamaño, lo cual posiblemente aumentó la seguridad hidráulica. La excepción fue el clon GU1, que no modificó este parámetro. Al comparar cómo varía la eficiencia del transporte en función de la fracción de lúmenes (F) entre distintos órganos, se observó que la $k_{St\text{theo}}$ es mayor en los tallos para un mismo valor de F. Esto sugiere que la distribución del tamaño de vasos (S) tiene un rol más importante que F en la eficiencia del transporte, a diferencia de lo reportado en varias especies de *Eucalyptus* por Barotto et al. (2017). Los clones GG y GU2 redujeron S y F en los tallos, mientras que GC y GT ajustaron solamente S, y GU1 modificó únicamente F. Estos patrones muestran la diversidad de respuestas entre genotipos, lo que indica diferencias notables en el balance entre seguridad y eficiencia aún dentro de especies emparentadas. Cabe destacar que en GG y GU2, la relación $k_{St\text{theo}}$ vs. F en tallos varió con el estrés, mostrando una disociación entre plantas control y plantas estresadas. Probablemente, esto se deba al refuerzo mecánico y a la reducción del tamaño de vasos en estos genotipos.

Los patrones de crecimiento fueron similares dentro de cada grupo de clones. En cuatro de los cinco genotipos, la caída del crecimiento en altura durante la sequía duplicó a la caída del crecimiento en diámetro. Sin embargo, GC fue el único clon que mantuvo valores de crecimiento similares entre las plantas control y las plantas

estresadas. Esto podría deberse, entre otros factores, a la activación de los mecanismos de respuesta morfofisiológicos e hidráulicos anteriormente mencionados, los cuales permitieron mantener la turgencia y el intercambio gaseoso durante el período de estrés. Los resultados evidencian la capacidad de GC para activar múltiples mecanismos de respuesta a la sequía. Al igual que el clon GT, los resultados sugieren que se trata de especies tolerantes, a diferencia de GG y GU2, que fueron particularmente sensibles y presentaron estrategias de respuesta similares a las especies evitadoras (Lambers et al., 2008; Levitt, 1980). La tendencia al mejor desempeño de los híbridos con eucaliptos colorados se observó también en árboles a campo, donde los clones GC y GT crecieron más que los otros, especialmente en condiciones de alta disponibilidad hídrica en el suelo, destacándose el clon GC por su crecimiento diamétrico superior (Gándara et al., 2020). En Sudáfrica, Drew et al. (2009) reportaron un comportamiento similar en clones GC creciendo a campo y lo compararon con el crecimiento de clones GU, que fue mayor durante períodos con buena disponibilidad hídrica y se redujo drásticamente en la estación seca.

Cabe destacar que los resultados de nuestros ensayos muestran una alta complejidad de respuestas, no siempre coincidente con los reportes de otros clones híbridos de *Eucalyptus* mencionados en los párrafos anteriores. Así, si bien se esperaba que los clones GC y GT tuvieran un mejor desempeño que el GG ante sequía, esto solo se verificó en el caso del GC en los ensayos controlados. Si bien ambos clones híbridos mostraron comportamientos anatomo-fisiológicos similares, el desempeño en crecimiento ante sequía fue mejor en GC que en GT. Asimismo, se esperaba que estos híbridos tuvieran un desempeño más pobre que el clon GG ante buenas condiciones hídricas, resultado que no se verificó en los ensayos de condiciones controladas ni en árboles a campo. En este sentido, el clon GC mostró siempre el mejor desempeño, tanto en el tratamiento control como bajo estrés. Por otro lado, los dos clones GU también tuvieron cierta similitud de comportamiento anatomo-fisiológico entre sí, pero el desempeño ante estrés —medido por el crecimiento en altura y diámetro— difirió entre clones, siendo GU2 más sensible que GU1. Estos resultados sugieren la necesidad de mediciones adicionales —como la asignación de carbono a raíces— para explicar la variabilidad de las respuestas observadas.

Por otro lado, contrariamente a lo postulado en nuestra segunda hipótesis, no se encontró evidencia concluyente de que el mejor desempeño ante la sequía estuviera asociado a una mayor plasticidad fenotípica en los híbridos. El clon GG, altamente sensible a la sequía, mostró diversas respuestas plásticas en términos fisiológicos (ejemplo, ajuste osmótico) y en la anatomía del xilema (ejemplo, marcada reducción de F y S de vasos, así como de las propiedades de las fibras). Si bien el clon de mejor desempeño, GC, se caracterizó por una alta plasticidad en varios caracteres, estos resultados sugieren que la plasticidad *per se* no es condición suficiente para alcanzar alta resistencia a la sequía en los eucaliptos estudiados, sino que el tipo de estrategia general —baja sensibilidad estomática, alta densidad de madera y posiblemente baja vulnerabilidad a la cavitación, alta capacidad de ajuste osmótico y elástico de los tejidos— es más importante para la adaptabilidad a condiciones variables de agua en suelo.

La finalidad central de esta tesis fue contribuir al conocimiento de caracteres que permitan la selección genética con foco en la adaptabilidad a la sequía. Para ello, más allá del análisis cualitativo precedente, se exploraron relaciones cuantitativas entre tasa media de crecimiento de los plantines bajo condiciones controladas y distintos caracteres de fácil medición explorados en la tesis. En este sentido, se planteó como tercera hipótesis de trabajo que existirían caracteres sencillos de medir que —por su asociación directa o indirecta con el desempeño de los distintos genotipos— podrían servir para la selección genética en programas de fenotipado de alto caudal. Los resultados del trabajo revelaron algunas relaciones significativas (figuras 4 y 5). Se trabajó con valores medios de los caracteres por clon y tratamiento, presentados en tablas por Gándara et al. (2025 a y b). Se analizó el desempeño del crecimiento relativo en altura y diámetro en ambos tratamientos de disponibilidad hídrica, así como la relación entre estas variables en el tratamiento de sequía respecto al control —como medida de la sensibilidad a la sequía—, considerando los siguientes caracteres de relativamente fácil medición: área foliar específica de las hojas (AFE), densidad de madera de ramas y tallos, k_{Smax} medida en tallos, k_{Stheo} de ramas y tallos, fracción de lúmenes de vasos (F) de ramas y tallos y composición de vasos (S) de ramas y tallos. Se presentan únicamente las relaciones con un coeficiente de determinación (R^2)

mayor a 0,5, que es equivalente a un coeficiente de correlación mayor a 0,7, indicativo de una asociación fuerte.

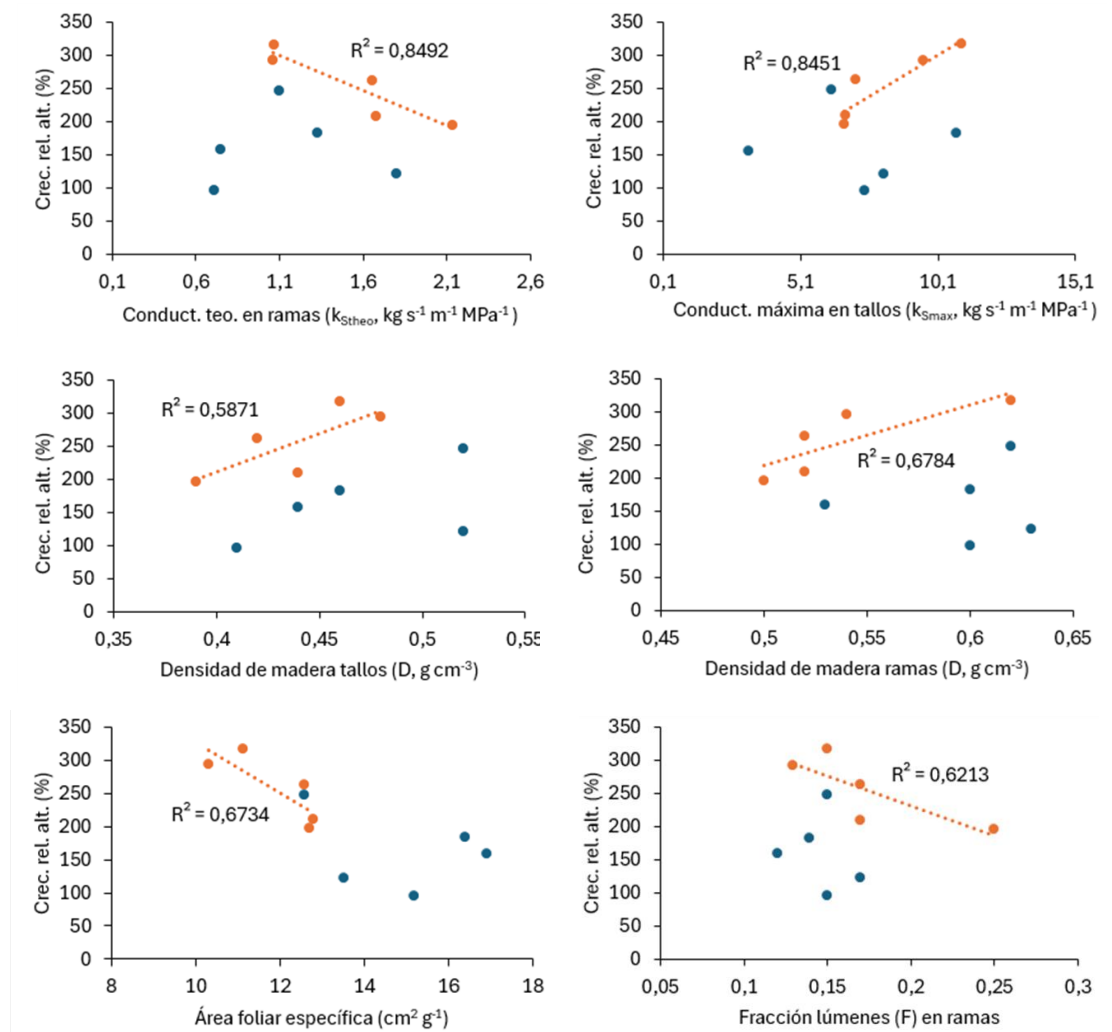
El crecimiento relativo en diámetro de los plantines presentó una baja asociación con todos los caracteres explorados ($R^2 < 0,3$ en todos los casos; datos no mostrados). Por el contrario, el crecimiento relativo en altura de los plantines presentó una alta asociación con varios caracteres funcionales, aunque se destaca que estas asociaciones solo fueron marcadas en los plantines creciendo en el tratamiento control, de alta disponibilidad hídrica (figura 4, símbolos naranjas). En los plantines creciendo bajo estrés hídrico, las relaciones se desacoplan (figura 4, símbolos azules), lo que sugiere que los cambios plásticos ocurridos en ellos no se trasladan de manera directa y lineal —análisis univariado— al desempeño de los plantines bajo esta condición. De acuerdo con estos resultados exploratorios, las tasas máximas de crecimiento en altura de los plantines estarían negativamente relacionadas con la $k_{S_{theo}}$ y la fracción de lúmenes (F) de ramas; ambas variables se correlacionan entre sí (Gándara et al., 2025b). Este resultado puede parecer contraintuitivo debido a la relación generalmente postulada entre la eficiencia del transporte de agua y la fijación de C en las especies leñosas (e. g., Hubbard et al., 2001; Sperry et al., 2008). Sin embargo, podría entenderse a la luz de la compleja arquitectura hidráulica de los eucaliptos, en los que especies como *E. grandis* se caracterizan por tener una alta eficiencia hidráulica en tallos, pero una baja eficiencia (baja k_s) en las ramas terminales. Este patrón se asocia con una alta vulnerabilidad a la cavitación (Fernández et al., 2019), donde las ramas, posiblemente, actúen como fusibles hidráulicos en el contexto de una estrategia evitadora de la deshidratación. Asimismo, se verificó una asociación negativa con el AFE, lo que indica que los genotipos que maximizan la superficie foliar por unidad de biomasa son aquellos con menor crecimiento en altura: nuevamente un resultado contraintuitivo. Sin embargo, este estaría a favor de la idea de estructuras terminales (ramas y hojas) conservativas del agua como asociadas a un mejor desempeño aun en condiciones de alta disponibilidad hídrica.

Por otro lado, el crecimiento relativo en altura de los plantines en condiciones de alta disponibilidad hídrica se relacionó positivamente con la conductividad hidráulica específica máxima ($k_{S_{max}}$) medida en los tallos y con la densidad de la

madera de tallos y ramas (figura 4). Estos resultados también contradicen el esperado compromiso en las especies leñosas entre eficiencia hidráulica y seguridad del sistema conductivo, reflejado en una alta densidad de la madera. Sin embargo, están a favor de la ausencia de estos compromisos postulada para genotipos de *Eucalyptus* de alto crecimiento por Fernández et al. (2019). Estos resultados respaldan la idea de que, en los eucaliptos, las altas tasas de crecimiento (al menos en altura) se logran combinando una alta eficiencia hidráulica en tallos con una alta densidad de madera, posiblemente como refuerzo para el sostenimiento de la función hidráulica en condiciones de alta demanda evaporativa.

Figura 4

Regresiones lineales entre el crecimiento relativo en altura (extraído de Gándara et al., 2025a) y distintos caracteres funcionales de ramas o tallos (extraídos de Gándara et al., 2025 a y b) en 5 clones de *Eucalyptus* (GG, GC, GT, GU1 y GU2) creciendo en condiciones controladas.



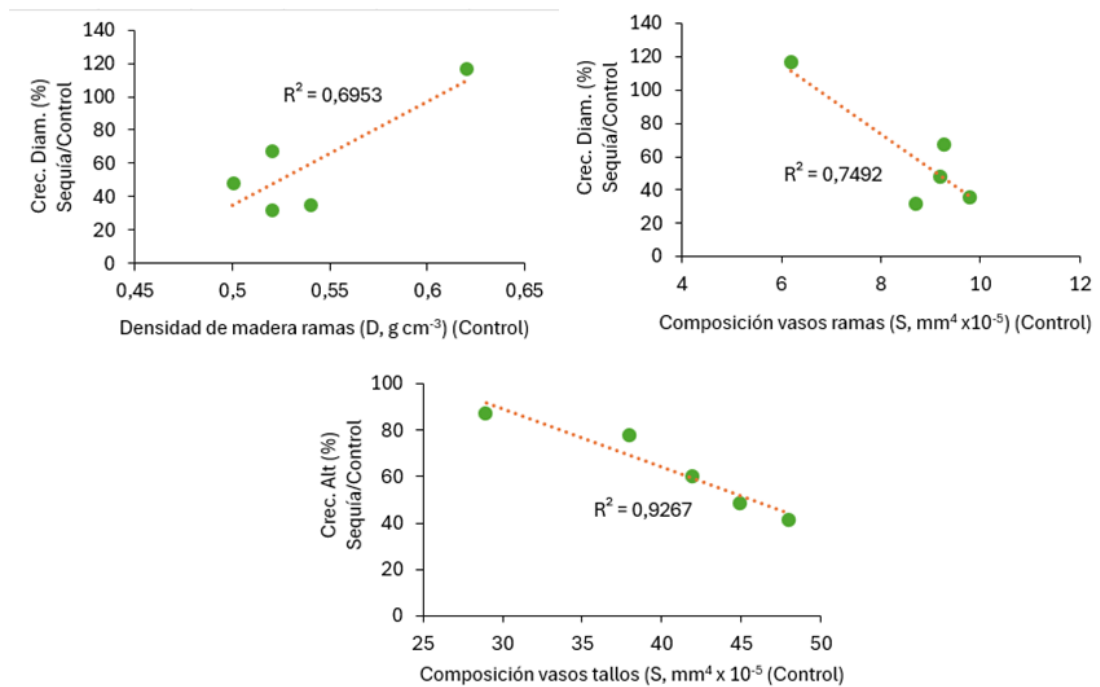
Nota. Cada punto es el promedio del genotipo. Los símbolos en naranja representan a las plantas creciendo bajo alta disponibilidad hídrica (control), y los símbolos azules, plantas en el tratamiento de estrés hídrico. Las relaciones mostradas poseen un coeficiente de determinación (R^2) de al menos 0,5 ($p < 0,05$) y corresponden en todos los casos a las plantas control.

Finalmente, se relacionó la sensibilidad a la sequía de los genotipos (cociente entre el crecimiento en sequía y el crecimiento en control, multiplicado por cien) con los distintos caracteres medidos en las plantas control, es decir, con aquellos caracteres que el genotipo expresa cuando tiene alta disponibilidad hídrica. Se exploraron estas relaciones considerando su posible aplicación en *screening* de plantines bajo riego frecuente, tratamiento que es más sencillo de aplicar que el de estrés controlado. Se encontraron solo tres relaciones significativas y altas (figura 5).

Dos de estas relaciones (primer y segundo panel de la figura 5) estuvieron muy traccionadas por el valor más disímil del genotipo GC. Este presentó la menor sensibilidad a la sequía (en realidad, un crecimiento medio incluso mayor que en el control, como se expresa en el porcentaje mayor a 100 %) con una alta densidad de madera y baja composición de vasos (S) de las ramas. Valores bajos de S, que es el cociente entre el tamaño medio y el número de vasos del xilema, se asocia en la bibliografía a una mayor seguridad hidráulica, ya que implica un número mayor de vasos con menor diámetro (Zanne et al., 2010). Por otro lado, se observó una relación muy significativa entre la sensibilidad del crecimiento en altura con la composición de vasos del tallo (tercer panel de figura 5). En este sentido, la mayor resistencia (o menor sensibilidad) ante la sequía se explicó por distintos caracteres del xilema de ramas o tallos, asociados en la literatura con una mayor seguridad del sistema de conducción de agua.

Figura 5

Regresión lineal entre la sensibilidad del crecimiento relativo en diámetro basal del tallo (paneles superiores) y el crecimiento en altura (panel inferior) frente a la sequía, en función de distintos caracteres funcionales de ramas o tallos (Gándara et al., 2025 a y b) en cinco clones de *Eucalyptus* (GG, GC, GT, GU1 y GU2) creciendo en condiciones controladas.



Nota. Se muestran solo las relaciones con un coeficiente de determinación (R^2) de al menos 0,5 ($p < 0,05$).

Estas exploraciones en relación con los caracteres que podrían usarse en fenotipado deben tomarse con cautela debido a que se trabajó con solo cinco genotipos. Sin embargo, permiten abrir promisorias líneas de trabajo a futuro con otros genotipos, de manera de verificar si se refuerzan o refutan estos patrones. De verificarse, estos resultados podrían tener importantes implicancias para el mejoramiento genético de *Eucalyptus* orientado a la optimización conjunta del crecimiento y la resistencia a la sequía.

Si bien los resultados de esta tesis aportan evidencias valiosas sobre rasgos potencialmente útiles para la selección genética orientada a la tolerancia a la sequía,

es necesario interpretar estas asociaciones con precaución. En particular, las relaciones que vinculan la densidad de la madera con un mayor desempeño bajo estrés estuvieron fuertemente influenciadas por el valor del clon GC, lo que evidencia el riesgo de extrapolar patrones basados en un número reducido de genotipos. Esto sugiere que la densidad de madera, aunque promisorio, no puede considerarse por sí sola un criterio general y robusto de *screening*. Su uso debería evaluarse en un conjunto más amplio de materiales genéticos y siempre en combinación con otros rasgos fisiológicos e hidráulicos para evitar sesgos genotípicos y fortalecer la predicción del desempeño en ambientes con disponibilidad hídrica variable.

6. Conclusiones

En este trabajo se evaluó la respuesta al déficit hídrico en plantines (en invernáculo) y árboles juveniles (a campo) de clones comerciales de *Eucalyptus grandis* (GG), *E. grandis* × *camaldulensis* (GC), *E. grandis* × *tereticornis* (GT) y *E. grandis* × *urophylla* (GU1 y GU2). Se analizaron variables fisiológicas, hidráulicas y anatómicas y su relación con el crecimiento. Los resultados revelaron diferentes estrategias de respuesta a la sequía entre los clones, consistentes en general dentro de los genotipos entre estadios ontogenéticos (plantín, árbol juvenil) y condiciones de crecimiento (invernáculo, campo).

Los híbridos con eucaliptos colorados, GC y GT, presentaron un menor control estomático durante la sequía, lo que favoreció una mayor transpiración y asimilación de carbono, y permitió mantener su capacidad de crecimiento, particularmente en el clon GC. Así, fueron menos eficientes en el uso del agua y mostraron una estrategia de tipo derrochadora, reforzada por su carácter anfiestomático. Como consecuencia del menor cierre estomático y de su comportamiento anisohídrico, estos híbridos registraron una caída sustancial de la conductividad hidráulica en tallos durante la sequía, a pesar de que, probablemente, tuvieron una menor vulnerabilidad a la cavitación inferida por este parámetro en sus parentales (*E. camaldulensis* y *E. tereticornis*), su alta densidad de madera y parámetros anatómicos que así lo sugieren (ejemplo, baja composición de vasos, S). Durante el estrés, todos los clones incrementaron la densidad de la madera de tallo y, al mismo tiempo, redujeron el diámetro de los vasos y aumentaron su frecuencia. Sin embargo, a diferencia de los otros clones, en GC y GT no se modificó la fracción de lúmenes de vasos (F) ni la longitud de las fibras, lo cual favoreció la eficiencia y la seguridad hidráulica. Curiosamente, GC presentó una alta conductividad hidráulica teórica y elevada densidad de la madera, lo que sugiere una adaptación simultánea para un transporte eficiente y resistencia. Estos caracteres del xilema, junto a su alta capacidad de ajuste osmótico y elástico en las hojas, resultaron en que haya sido el único clon que mantuvo el crecimiento en altura y diámetro durante la sequía respecto al tratamiento control. Esta alta resistencia (o baja sensibilidad) al estrés no se vio comprometida con el

crecimiento en condiciones de alta disponibilidad hídrica, tanto en plantines creciendo en condiciones controladas como en árboles jóvenes en el campo. Es decir, el clon GC optimizó el crecimiento en ambos tipos de condición.

E. grandis (GG) y, en menor medida GU1 y GU2, siguieron una estrategia más conservadora del uso de agua durante la sequía, caracterizada por un fuerte control estomático y una menor actividad transpiratoria —asociada a su carácter hipoestomático—, lo que indica que priorizaron la seguridad del sistema conductivo, principalmente el clon GG. Este clon presentó los ajustes más notables en rasgos de las fibras, con una reducción en su longitud, un aumento del espesor de sus paredes, así como también un temprano ajuste osmótico durante la sequía. A pesar de estas respuestas plásticas, este clon no fue capaz de mantener la apertura estomática durante la desecación del suelo y, por lo tanto, fue más sensible al estrés hídrico (*i. e.*, alta caída del crecimiento en altura y diámetro).

Ambos híbridos GU1 y GU2 exhibieron un comportamiento intermedio entre los híbridos con eucaliptos colorados y el clon de *E. grandis*. En términos de plasticidad, algunos rasgos de las fibras en estos híbridos variaron de manera similar a GG, mientras que otros se comportaron como en GC y GT no mostraron cambios durante la sequía. Si bien presentaron un perfil similar de respuestas morfofisiológicas, su sensibilidad a la sequía fue diferente, con una mayor sensibilidad —similar a GG— en el caso de GU2. Esto sugiere que, más allá de comportamientos fisiológicos similares (entre GC y GT o entre GU1 y GU2), el desempeño ante la sequía es variable inclusive dentro de combinaciones altamente emparentadas, lo que hace necesaria la evaluación de cada nuevo genotipo de manera particular.

La similitud de comportamiento entre estadios ontogenéticos en la mayoría de los clones sugiere que sería posible realizar selecciones tempranas basadas en caracteres morfofisiológicos durante las etapas iniciales del desarrollo de las plantas. Sin embargo, el clon GU1 difirió en parte en su comportamiento en invernáculo y campo, con mayor sensibilidad a sequía en el estadio juvenil que lo demostrado en el estadio de plantín, lo que sugiere la necesidad de más estudios.

Si bien se recomienda precaución debido a la necesidad de evaluar otros genotipos, se identificaron caracteres que podrían servir para el fenotipado de alto

rendimiento, tendiente a optimizar crecimiento y la tolerancia al estrés hídrico. En este sentido, la (alta) densidad de madera de tallos y ramas y la (baja) composición de vasos del xilema (S) aparecen como *proxies* de una baja sensibilidad a la sequía.

7. Bibliografía

- Agathokleous, E., Feng, Z. y Peñuelas, J. (2020). Chlorophyll hormesis: Are chlorophylls major components of stress biology in higher plants? *Science of the Total Environment*, 726, 138637. <https://doi.org/10.1016/j.scitotenv.2020.138637>
- Amatya, D. M., Munka, C., Gándara, J., Chescheir, G. M. y Skaggs, R. W. (2014). Evapotranspiration from a planted pine forest and a grassland site in Uruguay. En *Proceedings of the ASABE Conference on Evapotranspiration: Challenges in Measurement and Modeling from Leaf to the Landscape Scale and Beyond*. Raleigh. https://www.researchgate.net/publication/299582249_Evapotranspiration_from_a_Planted_Pine_Forest_and_a_Grassland_Site_in_Uruguay
- Anderegg, W. R. L., Klein, T., Bartlett, M., Sack, L., Pellegrini, A. F. A., Choat, B. y Jansen, S. (2020). Catastrophic hydraulic failure and tipping points in plants. *New Phytologist*, 226(4), 1180-1197. <https://doi.org/10.1111/nph.16410>
- Anderegg, W. R. L., Wolf, A., Arango-Velez, A., Choat, B., Chmura, D. J., Jansen, S., ... y Sperry, J. S. (2018). Woody plants optimise stomatal behaviour relative to hydraulic risk. *Ecology Letters*, 21(7), 968-977. <https://doi.org/10.1111/ele.12962>
- Balaguer, L., Martínez-Ferri, F., Valladares, M. y Pérez-Corona, F. (2002). Population divergence in the plasticity of the response of *Quercus coccifera* to the light environment. *Functional Ecology*, 15(1), 124-135.
- Barotto, A. J., Fernandez, M. E. y Gyenge, J. (2016). First insights into the functional role of vasicentric tracheids and parenchyma in *Eucalyptus* species with solitary vessels: Do they contribute to xylem efficiency or safety? *Tree Physiology*, 36(12), 1485-1497. <https://doi.org/10.1093/treephys/tpw072>
- Barotto, A. J., Monteoliva, S., Gyenge, J., Martínez-Meier, A. y Fernández, M. E. (2018). Functional relationships between wood structure and vulnerability to xylem cavitation in races of *Eucalyptus globulus* differing in wood density. *Tree Physiology*, 38(2), 243-251. <https://doi.org/10.1093/treephys/tpx138>

- Barotto, A. J., Monteoliva, S., Gyenge, J., Martínez-Meier, A., Moreno, K., Tesón, N. y, Fernández, M. E. (2017). Wood density and anatomy of three *Eucalyptus* species: Implications for hydraulic conductivity. *Forest Systems*, 26, e010. <https://doi.org/10.5424/fs/2017261-10446>
- Blackman, C. J., Pfautsch, S., Choat, B., Delzon, S., Gleason, S. M. y Duursma, R. A. (2016). Toward an index of desiccation time to tree mortality under drought. *Plant, Cell & Environment*, 39(10), 2342-2345. <https://doi.org/10.1111/pce.12758>
- Bond, B. J. y Kavanagh, K. L. (1999). Stomatal behavior of four woody species in relation to leaf-specific hydraulic conductance and threshold water potential. *Tree Physiology*, 19(8), 503-510. <https://doi.org/10.1093/treephys/19.8.503>
- Bourné, A. E., Haigh, A. M. y Ellsworth, D. S. (2015). Stomatal sensitivity to vapour pressure deficit relates to climate of origin in *Eucalyptus* species. *Tree Physiology*, 35(3), 266-278. <https://doi.org/10.1093/treephys/tpv014>
- Brodribb, T. J. y Holbrook, N. M. (2004). Stomatal closure during leaf dehydration, correlation with other leaf physiological traits. *Plant Physiology*, 134(4), 224-235.
- Cano, D., Cacciuttolo, C., Custodio, M. y Nosetto, M. (2023). Effects of Grassland Afforestation on Water Yield in Basins of Uruguay: A Spatio-Temporal Analysis of Historical Trends Using Remote Sensing and Field Measurements. *Land*, 12(1), 185. <https://doi.org/10.3390/land12010185>
- Carraro, E. y Di Iorio, A. (2022). Eligible strategies of drought response to improve drought resistance in woody crops: A mini-review. *Plant Biotechnology Reports*, 16, 265-282. <https://doi.org/10.1007/s11816-021-00733-x>
- Choat, B., Brodribb, T. J., Brodersen, C. R., Duursma, R. A., López, R. y Medlyn, B. E. (2018). Triggers of tree mortality under drought. *Nature*, 558(7711), 531-539. <https://doi.org/10.1038/s41586-018-0240-x>
- Choat, B., Jansen, S., Brodribb, T. J., Cochard, H., Delzon, S., Bhaskar, R., ... y Zanne, A. E. (2012). Global convergence in the vulnerability of forests to drought. *Nature*, 491(7426), 752-755. <https://doi.org/10.1038/nature11688>

- Corcuera, L. (2003). Comparación de dos métodos para generar curvas presión-volumen en especies del género *Quercus*. *Investigación Agraria: Sistemas y Recursos Forestales*, 12(1), 111-121.
- Dalla-Salda, G., Martínez-Meier, A., Cochard, H. y Rozenberg, P. (2011). Genetic variation of xylem hydraulic properties shows that wood density is involved in adaptation to drought in Douglas-fir (*Pseudotsuga menziesii* (Mirb.)). *Annals of Forest Science*, 68(4), 747-757. <https://doi.org/10.1007/s13595-011-0091-1>
- Dellacassa, P. y Figarola Sosa, G. (2016). *Estudio del estado hídrico y eficiencia en el uso del agua en clones de Eucalyptus grandis e híbridos interespecíficos* [tesis de grado, Universidad de la República]. Repositorio institucional de la Universidad de la República.
- Dellepiane, J. (2023). *Estudio de la eficiencia de uso del agua (EUA) en una plantación de eucaliptus híbridos de origen clonal* [tesis de grado, Universidad de la República]. Repositorio institucional de Facultad de Agronomía.
- Dogliotti, G., Rizzo, I., Baietto, A., Posse, J. P., Aubet, N. y González-Tálice, J. (2023). Crown segmentation using Airborne Laser Scanning data in a silvopastoral system with *Eucalyptus grandis*. *Agrociencia Uruguay*, 27(NE2), e1311. <https://doi.org/10.31285/AGRO.27.1311>
- Drew, D. M., Downes, G. M., Grzeskowiak, V. y Naidoo, T. (2009). Differences in daily stem size variation and growth in two hybrid eucalypt clones. *Trees: Structure and Function*, 23(3), 585-595. <https://doi.org/10.1007/s00468-008-0303-y>
- Eamus, D., O'Grady, A. P. y Hutley, L. (2000). Dry season conditions determine wet season water use in the wet-tropical savannas of Northern Australia. *Tree Physiology*, 20(18), 1219-1226. <https://doi.org/10.1093/treephys/20.18.1219>
- England, J. R. y Attiwill, P. M. (2011). Changes in stomatal frequency, stomatal conductance, and cuticle thickness during leaf expansion in the broad-leaved evergreen species, *Eucalyptus regnans*. *Trees: Structure and Function*, 25(6), 987-996. <https://doi.org/10.1007/s00468-011-0573-7>
- Fernández, M. E. y Gyenge, J. E. (eds.). (2010). *Técnicas de medición en ecofisiología vegetal*. Instituto Nacional de Tecnología Agropecuaria.

- Fernández, M. E., Barotto, A. J., Martínez-Meier, A. y Monteoliva, S. (2019). New insights into wood anatomy and function relationships: How *Eucalyptus* challenges what we already know. *Forest Ecology and Management*, 454, 117638. <https://doi.org/10.1016/j.foreco.2019.117638>
- Fichot, R., Brignolas, F., Cochard, H. y Ceulemans, R. (2015). Vulnerability to drought-induced cavitation in poplars: Synthesis and future opportunities. *Plant, Cell & Environment*, 38(7), 1233-1251. <https://doi.org/10.1111/pce.12491>
- Gándara, J. M. (2013). *Curso estacional del estado hídrico, crecimiento y actividad fotosintética en un rodal de Pinus taeda L. en Uruguay* [tesis de maestría, Universidad de la República]. Colibri. <https://hdl.handle.net/20.500.12008/1852>
- Gándara, J. M., Viega, L., Ross, S., Munka, C. y Bentancourt, Ó. (2014). Variación estacional del estado hídrico y crecimiento de *Pinus taeda* L. bajo diferente manejo silvícola en el noreste de Uruguay. *Agrociencia Uruguay*, 18(1), 1-11. <https://doi.org/10.31285/AGRO.18.432>
- Gándara, J., Nión, M., González-Tálice, J., Ross, S., Villar, J. y Fernández, M. E. (2025a). Similar but unique: physiological response to drought and growth of pure species and interspecific hybrid clones of *Eucalyptus*. *Trees*, 39(36). <https://doi.org/10.1007/s00468-025-02609-x>
- Gándara, J., Nión, M., Ross, S., González-Tálice, J., Tabeira, P. y Fernández, M. E. (2025b). Xylem functional anatomy of pure-species and interspecific hybrid clones of *Eucalyptus* differing in drought resistance. *Forests*, 16(8), 1267. <https://doi.org/10.3390/f16081267>
- Gándara, J., Ross, S., Quero, G., Nión, M., Dellacassa, P., Dellepiane, J. y Viega, L. (2020). Differential water-use efficiency and growth among *Eucalyptus grandis* hybrids under two different rainfall conditions. *Forest Systems*, 29(2), e006. <https://doi.org/10.5424/fs/2020292-16011>
- Gleason, S. M., Westoby, M., Jansen, S., Choat, B., Hacke, U. G., Pratt, R. B., Bhaskar, R., Brodribb, T. J., Bucci, S. J., Cao, K.-F., Cochard, H., Delzon, S., Domec, J.-C., Fan, Z.-X., Feild, T. S., Jacobsen, A. L., Johnson, D. M., Lens, F., Maherali, H. ... Zanne, A. E. (2016). Weak tradeoff between xylem safety and

- xylem-specific hydraulic efficiency across the world's woody plant species. *New Phytologist*, 209(1), 123-136. <https://doi.org/10.1111/nph.13646>
- Gonçalves, J. L. M., Alvares, C. A., Rocha, J. H. T., Brandani, C. B. y Hakamada, R. E. (2017). Eucalypt plantation management in regions with water stress. *Southern Forests: A Journal of Forest Science*, 79(3), 169-183. <https://doi.org/10.2989/20702620.2016.1255415>
- González-Tálice, J. y Dogliotti, G. (2024). Characterizing microenvironmental factors and the forest component in the production of natural grasslands in a silvopastoral system with *Eucalyptus grandis*. *Agroforestry Systems*, 98(7), 2071-2085. <https://doi.org/10.1007/s10457-024-01028-0>
- Guarnaschelli, A. B., Lemcoff, J. H., Prystupa, P. y Garau, A. M. (2003). Responses to drought preconditioning in *Eucalyptus globulus* Labill. provenances. *Trees: Structure and Function*, 17(6), 501-509. <https://doi.org/10.1007/s00468-003-0264-0>
- Hacke, U. G., Sperry, J. S., Pockman, W. T., Davis, S. D. y McCulloh, K. A. (2001). Trends in wood anatomy and hydraulic traits of angiosperms: Evidence for a tradeoff between conduit safety and efficiency. *Tree Physiology*, 21(10), 689-717. <https://doi.org/10.1007/s004420100628>
- Hacke, U. G., Sperry, J. S., Wheeler, J. K. y Castro, L. (2006). Scaling of angiosperm xylem structure–function relationships. *Plant, Cell & Environment*, 29(1), 125-136. <https://doi.org/10.1093/treephys/26.6.689>
- Hammond, W. M. y Adams, H. D. (2019). Dying on time: Traits influencing the dynamics of tree mortality risk from drought. *Tree Physiology*, 39(6), 906-909. <https://doi.org/10.1093/treephys/tpz050>
- Harper, R. J., Smettem, K. R. J., Carter, J. O. y McGrath, J. F. (2009). Drought deaths in *Eucalyptus globulus* plantations in relation to soils, geomorphology and climate. *Plant and Soil*, 324(1-2), 199-207. <https://doi.org/10.1007/s11104-009-9944-x>
- Hmidi, D., Muraya, F., Fizames, C., Véry, A. -A. y Roelfsema, M. R. G. (2025). Potassium extrusion by plant cells: Evolution from an emergency valve to a

- driver of long-distance transport. *New Phytologist*, 245(1), 69-87.
<https://doi.org/10.1111/nph.20207>
- Hubbard, R. M., Ryan, M. G., Stiller, V. y Sperry, J. S. (2001). Stomatal conductance and photosynthesis vary linearly with plant hydraulic conductance in ponderosa pine. *Plant, Cell & Environment*, 24(2), 113-121.
- Ilic, J., Boland, D., McDonald, M., Downes, G. y Blakemore, P. (2000). *Wood density: Phase 1—State of knowledge* [reporte técnico n.º 18]. Australian Greenhouse Office; National Carbon Accounting System.
<https://www.dceew.gov.au/themes/custom/awe/fullcam/Help-FullCAM2020/reps/TR18%20Woody%20Density%20Phase%201%20-%20State%20of%20Knowledge.pdf>
- Intergovernmental Panel on Climate Change (IPCC), Lee, H. (ed.) y Romero, J. (ed.). (2023). *Climate change 2023: Synthesis report: Contribution of Working Groups I, II and III to the Sixth Assessment Report of the Intergovernmental Panel on Climate Change*. <https://doi.org/10.59327/IPCC/AR6-978929169164>
- Jacobsen, A. L., Pratt, R. B., Ewers, F. W. y Davis, S. D. (2007). Cavitation resistance and seasonal hydraulics differ among three arid California plant communities. *Plant, Cell & Environment*, 30(12), 1599-1612. <https://doi.org/10.1111/j.1365-3040.2007.01729.x>
- Johnson, D. M., Katul, G. y Domec, J. C. (2022). Catastrophic hydraulic failure and tipping points in plants. *Plant, Cell & Environment*, 45(7), 2073-2084. <https://doi.org/10.1111/pce.14327>
- Kapilan, R., Vaziri, M. y Zwiazek, J. J. (2019). Regulation of aquaporins in plants under stress. *Biological Research*, 51, artículo 4. <https://doi.org/10.1186/s40659-018-0152-0>
- Kerstiens, G. (1996). Cuticular water permeability and its physiological significance. *Journal of Experimental Botany*, 47(12), 1813-1832. <https://doi.org/10.1093/jxb/47.12.1813>
- Körner, C. y Cochrane, P. M. (1985). Stomatal responses and water relations of *Eucalyptus pauciflora* in summer along an elevational gradient. *Oecologia*, 66(4), 443-455. <https://doi.org/10.1007/BF00378313>

- Lachenbruch, B. y McCulloh, K. A. (2014). Traits, properties, and performance: How woody plants combine hydraulic and mechanical functions in a cell, tissue, or whole plant. *New Phytologist*, 204(4), 747-764. <https://doi.org/10.1111/nph.13035>
- Lambers, H., Chapin, F. S. y Pons, T. L. (2008). *Plant physiological ecology*. Springer.
- Lamy, J. B., Delzon, S., Bouche, P. S., Alia, R., Vendramin, G. G., Cochard, H. y Plomion, C. (2014). Limited genetic variability and phenotypic plasticity detected for cavitation resistance in a Mediterranean pine. *New Phytologist*, 201(3), 874-886. <https://doi.org/10.1111/nph.12556>
- Larcher, W. (2003). *Physiological plant ecology: Ecophysiology and stress physiology of functional groups* (4.^a ed.). Springer.
- Lemcoff, J. H., Guarnaschelli, A. B., Garau, A. M. y Prystupa, P. (2002). Elastic and osmotic adjustments in rooted cuttings of several clones of *Eucalyptus camaldulensis* Dehn. from southeastern Australia after a drought. *Flora*, 197(2), 134-142. <https://doi.org/10.1078/0367-2530-00023>
- Lens, F., Sperry, J. S., Christman, M. A., Choat, B., Rabaey, D. y Jansen, S. (2011). Testing hypotheses that link wood anatomy to cavitation resistance and hydraulic conductivity in angiosperm trees. *New Phytologist*, 190(3), 709-723. <https://doi.org/10.1111/j.1469-8137.2010.03518.x>
- Lenz, T. I., Wright, I. J. y Westoby, M. (2006). Interrelations among pressure–volume curve traits across species and water availability gradients. *Physiologia Plantarum*, 127(3), 423-433. <https://doi.org/10.1111/j.1399-3054.2006.00680.x>
- Leuschner, C., Wedde, P. y Lübbe, T. (2019). The relation between pressure–volume curve traits and stomatal regulation of water potential in five temperate broadleaf tree species. *Annals of Forest Science*, 76, 60. <https://doi.org/10.1007/s13595-019-0838-7>
- Levit, J. (1980). *Responses of plants to environmental stresses* (vol. II, 2.^a ed.). Academic Press.
- Li, S., Wang, J., Lu, S., Salmon, Y., Liu, P. y Guo, J. (2023). Trade-off between hydraulic safety and efficiency in plant xylem and its influencing factors. *Forests*, 14(9), 1817. <https://doi.org/10.3390/f14091817>

- Li, Y., Huang, Y., Zheng, Y., Zhang, J., Zou, Y., Heal, K. R. y Zhou, Y. (2024). Xylem plasticity of root, stem, and branch in *Cunninghamia lanceolata* under drought stress: Implications for whole-plant hydraulic integrity. *Frontiers in Plant Science*, 15, 10910014. <https://doi.org/10.3389/fpls.2024.1308360>
- Li, J., Wang, J., Chen, L., Wu, C., Li He, Cheng, Z. y Gao, J. (2025). Embolism formation and repair of *Phyllostachys vivax* f. *aureocaulis* in winter and the role of non-structural carbohydrates in this process. *Frontiers in Plant Science*, 16. <https://doi.org/10.3389/fpls.2025.1539320>
- Lin, Y. -S., Medlyn, B. E., Duursma, R. A., Prentice, I. C., Wang, H., Baig, S., Eamus, D. y Ellsworth, D. S. (2015). Optimal stomatal behaviour around the world. *Nature Climate Change*, 5(5), 459-464. <https://doi.org/10.1038/nclimate2550>
- Linderman, T., Plata, V., Sancho, D. y Oyhantcabal, W. (2013). *Clima de cambios: nuevos desafíos de adaptación en Uruguay*. Ministerio de Ganadería, Agricultura y Pesca. <http://www.fao.org/climatechange/84982/es/>
- Maherali, H., Pockman, W. T. y Jackson, R. B. (2004). Adaptive variation in the vulnerability of woody plants to xylem cavitation. *Ecology*, 85(8), 2184-2199. <https://doi.org/10.1890/02-0538>
- Martínez-Vilalta, J. y Garcia-Forner, N. (2016). Water potential regulation, stomatal behaviour and hydraulic transport under drought: Deconstructing the iso/anisohydric concept. *Plant, Cell & Environment*, 40(6), 962-976. <https://doi.org/10.1111/pce.12846>
- Martínez-Vilalta, J., García-Valdés, R., Jump, A., Vilà-Cabrera, A. y Mencuccini, M. (2023). Accounting for trait variability and coordination in predictions of drought-induced range shifts in woody plants. *New Phytologist*, 240(1), 23-40. <https://doi.org/10.1111/nph.19138>
- Martínez-Vilalta, J., Prat, E., Oliveras, I. y Piñol, J. (2002). Xylem hydraulic properties of roots and stems of nine Mediterranean woody species. *Oecologia*, 133(1), 19-29. <https://doi.org/10.1007/s00442-002-1009-2>
- Martin-St. Paul, N., Delzon, S. y Cochard, H. (2017). Plant resistance to drought depends on timely stomatal closure. *Ecology Letters*, 20(11), 1437-1447. <https://doi.org/10.1111/ele.12851>

- Matos, I. S., Cornelissen, J. H. C. y Sack, L. (2024). Negative allometry of leaf xylem conduit diameter and double-wall thickness: implications for implosion safety. *New Phytologist*, 242(6), 2464-2478. <https://doi.org/10.1111/nph.19771>
- Mattson, M. P. (2008). Hormesis defined. *Ageing Research Reviews*, 7(1), 1-7. <https://doi.org/10.1016/j.arr.2007.08.007>
- McCulloh, K. A., Johnson, D. M., Meinzer, F. C. y Woodruff, D. R. (2014). The dynamic pipeline: Hydraulic capacitance and xylem hydraulic safety in four tall conifer species. *Plant, Cell & Environment*, 37(5), 1171-1183. <https://doi.org/10.1111/pce.12225>
- McDowell, N. G., Pockman, W. T., Allen, C. D., Breshears, D. D., Cobb, N., Kolb, T., Plaut, J., Sperry, J., West, A., Williams, D. G. y Yezpez, E. A. (2008). Mechanisms of plant survival and mortality during drought: Why do some plants survive while others succumb to drought? *New Phytologist*, 178(4), 719-739. <https://doi.org/10.1111/j.1469-8137.2008.02436.x>
- Meinzer, F. C. y McCulloh, K. A. (2013). Xylem recovery from drought-induced embolism: Where is the hydraulic point of no return? *Tree Physiology*, 33(3), 331-334. <https://doi.org/10.1093/treephys/tpt022>
- Merchant, A., Callister, A., Arndt, S., Tausz, M. y Adams, M. (2007). Contrasting physiological responses of six *Eucalyptus* species to water deficit. *Annals of Botany*, 100(7), 1507-1515. <https://doi.org/10.1093/aob/mcm234>
- Mielke, M. S., Oliva, M. A., Barros, N. F. de, Penchel, R. M. y Martinez, C. A. (2000). Leaf gas exchange in a clonal eucalypt plantation as related to soil moisture, leaf water potential and microclimate variables. *Forest Ecology and Management*, 130(1-3), 263-270. <https://doi.org/10.1007/s004680050012>
- Mokotedi, M. O. (2013). Water relations of *Eucalyptus nitens* × *Eucalyptus grandis*: Is there interclonal variation in response to experimentally imposed water stress? *Southern Forests: A Journal of Forest Science*, 75(4), 213-220. <https://doi.org/10.2989/20702620.2013.858212>
- Monteoliva, S., Barotto, J. y Fernández, M. E. (2015). Anatomía y densidad de la madera en *Eucalyptus*: variación interespecífica e implicancia en la resistencia al estrés abiótico. *Revista de la Facultad de Agronomía*, 114(2), 1-12.

- Nicotra, A. B., Atkin, O. K., Bonser, S. P., Davidson, A. M., Finnegan, C., Mathesius, U., Purugganan, M. D., Richards, C. L., Valladares, F. y van Kleunen, M. (2010). Plant phenotypic plasticity in a changing climate. *Trends in Plant Science*, 15(12), 684-692. <https://doi.org/10.1016/j.tplants.2010.09.008>
- Niinemets, Ü. (2001). Global-scale climate controls of leaf dry mass per area, density and thickness in trees and shrubs. *Ecology*, 82(2), 453-469. <https://doi.org/10.2307/2679872>
- Ni3n, M., G3ndara, J., Ross, S., Sainz, M. M. y Viega, L. (2024). Photosynthesis adaptation to long- and short-term water restriction in commercial plantlets of *Eucalyptus grandis* and hybrids with Red Gums. *Trees*, 38(3), 537-547. <https://doi.org/10.1007/s00468-024-02503-y>
- Nouri, A. (2012). Variation of Basic Density in *Eucalyptus camaldulensis* Dehnh Wood Grown in Iran. *Middle-East Journal of Scientific Research*, 11(10), 1621-1623. [https://www.idosi.org/mejsr/mejsr11\(10\)12/20.pdf](https://www.idosi.org/mejsr/mejsr11(10)12/20.pdf)
- Oficina de Estadísticas Agropecuarias (DIEA). (2023). *Anuario estadístico agropecuario (2022)*. Ministerio de Ganadería, Agricultura y Pesca. <https://descargas.mgap.gub.uy/DIEA/Anuarios/Anuario2023/ANUARIO2023WEB.pdf>
- O'Sullivan, K. L. y Schenk, H. J. (2012). Conduit reinforcement of *Juniperus* species enhances cavitation resistance in arid environments. *American Journal of Botany*, 99(3), 299-306. <https://doi.org/10.3732/ajb.1100271>
- Pallardy, S. G. (2008). *Physiology of woody plants* (3.^a ed.). Academic Press.
- Pechi, E. I. y Ram3rez, N. (2013). *Efecto de la poda en el control de la din3mica del agua en 3rboles de Pinus taeda* [tesis de grado, Universidad de la Rep3blica]. Colibri. <https://hdl.handle.net/20.500.12008/1765>
- Pfautsch, S. (2016). Hydraulic anatomy and function of trees—basics and critical developments. *Current Forestry Reports*, 2(4), 236-248. <https://doi.org/10.1007/s40725-016-0046-8>
- Pfautsch, S., Aspinwall, M., Drake, J., Chac3n-Doria, E., Langela, R., Tissue, D., Tjoelker, M. y Lens, F. (2018). Traits and trade-offs in whole-tree hydraulic

- architecture along the vertical axis of *Eucalyptus grandis*. *Annals of Botany*, 121(1), 129-141. <https://doi.org/10.1093/aob/mcx137>
- Pillai, P. K. C., Pandalai, R. C., Dhamodaran, T. K. y Sankaran, K. V. (2013). Wood density and heartwood proportion in Eucalyptus trees from intensively-managed short-rotation plantations in Kerala, India. *Journal of Tropical Forest Science*, 25(2), 220-227.
- Pita, P. y Pardos, J. A. (2001). Growth, leaf morphology, water use and tissue water relations of *Eucalyptus globulus* clones in response to water deficit. *Tree Physiology*, 21(9), 599-607. <https://doi.org/10.1093/treephys/21.9.599>
- Pyrke, A. F. y Kirkpatrick, J. B. (1994). Growth rate and basal area response curves of four *Eucalyptus* species on Mt. Wellington, Tasmania. *Journal of Vegetation Science*, 5(1), 13-24.
- Ripullone, F., Guerrieri, M. R., Nole, A., Magnani, F. y Borghetti, M. (2007). Stomatal conductance and leaf water potential responses to hydraulic conductance variation in *Pinus pinaster* seedlings. *Trees: Structure and Function*, 21(3), 371-378. <https://doi.org/10.1007/s00468-007-0130-6>
- Rowland, L., Ramírez-Valiente, J.-A., Hartley, I. P. y Mencuccini, M. (2023). How woody plants adjust above- and below-ground traits in response to sustained drought. *New phytologist*, 239(4), 1173-1189. <https://doi.org/10.1111/nph.19000>
- Ryan, M., Phillips, N. y Bond, B. (2006). The hydraulic limitation hypothesis revisited. *Plant, Cell & Environment*, 29(3), 367-381. <https://doi.org/10.1111/j.1365-3040.2005.01478.x>
- Saito, T. y Terashima, I. (2004). Reversible decreases in the bulk elastic modulus of mature leaves of deciduous *Quercus* species subjected to two drought treatments. *Plant, Cell & Environment*, 27, 863-875. <https://doi.org/10.1111/j.1365-3040.2004.01192.x>
- Santiago, L. S., Goldstein, G., Meinzer, F. C., Fisher, J. B., Machado, K., Woodruff, D. R. y Jones, T. (2004). Leaf photosynthetic traits scale with hydraulic conductivity and wood density in Panamanian forest canopy trees. *Oecologia*, 140(4), 543-550. <https://doi.org/10.1007/s00442-004-1624-1>

- Scholz, F. G., Bucci, S. J., Goldstein, G., Meinzer, F. C., Franco, A. C. y Miralles-Wilhelm, F. (2007). Biophysical properties and functional significance of stem water storage tissues in Neotropical savanna trees. *Plant, Cell & Environment*, 30(2), 236-248. <https://doi.org/10.1111/j.1365-3040.2006.01623.x>
- Searson, M. J., Thomas, D. S., Montagu, K. D. y Conroy, J. P. (2004). Wood density and anatomy of water-limited eucalypts. *Tree Physiology*, 24(11), 1295-1302. <https://doi.org/10.1093/treephys/24.11.1295>
- Singh, U. (2005). Comparative study of transpiration rates by different Eucalyptus species under various soil moisture and climatic conditions. *Indian Journal of Forestry*, 28(2), 112-115. <https://doi.org/10.54207/bsmps1000-2005-I4XII9>
- Skaggs, R. W., Chescheir, G. M., Amatya, D. M. y Gilliam, J. W. (2008). Simulation of the Hydrologic Effects of Afforestation in the Tacuarembó River Basin, Uruguay. *Journal of Hydrology*, 348(3-4), 129-140. <https://www.researchgate.net/publication/43262615>
- Soro, A., Lenz, P., Roussel, J. -R. y Achim, A. (2023). The phenotypic and genetic effects of drought-induced stress on wood specific conductivity and anatomical properties in white spruce seedlings, and relationships with growth and wood density. *Frontiers in Plant Science*, 14, 1297314. <https://doi.org/10.3389/fpls.2023.1297314>
- Sperry, J. S. y Hacke, U. G. (2004). Analysis of circular bordered pit function: I. Angiosperm vessels with homogeneous pit membranes. *American Journal of Botany*, 91(3), 369-385. <https://doi.org/10.3732/ajb.91.3.369>
- Sperry, J. S., Hacke, U. G., Oren, R. y Comstock, J. P. (2002). Water deficits and hydraulic limits to leaf water supply. *Plant, Cell & Environment*, 25(2), 251-263. <https://doi.org/10.1046/j.0016-8025.2001.00799.x>
- Sperry, J. S., Meinzer, F. C. y McCulloh, K. A. (2008). Safety and efficiency conflicts in hydraulic architecture: Scaling from tissues to trees. *Plant, Cell & Environment*, 31(5), 632-645. <https://doi.org/10.1111/j.1365-3040.2008.01807.x>

- Stape, J. L. y Binkley, D. (2010). Insights from full-rotation Nelder spacing trials with *Eucalyptus* in São Paulo, Brazil. *Southern Forests: A Journal of Forest Science*, 72(2), 91-98. <https://doi.org/10.2989/20702620.2010.507031>
- Tampori, K., Amoah, M., Dadzie, K. y Siam, N. A. (2024). Characterization of Wood Cellular Structure of Plantation Grown *Anogeissus leiocarpa* and *Eucalyptus camaldulensis* in the Savannah Ecological Zone, Ghana. *SEEFOR South-East European Forestry*, 15 (2), 201-210. <https://doi.org/10.15177/seeфор.24-22>
- Tricerri, N., Tomasella, M., Cavalletto, S., Petruzzellis, F., Natale, S., Crivellaro, A., Gamba, R., Piermattei, A., D'Amico, L., Tromba, G., Nardini, A., Zwieniecki, M. A. y Secchi, F. (2025). Fibers beyond structure: Do they contribute to embolism reversal after drought relief in poplar? *New Phytologist*, 247(2), 612-624. <https://doi.org/10.1111/nph.70179>
- Tyree, M. T. (2003). Hydraulic limits on tree performance: Transpiration, carbon gain and growth of trees. *Trees: Structure and Function*, 17(2), 95-100. <https://doi.org/10.1007/s00468-002-0227-x>
- Tyree, M. T. y Jarvis, P. G. (1982). Water in tissues. En O. L. Lange, P. S. Nobel, C. B. Osmond y H. Ziegler (eds.), *Water relations and carbon assimilation: Physiological plant ecology II: Encyclopedia of Plant Physiology, New Series, 12b* (pp. 36-71). Springer-Verlag.
- Tyree, M. T. y Zimmermann, M. H. (2002). *Xylem structure and the ascent of sap* (2.^a ed.). Springer.
- USDA Forest Service. (2023). *Understanding i-Tree — Appendix 11: Wood density values* (GTR-NRS200-2023 Appendix 11). U. S. Department of Agriculture, Forest Service.
- Valladares, J., Figueiredo de Paula, N. y De Paula, C. (2014). Physiological changes in *Eucalyptus* hybrids under different irrigation regimes. *Revista Ciência Agronômica*, 45(4), 805-814. <https://doi.org/10.1590/S1806-66902014000400019>
- Valverde, J. C., Rubilar, R. A., Medina, A., Pincheira, M., Emhart, V., Espinoza, Y., Bozo, D. y Campoe, O. C. (2025). Transpiration and Water Use Efficiency of

- Mediterranean *Eucalyptus* Genotypes Under Contrasting Irrigation Regimes. *Plants*, 14(14), 2232. <https://doi.org/10.3390/plants14142232>
- Vander Willigen, C. y Pammenter, N. W. (1998). Relationship between growth and xylem hydraulic characteristics of clones of *Eucalyptus* spp. at contrasting sites. *Tree Physiology*, 18(8), 595-600. <https://doi.org/10.1093/treephys/18.8-9.595>
- Vieira, T. A. S., Arriel, T. G., Zanuncio, A. J. V., Carvalho, A. G., Branco-Vieira, M., Carabineiro, S. A. C. y Trugilho, P. F. (2021). Determination of the chemical composition of *Eucalyptus* spp. for cellulosic pulp production. *Forests*, 12(12), 1649. <https://doi.org/10.3390/f12121649>
- Wang, P., Zhao, Y., Li, Z., Hsu, C. C., Liu, X., Fu, L., Hou, Y. J., Du, Y., Xie, S., Zhang, C., Gao, J., Cao, M., Huang, X., Zhu, Y., Tang, K., Wang, X., Tao, W. A., Xiong, Y., & Zhu, J. K. (2018). Reciprocal Regulation of the TOR Kinase and ABA Receptor Balances Plant Growth and Stress Response. *Molecular cell*, 69(1), 100–112.e6. <https://doi.org/10.1016/j.molcel.2017.12.002>
- Willson, C. J., Manos, P. S. y Jackson, R. B. (2008). Hydraulic traits are influenced by phylogenetic history in the drought-resistant, invasive genus *Juniperus* (Cupressaceae). *American Journal of Botany*, 95(3), 299–314. <https://doi.org/10.3732/ajb.95.3.299>
- White, D. A., Turner, N. C. y Galbraith, J. H. (2000). Leaf water relations and stomatal behavior of four allopatric *Eucalyptus* species planted in Mediterranean southwestern Australia. *Tree Physiology*, 20(17), 1157-1165. <https://doi.org/10.1093/treephys/20.17.1157>
- Whitehead, D. y Beadle, C. L. (2004). Physiological regulation of productivity and water use in *Eucalyptus*: A review. *Forest Ecology and Management*, 193(1-2), 113-140. <https://doi.org/10.1016/j.foreco.2004.01.026>
- Xu, H., Wang, H., Prentice, I. C., Harrison, S. P. y Wright, I. J. (2021). Coordination of plant hydraulic and photosynthetic traits: confronting optimality theory with field measurements. *New Phytologist*, 232(3), 1286-1296. <https://doi.org/10.1111/nph.17656>
- Zanne, A. E., Westoby, M., Falster, D. S., Ackerly, D. D., Loarie, S. R., Arnold, S. E. J. y Coomes, D. A. (2010). Angiosperm wood structure: Global patterns in vessel

- anatomy and their relation to wood density and potential conductivity. *American Journal of Botany*, 97(2), 207-215. <https://doi.org/10.3732/ajb.0900178>
- Zhang, Z. Z., Zhao, P., Oren, R., McCarthy, H. R., Niu, J. F., Zhu, L. W. y Huang, Y. Q. (2015). Water use strategies of a young *Eucalyptus urophylla* forest in response to seasonal change of climatic factors in South China. *Biogeosciences Discussions*, 12(13), 10469-10510. <https://doi.org/10.5194/bgd-12-10469-2015>
- Zhou, S. -X., Medlyn, B. E., y Prentice, I. C. (2016). Long-term water stress leads to acclimation of drought sensitivity of photosynthetic capacity in xeric but not riparian *Eucalyptus* species. *Annals of Botany*, 117(1), 133-144. <https://doi.org/10.1093/aob/mcv161>
- Wang, P., Zhao, Y., Li, Z., Hsu, C.-C., Liu, X., Fu, L., Hou, Y. -J., Du, Y., Xie, S., Zhang, C., Gao, J., Cao, M., Huang, X., Tang, K., Wang, X., Tao, W.-A., Xiong, Y. y Zhu, J. -K. (2018). Reciprocal regulation of the TOR kinase and ABA receptor balances plant growth and stress response. *Molecular Cell*, 69(1), 100-112. <https://doi.org/10.1016/j.molcel.2017.12.002>
- Zimmermann, J., Link, R. M., Hauck y Schuldt, B. (2021). 60-year record of stem xylem anatomy and related hydraulic modification under increased summer drought in ring- and diffuse-porous temperate broad-leaved tree species. *Trees*, 35(3), 919-937. <https://doi.org/10.1007/s00468-021-02090-2>